NASA-CR65136

THE EFFECT OF THE LUNAR ENVIRONMENT ON MAGMA GENERATION, MIGRATION, AND CRYSTALLIZATION

report to

NATIONAL AERONAUTICS and SPACE ADMINISTRATION MANNED SPACECRAFT CENTER

Contract NAS 9-3449

Arthur D. Little, Inc.

THE EFFECT OF THE LUNAR ENVIRONMENT ON MAGMA GENERATION, MIGRATION, AND CRYSTALLIZATION

Contract No. NAS 9-3449

To

NATIONAL AERONAUTICS AND SPACE ADMINISTRATION
MANNED SPACECRAFT CENTER
2101 WEBSTER-SEABROOK ROAD
HOUSTON, TEXAS 77058

Prepared by

ARTHUR D. LITTLE, INC.
15 ACORN PARK
CAMBRIDGE, MASSACHUSETTS

R. K. McConnell
R. V. Allen
J. Aronson
G. Feick
D. W. Lee
L. McClaine
B. Vonnegut

November 1, 1965

FOREWARD

This report was prepared by the Research and Development Division of Arthur D. Little, Inc., and covers work carried out under contract NAS 9-3449 during the period August 13, 1964 to August 20, 1965. The work was administered by the National Aeronautics and Space Administration, Manned Spacecraft Center with Elbert A. King, Technical Initiator. In addition to those listed as authors, the following persons made invaluable contributions to the study: J. Berkowitz, P. E. Blackburn, J. L. Engelke, and F. F. Surprenant. Professor R. Bisque of the Colorado School of Mines and Dr. S. Thorarinsson of the Museum of Natural History, Reykjavik, acted as consultants.

ABSTRACT

Studies of several models of lunar composition indicate that a period of intense volcanic activity with sudden onset and approximately exponential decline is entirely likely. A mechanism for sudden generation of magma is proposed on the basis of the thermal properties of a basalt-dunite mixture. Factors controlling the migration of magma through a dike, the formation of magma chambers and the deposition of volatile species on the moon's surface are discussed.

TABLE OF CONTENTS

LIST OF FIGURES

INTRODUCTION

Most present models of the lunar surface rocks assume that they are similar in composition to terrestrial igneous rocks. While there is considerable controversy as to whether the surface morphology is predominantly a result of volcanic activity or meteorite impacts, most students of lunar geology are willing to accept both types of activity to some extent. Because of the relative importance of volcanic terrain from the point of view of natural resources as well as from a scientific point of view, it is important that the Apollo astronauts be able to recognize, and be prepared to cope with, any volcanic rocks which they might encounter.

The diversity of igneous rocks on the earth illustrates the profound effect that relatively small changes in environment may have. Under lunar conditions of reduced gravity, high vacuum, and different thermal conditions it has been suggested that the properties of the rocks may be so unique that their igneous origin may be unrecognizable to an astronaut trained in terrestrial geology. In addition to the problem of recognition, the morphology and texture of the lunar rocks may be of such a character as to present engineering and mobility problems. Highly reactive volatiles emitted from volcanos on the moon's surface and trapped in perpetually shaded areas may present a hazard if accidently unfrozen.

In order to be able to anticipate and plan against these unknown variables, it is necessary to establish a coherent quantitative theory of igneous activity which may be tested on the earth and then extrapolated to the moon. This report presents the results of a program in which we have tried to develop such a theory for some of the better known aspects of igneous activity.

Our approach to the study has been to subdivide each of the three major problems of generation, migration, and crystallization into smaller well-defined partial problems which are more susceptible to theoretical treatment. For each partial problem we have attempted to develop a mathematical model whose degree of sophistication is consistent with

available experimental and/or field data, or data which may be obtained in later studies. We have tried, wherever possible, to present our models in such a way, that as data improves, modifications may be easily made with as minor effects as possible on the value of the study.

The models include dimensional analysis, algebraic expression, and simulation by means of digital computers. While the numerical models frequently represent gross over-simplifications of the processes taking place in nature, they have usually made it possible to arrive at a more quantitative understanding of many of the igneous features observed on earth. Where there is direct evidence that one of the factors controlling a particular phenomenon differs significantly on the moon from that observed on the earth, we have tried to determine how the phenomenon itself will differ. Where there is no clear evidence how controlling factors would differ, we have chosen to assume that they are identical. Where there appears to be insufficient experimental data available to construct a satisfactory model we have tried to indicate this.

As the study progressed, it became apparent that there was a much wider variety of volcanic features which were potentially susceptible to quantitative analysis than we had initially suspected, and we found it necessary to concentrate on a few of the more important ones. In general, we believe that enough understanding of the processes of generation and intrusion has been gained to predict a number of aspects of their nature on the moon; however, much experimental and theoretical work appears to be required before one can make such a claim about extrusion.

2. MAGMA GENERATION

Generation of magma is one of many possible events in the evolutionary history of any planetary body. This history (barring astronomical accidents) is essentially determined by four sets of initial conditions:

mass,
distribution of elements,
distribution of heat sources,
initial temperature distribution.

These conditions are not independent. Mass depends on the density which is a function of composition. Distribution of heat sources depends on minor percentages of radioactive elements. The initial temperature distribution is probably related to all the above as well as the mechanism of formation.

If the planet consists of more than one material phase there will be a natural tendency towards attaining the lowest possible gravitational potential energy by bringing denser materials closer to the center and allowing the lighter ones to move away. By far the most effective mechanism for this differentiation is by flow of one of the phases, as a fluid or magma.

The basic problem then, is one of determining the thermal history of the planet and then seeing how magma generation is related to this thermal history.

In order to compare magma generation on the moon with generation on the earth we have tried first to determine what processes taking place in the upper mantle of the earth would be consistent with terrestrial igneous activity and then to estimate how these processes would be changed by the lunar environment. To make the comparison one must define magma generation in terms which are both geologically and mathematically meaningful. A suitable geological definition might be: partially melting <u>enough</u> mantle material that some or all of it is potentially able to migrate upward. As this definition is too complex for our initial studies, in this chapter we shall assume that partial melting and magma generation are synonymous and that <u>any</u> melt generated will move to the surface resulting in diverse events which we shall collectively call volcanism.

2.1 DEVELOPMENT OF THE MODEL

Models for the thermal history of planetary bodies are becoming increasingly sophisticated. Fourier (1822) derived an analytic expression for the cooling of a uniform initially hot earth. Jacobs (1956) investigated the thermal history of a layered earth with different distributions of radioactive elements and constant temperature-independent thermal conductivity. Lubimova (1958) considered the effects of radiative transfer on the earth's thermal history using an analog computer. MacDonald (1959, 1962) used a finite difference technique to investigate the thermal history of the earth and the moon taking into account the effects of radiative transfer. Using chondritic ratios of the heat producing isotopes, a variety of initial conditions and heat source distributions were simulated. Fricker and Reynolds (1965) have extended MacDonald's approach by considering the heat of fusion and trying to simulate the effects of convection in a molten layer.

To investigate the interaction between volcanism and the thermal history of the moon, we have extended MacDonald's approach in a different direction by developing a computer program which simulates a planetary body with the following characteristics:

(1) The body consists of two phases each with a distinct density.

(2) The first phase has a discrete melting temperature, independent of the amount of second phase present, which is a known linear function of pressure. The melting temperature of the other phase is very much greater than that of the first.

(3) The heat of fusion of the first phase is independent of pressure and of the concentration of the second phase.

(4) The specific heats of both phases are the same and are independent of temperature and pressure.

(5) The thermal conductivity of both phases are the same known temperature dependent functions of conductivity, index of refraction, and photon mean free path at a reference temperature.

(6) The ratios of heat producing radioactive isotopes are those of terrestrial rocks and these isotopes may be either entirely localized in the low melting phase or equally distributed between the two phases.

(7) Any melt produced moves rapidly to the surface maintaining a constant temperature and the unmelted material moves downward to replace it. This model obviously represents only a first approximation of the actual properties of the moon or of any other small planetary body yet with it it is possible to demonstrate many of the most significant features of the role of volcanism in planetary evolution. Only when these more significant features have been determined will increasing the complexity of the model be justifiable. The following sections are concerned with the estimation of the appropriate input data to be used in the computer simulation.

2.11 Density and Composition

2.111 Density and Pressure

The mean density of the moon is 3.34. If the temperature, elastic constants and coefficient of thermal expansion were known the density at atmospheric pressure could be computed. Fortunately, the effects of pressure and temperature to some extent offset one another and the pressures are low enough (about 45 kilobars at the center of the moon) that if the moon were composed primarily of silicates similar to those found in the earth's mantle no large pressure induced density changes would be expected. As the moon's mean density is very close to that observed in the earth's oceanic mantle at depths of about 30 km (Anderson, 1964) and the density is highly sensitive to minor changes in iron content, we see no reason to discard a terrestrial mantle composition on the basis of density alone. As the melting temperature is a function of pressure it is important to determine the variation of the pressure with depth. Fortunately, the pressure is relatively insensitive to minor changes in density due to compressibility and thermal expansion. As there is no apriori reason for assuming a differentiated moon, as a first approximation we shall assume it has a uniform density. Using this assumption, hydrostatic pressures have been calculated by Lowman (1963) and others. In terms of the mass m and the radius a the pressure p of a spherical planet is given by

$$p = \frac{3}{8}\frac{Gm^2}{a^4}\left(1 - \frac{r^2}{a^2}\right) \qquad (2.11\text{-}1)$$

Where r is the distance from the center and G is the gravitational constant 6.673×10^{-8} cm^3 gm^{-1} sec^{-2}.

For the earth we have adopted densities from Anderson's (1964) model "CITI3F" for the oceanic upper mantle based on Love wave information. From this it is relatively straightforward to determine a standard pressure distribution within the uppermost several hundred kilometers of the earth's mantle by numerical integration.

A comparison of pressures as a function of depth in the moon and earth calculated from the above expressions are shown in Figure 2.11-1.

2.112 Composition of Earth's upper Mantle

While there is considerable argument about the compositions of the upper mantle most theories propose a material lying somewhere between dunite or peridotite and eclogite (high pressure basalt) as proposed by Lovering (1958) and others. Chondritic models have long been proposed for the composition of both the earth and the moon. As the moon's density and the density of the earth's upper mantle are closer to the silicate phase of chondrite rather than to chondrite as a whole (about 3.6 gm/cm^3) the silicate phase alone is usually considered to correspond most closely to the earth's upper mantle and to the moon. The average composition of the silicate phase of 94 chondrites from Urey and Craig (1953) is shown as Model (1) in Table 2.11-1. With more refined studies the chondrite model of the earth has had to be modified in some respects, esspecially the ratios of the minor elements such as K/U and Fe/Mg.

Ringwood (1959) has presented rather convincing arguments for adjusting the FeO/MgO ratio from 1/2 to 1/5, reducing the SiO_2 content slightly, and making the other minor modifications to obtain a material more consistent with existing evidence for the earth's upper mantle (Model 2). He has pointed out the similarity of this material to a mixture of one part basalt (average between tholeiite and alkali basalts) to three parts dunite (Model 3). Ringwood has called this mixture pyrolite and used it to present a qualitative explanation of differentiation within the earth's mantle.

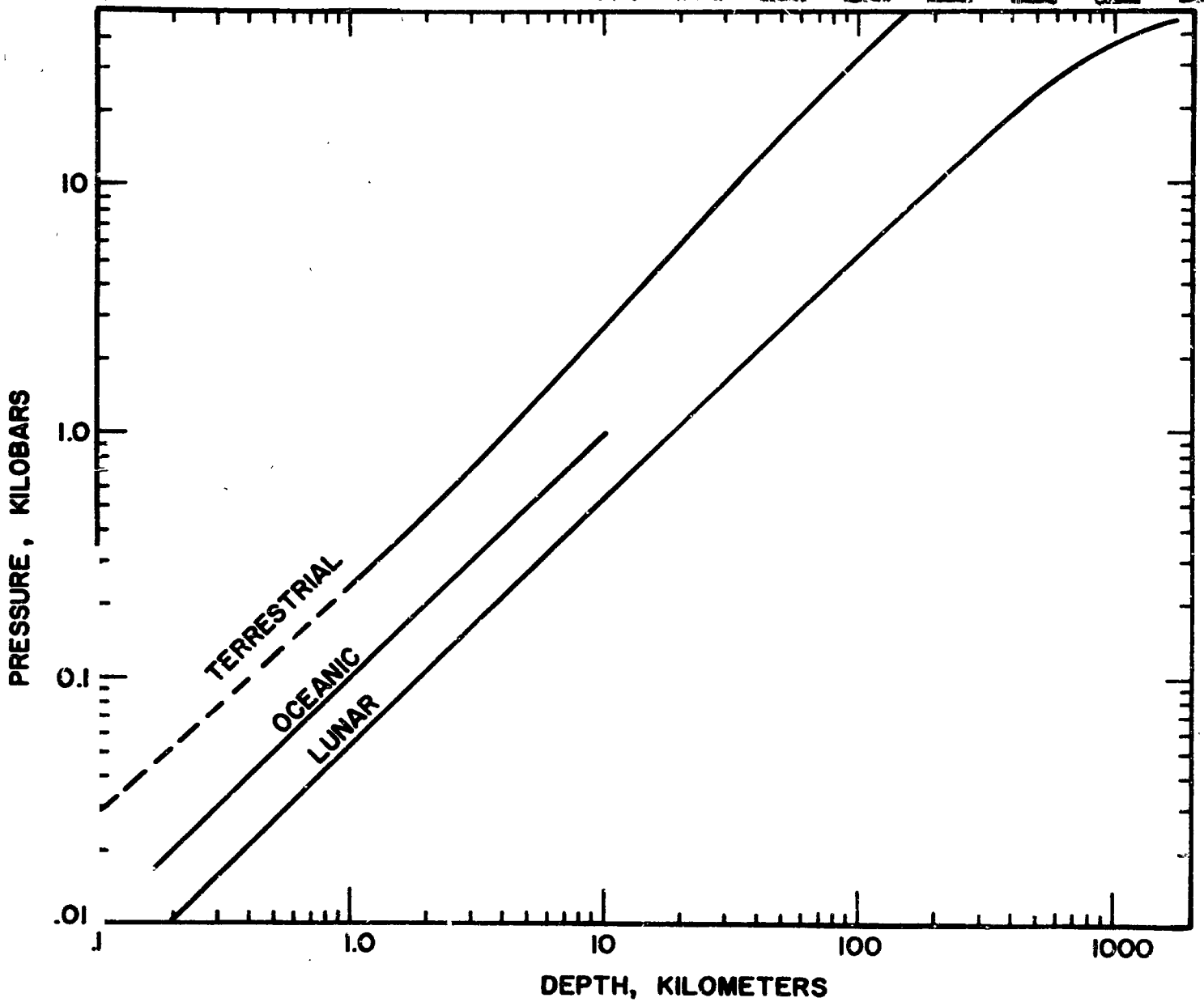

FIGURE 2.11-1 Comparison of pressures at various depths in the moon, earth, and undersea.

TABLE 2.11-I

	(1) Urey and Craig (1953)* Silicate Phase of 94 Chondrites	(2) Ringwood (1959) Modified Chondrite	(3) Green and Ringwood (1963) Pyrolite
SiO_2	47.86	44.69	43.06
MgO	30.00	39.08	39.32
FeO	15.67	7.81	8.15
Al_2O_3	3.14	4.09	3.99
CaO	2.45	3.19	2.65
Na_2O	0.88	1.14	0.61
Other			2.66

* Neglecting minor constituents.

Thus we may say that to a first approximation the silicate phase of a chondrite and "pyrolite" represent a composition intermediate between dunite and eclogite.

A normative mineral assemblage for this pyrolite, calculated using the C.I.P.W. method (Johannsen, 1939), is shown in Table 2.11-II. This provides an approximate guide to the distribution of the oxides among the various minerals but does not necessarily represent the equilibrium mineral assemblage at any depth in the mantle of the earth or in the moon.

As it is difficult to determine the exact ratio of basalt to dunite which is most appropriate for the mantle we shall call the pyrolite composition discussed above "pyrolite-1:3", with the numbers representing the ratio of basalt to dunite.

Among the more significant features of the Ringwood model is that it is approximately chondritic yet is able to produce a basalt magma of approximately the composition and normative mineral assemblage shown in Table 2.11-III, upon partial melting (Green and Ringwood, 1963). After melting and removal of the basalt melt a residue of peridotite or dunite would be left behind.

2.113 Assumed Composition for the Moon

Because of the lack of direct experimental evidence proposed models of the moon's composition have not been refined as extensively as the models for the earth's upper mantle. There is, however, no evidence

TABLE 2.11-II

PYROLITE-1:3 NORMATIVE MINERAL ASSEMBLAGE

Oxide	Wt. %	Mol.	Chro-mite	Ilmen-ite	Ortho-clase	Albite	Anor-thite	Mag-netite	Diop-side	Hyper-sthene	Oli-vine
SiO_2	43.06	0.717			.012	.054	.056		.038	.073	.484
MgO	39.32	0.983							.018	.067	.898
FeO	6.66	0.092	.002	.007				.010	.001	.006	.070
Fe_2O_3	1.66	0.010						.010			
Al_2O_3	3.99	0.039			.002	.009	.028				
CaO	2.65	0.047					.028		.019		
Na_2O	0.61	0.009				.009					
K_2O	0.22	0.002			.002						
Cr_2O_3	0.42	0.002	.002								
NiO	0.39	0.005									
CoO	0.02	0.0002									
Mn[illegible]	0.13	0.001									
P_2O_5	0.08	0.0006									
H_2O	0.21	0.01									
TiO_2	0.58	0.007		.007							
Weight % of Mineral			.448	1.06	1.11	4.72	7.78	2.32	4.13	7.49	70.00

TABLE 2.11-III

MODEL BASALT NORMATIVE MINERAL ASSEMBLAGE

Oxide	Wt. %	Mol.	Apatite	Ilmenite	Orthoclase	Albite	Anorthite	Magnetite	Diopside	Hypersthene	Olivine
SiO_2	48.30	.805			.054	.234	.184		.182	.105	.045
MgO	7.36	.197							.065	.075	.057
FeO	8.89	.123		.029				.019	.025	.030	.033
Fe_2O_3	3.02	.019						.019			
Al_2O_3	14.35	.140			.009	.039	.092				
CaO	10.58	.189	.006				.092		.091		
Na_2O	2.43	.039				.039					
K_2O	.88	.009			.009						
MnO	.19	.003									
P_2O_5	.31	.002	.002								
H_2O	.83	.046									
TiO_2	2.33	.029		.029							
Weight % of Mineral			0.67	4.41	5.00	20.44	25.58	4.41	20.34	11.46	7.28

that to a first approximation the moon is significantly different from the upper mantle and we shall therefore assume they are the same until this assumption leads to conclusions which are in contradiction to direct observations. No such contradictions have yet appeared. If tektites come from the moon, their K/U ratios, discussed below in conjunction with heat sources, would tend to point toward the similarity of the upper mantle composition and the moon.

The assumption of equality between upper mantle and moon does not of course remove all the compositional difficulties but it does make it possible, using the additional assumption of a mantle whose composition may be approximated by a mixture of dunite and basalt to try to find a mixture which will be thermally and volcanologically consistent with terrestrial observations.

2.12 Heat Sources

For material of bulk density ρ and concentrations $C_i(t)$ of n elements A_i which decay to B_i with decay constants λ_i liberating amount of heat Q_i per gram in the process, the rate of heat production per unit volume $q(t)$ at time t is

$$q(t) = \rho \sum_{i=i}^{n} Q_i \lambda_i C_i(t_o) \exp[\lambda_i (t_o - t)]. \qquad (2.12\text{-}1)$$

It is normally assumed that the only isotopes producing enough heat and with long enough half life to have significantly influenced the thermal history of the earth and moon are U^{238}, U^{235}, Th^{232}, and K^{40}. The reactions involved (neglecting intermediate steps) are (Jacobs, Russell and Wilson, 1959):

$$U^{238} \rightarrow Pb^{206} + 8He^4 + 6\beta$$
$$U^{235} \rightarrow Pb^{207} + 7He^4 + 4\beta$$
$$Th^{232} \rightarrow Pb^{208} + 6He^4 + 4\beta$$
$$K^{40} + e^C \rightarrow A^{40} + \gamma + \text{X-ray}$$
$$\text{or} \quad K^{40} \rightarrow Ca^{40} + \beta$$

Additional shorter lived isotopes may have been important in the early thermal history of the planet but they have not yet been satisfactorily studied. The main effect of these sources will be to raise the temperature at the time of formation.

We may then make up a table (see for example MacDonald, 1959) for the longer lived isotopes.

TABLE 2.12-I

Isotope	U^{238}	U^{235}	Th^{232}	K^{40}
Half-life (10^9 years)	4.51	.713	13.9	1.25
$\lambda\ 10^{-18}\ sec^{-1}$	4.87	30.80	1.58	17.57
Heat production $Q\lambda$ ergs/gm/sec	0.94	5.7	0.26	0.298

Thus the uranium heat production per cubic centimeter of rock is

$$q_U(t) = \rho C_U(t_o)\{\ 0.9332\exp[4.87\times10^{-18}(t_o-t)] + 0.04047\exp[3.09\times10^{-17}(t_o-t)]\} \quad (2.12\text{-}2)$$

The heat production from thorium is

$$q_{Th}(t) = \rho C_U(t_o)\{(C_{Th}/C_U)0.26\exp[1.58\times10^{-18}(t_o-t)]\} \quad (2.12\text{-}3)$$

Similarly for potassium we obtain

$$q_K(t) = \rho C_U(t_o)\{(C_{K^{40}}/C_K)\ (C_K/C_U)\ 0.298\exp[1.76\times10^{-17}(t_o-t)]\} \quad (2.12\text{-}4)$$

2.121 Isotope Ratios in Terrestrial Rocks and Meteorites

While the absolute concentrations of the different radioactive isotopes vary significantly within the earth and meteorites, the ratios relative to total uranium are much more constant (Wasserburg et al, 1964). As a result of essentially identical chemical behavior of the uranium isotopes their ratios within exposed terrestrial rocks and meteorites do not vary significantly from

$$U^{238} = .9928\ U^{total}$$
$$U^{235} = .0071\ U^{total}$$

(Handbook of Chemistry and Physics, 1962).

Because of considerable chemical similarity uranium and thorium tend to move together; thorium to uranium ratios in terrestrial igneous rocks do not vary much from 4. MacDonald (1964) has chosen the ratio

$$Th/U = 3.7$$

as being the most representative of terrestrial rocks. While there are not enough good determinations of the Th/U ratio for meteorites to provide a reliable estimate (Wasserburg et al, 1964), a value in the neighborhood of 4 is not inconsistent with most data available for chondrites (MacDonald, 1959).

The ratio of the potassium isotopes do not vary significantly from

$$K^{40} = 1.19 \times 10^{-4} K^{total}$$

but there is increasing evidence that the K/U ratio may be considerably different in chondrites than it is in the earth. After examining the available evidence Wasserburg et al (1964) conclude that the ratio of K/U of chondrites is close to 8×10^4 while for igneous rocks exposed to the earth's surface it averages around 1×10^4. Because of the chemical dissimilarity of K and U there is no obvious theoretical reason that the two should maintain a constant ratio. Nevertheless the observed values of the K/U ratio on the earth are sufficiently constant that it seems appropriate to follow the lead of Wasserburg et al (1964) and MacDonald (1964) and choose the ratio for our model composition 1.0×10^4.

2.122 Isotope Ratios in Tektites

Some additional justification for selecting the above ratios for our model may be obtained by considering the chemical composition of tektites.

TABLE 2.12-I

ELEMENT RATIOS IN TEKTITES -- Data compiled by Chao (1963)

	K_2O wt %	K wt %	U ppm	Th ppm	K/U	Th/U
Moldavites	3.04	2.52	2.05 (4)*	15.4 (1)*	1.22×10^4	7.50
Javanites) Billitonites)	2.20	1.82	2.1 (2)	9.6	$.87 \times 10^4$	4.60
Philippinites	2.31	1.92	2.13 (3)		.90	
Indochinites	2.40	1.99	2.23 (4)		.89	
Australites	2.20	1.83	2.03 (4)	10.8 (2)	.90	5.32
North America	2.13	1.77	1.55 (2)	4.0 (1)	1.14	
Ivory Coast	1.53	1.27	1.1 (1)	____	1.15	2.58
		1.87	1.88	9.95	1.01×10^4	5.0

Mean (K/U) = 1.01×10^5

Mean K/Mean U = $.995 \times 10^4$

Mean Th/Mean U = 5.3

*Numbers in parentheses are number of analyses reported.

Chao (1963) has assembled chemical analyses of a large number of tektites. From these analyses it is possible to make a crude estimate of the Th/U and K/U ratio for different types of tektites (Table 2.12-I).

While there is relatively little information on the thorium values the mean Th/U ratio seems to be of the order of 5.0. This ratio is not significantly different from that derived from the few analyses assembled by MacDonald (1959), or from the values for terrestrial rocks, especially the basalts reported by Wasserburg et al. (1964), and is subject to the same limitations of reliability.

If we look at the mean K/U ratio estimated from Chao's tektite data we see it is remarkably constant and very close to 1.0×10^4; this is the same as that chosen by Wasserburg as being the most representative of terrestrial rocks. While this ratio may be interpreted as evidence for the terrestrial origin of tektites, if we are to accept the many arguments for the moon as their source, then the K/U ratio of those lunar surface rocks represented by tektites would be consistent with the values selected for our model.

2.123 Heat Production in Model

From the above arguments it appears that the ratios chosen by Wasserburg et al. for the composition of the minor, heat producing components earth's mantle are not inconsistent with our present knowledge of the composition of the moon and it is appropriate to adopt them for our model. The selected concentrations in terms of the total uranium content of the model are summarized in Table 2.12-II.

TABLE 2.12-II

Isotope	Concentration	Basis for Estimate	Reference
U^{238}	$.9928\ U^{total}$	Terrestrial abundances	(1)
U^{235}	$.0071\ U^{total}$	Terrestrial abundances	(1)
Th	$3.7\ U^{total}$	Estimated averag terrestrial abundances (not inconsistent with present chondrite and tektite data)	(2) (3),(4)
K^{40}	$1.19\ U^{total}$	K^{40}/K^{total}; K^{total}/U^{total}	
K^{40}	$1.19 \times 10^{-4}\ K^{total}$	Terrestrial abundances	(1)
K^{total}	$1 \times 10^4\ U^{total}$	Estimated avg. terrestrial abundances	(2)

References:

(1) Handbook of Chemistry and Physics (1962)

(2) Wasserburg et al. (1964)

(3) MacDonald (1959)

(4) This report, calculated from Chao (1963)

In terms of the uranium concentration in grams/gram the total power supplied in watts per cubic centimeter is then given by

$$\begin{aligned} q(t) &= q_U + q_{Th} + q_K \\ &= \rho C_U(t_o)\times 10^{-7}\{0.9332\exp[4.87\times 10^{-18}(t_o-t)] \\ &\quad +0.04047\exp[3.08\times 10^{-17}(t_o-t)] \\ &\quad + 0.962\exp[1.58\times 10^{-18}(t_o-t)] \\ &\quad + 0.355\exp[1.87\times 10^{-17}(t_o-t)]\} \end{aligned} \qquad (2.12\text{-}5)$$

Since we have fixed the ratios of all the heat producing isotopes in the model relative to the total uranium content we may now discuss any single component, and include, by implication, the combined amounts of uranium, thorium and potassium.

It remains to select the uranium concentration in the basalt and in the model planet. Although MacDonald (1959, 1964) has shown that a measurement of the present heat flow does not provide adequate constraints to uniquely determine both the concentration and vertical distribution of heat sources within a planet one can seek a distribution which is consistent with an initially uniform mantle differentiated through igneous activity alone.

Engel and Engel, (1964) have presented strong evidence for low potassium (and hence low uranium) tholeiites being by far the largest constituent of the basaltic crust in the deep oceans. As tholeiites average less than .2 per cent K if we assume that they have the normal K/U ratio of about 10^4 then the uranium concentration is less than .2 ppm. Uranium concentrations in dunites sampled at the earth's surface are normally very low. Tilton and Reed (1963) have presented analyses of five ultramafic rocks: three olivine nodules and two dunites. The mean uranium concentrations observed were 0.006 ppm, and the highest reported was 0.015 ppm (in a dunite from St. Paul's Rock). All these values are an order of magnitude

below the reported concentrations in low-uranium tholeiitic basalts and thus, in the simple approximation represented by our model, the assumption of all the heat sources localized in the low melting phase seems to be justified.

Only the ratio of basalt to dunite in the mixture remains to be estimated before proceeding with the calculations of the thermal history. One way to calculate the ratio is to determine what uranium content of the mixture is consistent with observed heat flow. Present terrestrial heat flow averages 6.3×10^{-6} watts per square centimeter (Lee, 1963). The area of an equivalent spherical earth is 5.1×10^{18} cm^2 and the mass of the combined crust and mantle is of the order of 4.0×10^{27} gm. (Birch, 1964). If we take the present rate of heat flow as an estimate of the present rate of heat production, the average heat production in the earth is 8.0×10^{-15} watts/gm.

From equation (2.12-5) it can be seen that the present rate of heat production from a rock with terrestrial isotope ratios is about 2.29×10^{-7} watts per gram of uranium present. Thus the uranium concentration in a mixture producing 8.0×10^{-15} watts/gm is .035 ppm. Figure 2.12-1 shows the relationship between concentration of uranium in basalt and the concentration of uranium in the mixture, for a number of basalt to dunite ratios. The intersection between the 0.035 ppm uranium in the mixture and the 0.2 ppm uranium in basalt lies at a basalt:dunite ratio of .21.

MacDonald (1964) has found that for the "terrestrial" isotope ratios observed values of terrestrial heat flow are consistent with uranium contents between .04 ppm and .05 ppm if the temperature at the time of formation were 1000°C. A content of .045 ppm corresponds to a basalt to dunite ratio around .30. Thus, mantle compositions estimated from the heat flow data lie well within the range of Ringwood's models and well within the accuracy required for our analyses.

There is another possible source of error which should be mentioned. From the phase relationships to be discussed below it is apparent that the alkalis will be concentrated in the first melting material which, assuming a constant K/U ratio, will result in a relative enrichment of heat producing isotopes in the melt fraction. If part of the basalt is left behind in the mantle it may be depleted in the heat producing isotopes

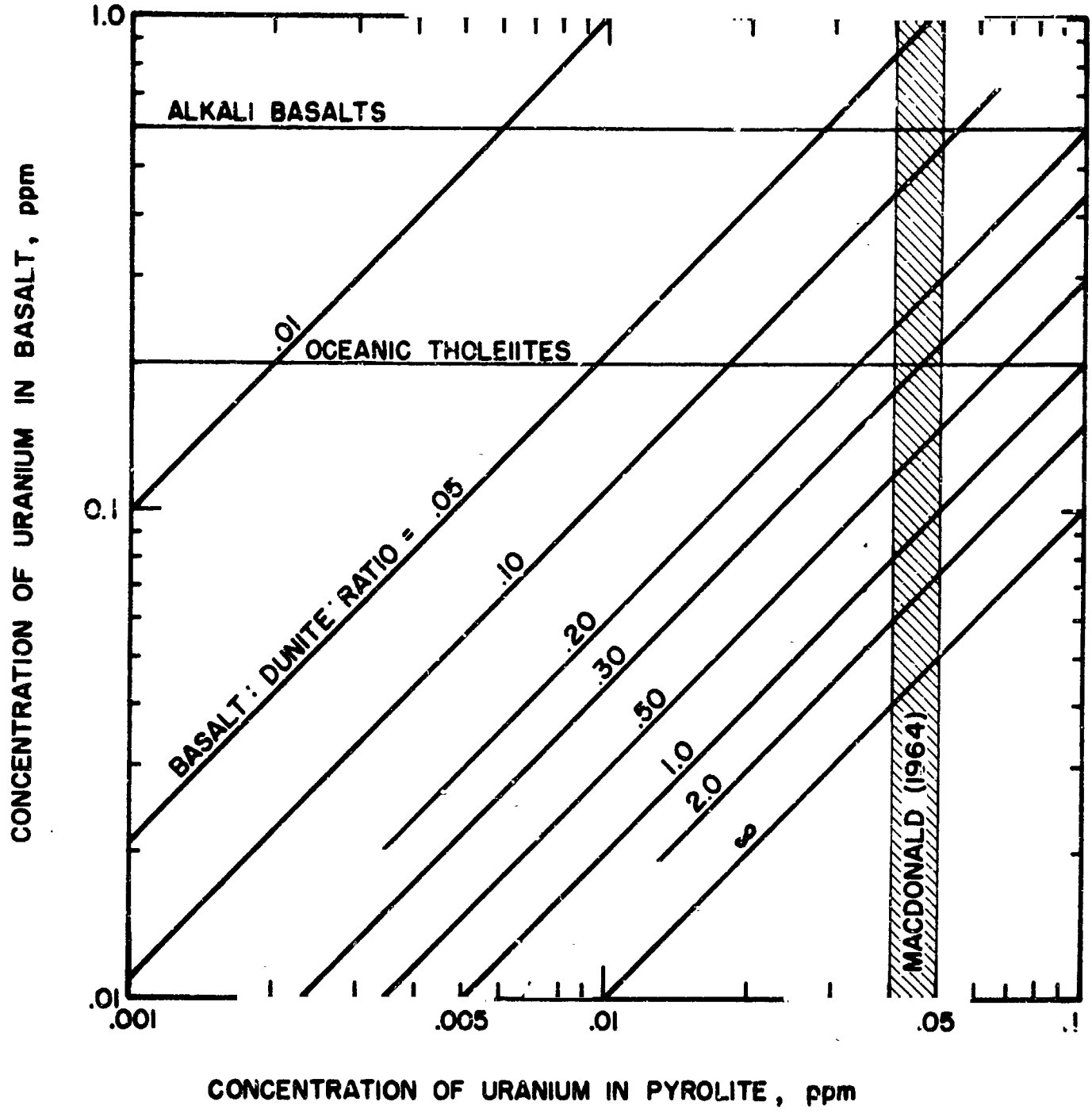

FIGURE 2.12-1 Relationship between concentration of uranium in basalt and concentration in pyrolite as a function of basalt to dunite ratio.

and the basalt sampled at the surface may be correspondingly enriched in these isotopes. Calculations based on the enriched basalt will result in an underestimate of the amount of basalt originally present. We shall neglect such possible underestimation in our theoretical analysis but if it were to occur it should not alter the findings of this study because only the mobile radioactive fraction of the basalt is significant in volcanism. Evidence that a great error in the estimate of the mobile fraction is unlikely may be obtained by comparing the thickness of the "basaltic" crust under the oceans with the apparent depth of magma sources. McConnell and McTaggert-Cowan (1963) have computed the arithmetic mean of the reported thicknesses of the crust under the ocean basin floors from 148 seismic refraction profiles as 9.05 km. This would represent the entire basalt content of about 40 km. of primary mantle material and is not inconsistent with reported depths of 60 km. for magma sources under Hawaii (Eaton and Murata, 1960) and the apparent beginning of the low velocity zone under the ocean around this depth (see for example Anderson, 1964).

2.13 Melting Behavior

To determine the melting behavior of the model composition we have studied the melting behavior of pyrolite-1:3 which is compositionally equivalent to one part of basalt to three parts of dunite. Should it become apparent, on the basis of other evidence, that a different ratio is more appropriate the analysis outlined below can be modified appropriately. Nevertheless, we believe that for small changes of this ratio the important qualitative aspects of the melting behavior will not be appreciably modified.

Recalculation of the composition of the pyrolite-1:3 in terms of moles/100 grams and mole percent are shown in Table 2.13-I. We shall first consider the melting behavior at atmospheric pressure and then estimate how this behavior is affected by changes in pressure and by the presence of water and other volatiles.

TABLE 2.13-I

COMPOSITION OF "PYROLITE"-1:3

Oxide	Wt. %	Moles/100 g.	Mole %
SiO_2	43.06	.718	37.7
MgO	39.32	.975	51.3
FeO	8.15	.113	5.94
Al_2O_3	3.99	.039	2.05
CaO	2.65	.047	2.47
Na_2O	0.61	.01	.525
Other	2.66	-	-

2.131 The Melting Curve of Pyrolite-1:3 at Atmospheric Pressure

To derive a melting curve for pyrolite from existing phase studies one must assume that the mineral assemblage to be melted was formed under equilibrium conditions, where the melting curve is identical to the crystallization curve. As data for six component systems involving the primary oxides in pyrolite-1:3 are not availab e the system must be further simplified by examining available phase diagrams containing the major constituents MgO and SiO_2 plus one or two of the other oxide components.

From the diagram of the MgO SiO_2-Al_2O_3 system (Levin, et al, 1964, Fig. 712) we can derive the crystallization curve (Figure 2.13-1) for a mixture of MgO-SiO_2-Al_2O_3 in the same ratio as in pyrolite; in effect we are then examining the behavior before the addition of the other components. While the melting point of pure forsterite (Mg_2SiO_4) is about 2170°K, in this system precipitation of forsterite commences at 2040°K and continues until the solution composition reaches the enstatite ($MgSiO_3$) boundary at about 1750°K. From this point on enstatite precipitates while forsterite redissolves until the ternary eutectic at 1640°K is reached, at which point a compound $2MgO.2Al_2O_3.5SiO_2$ commences to precipitate along with enstatite until the system becomes completely solid.

The MgO-FeO-SiO_2 system is presented as Figure 682 in Levin, et al. (1964). Again we may consider a system of the three oxides in the same proportions as in pyrolite. Both forsterite and enstatite can incorporate

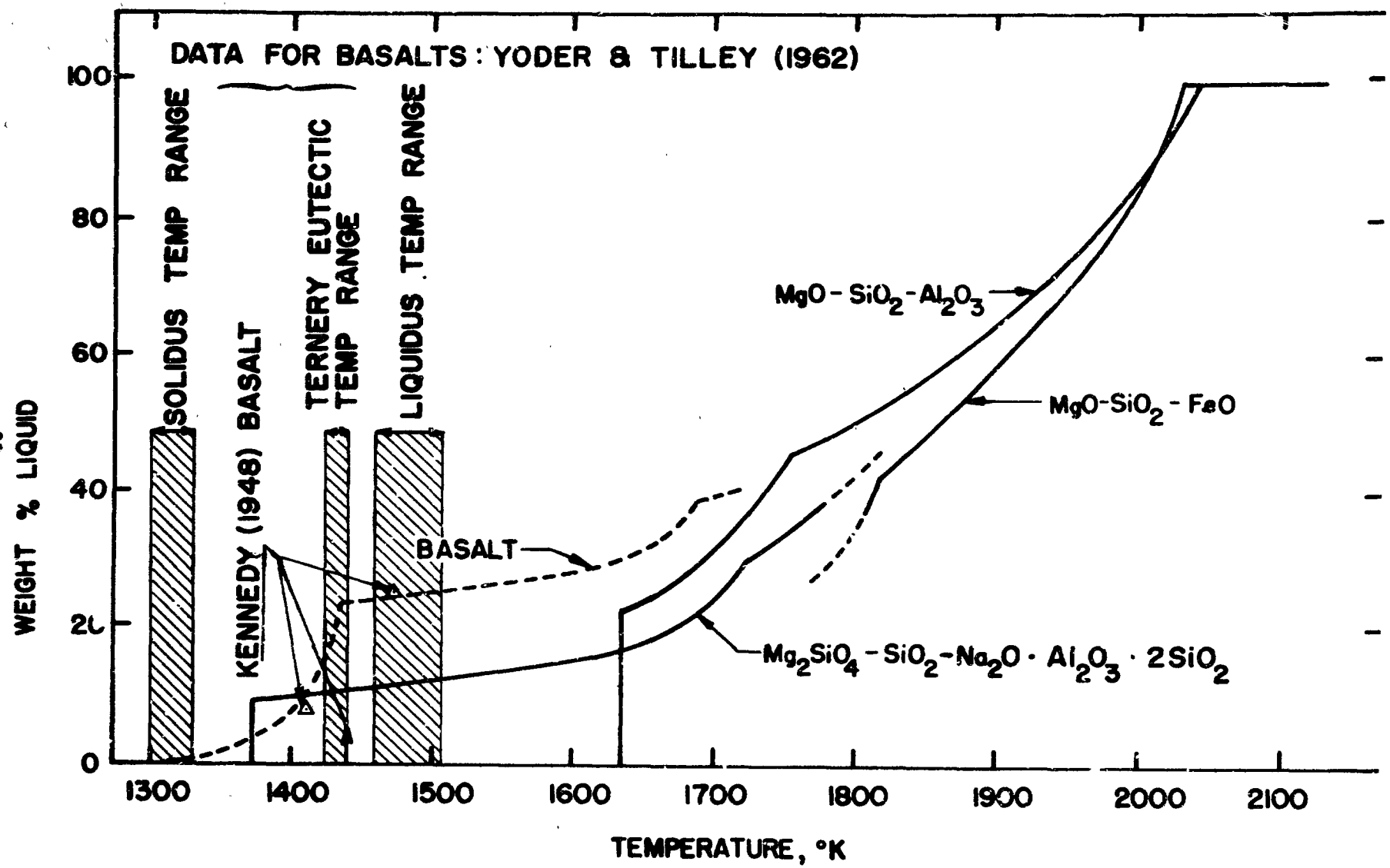

FIGURE 2.13-1 Melting curves for selected phase systems.

iron into their lattice structure in place of magnesium and these solid solutions are indicated on this phase diagram. This behavior makes it more difficult to completely represent all the necessary phase information on a single diagram. However, in conjunction with Figure 683 of the same reference, which presents tie lines at specific temperatures, we can derive a crystallization curve over the temperature range where the ortho-silicate (olivine) phase is precipitating. The phase diagram indicates that precipitation commences at about 2040°K and that crystallization follows the path indicated on our Figure 2.13-1 until about 1820°K when the metasilicate (pyroxene) phase commences to precipitate. The olivine phase precipitates initially at about a 1:11 ratio of Fe:Mg. As in the previous system, when pyroxene commences to precipitate, olivine will redissolve, but if equilibrium is maintained between the solid and the solution the remaining olivine will gradually increase its iron content as the liquid composition changes along the olivine-pyroxene boundary line.

A plane from the four component system $MgO-SiO_2Al_2O_3-Na_2O$ is also shown in Levin et al. (1964, Figure 855). The three components of the resulting ternary system are forsterite (Mg_2SiO_4), silica (SiO_2), and carnegeite ($Na_2O.Al_2O_3.2SiO_2$). To examine the behavior of this system we will calculate the quantity of forsterite based on the moles of MgO and FeO in pyrolite, the moles of carnegeite based on the Al_2O_3 content of pyrolite, and the moles of silica based on the moles of SiO_2 in pyrolite remaining after the forsterite and carnegeite compositions have been satisfied. This crystallization curve is also shown in our Figure 2.13-1. From the published isotherms the highest point of the curve which can be determined is 1770°K. Again, in this case, the olivine precipitates first, pyroxene precipitation commences at about 1720°K and continues while olivine redissolves. A ternary eutectic is reached at about 1370°K at which temperature albite ($Na_2O.Al_2O_3.6SiO_2$) begins to precipitate and crystallization is completed.

We believe that the examination of the above three systems provides a good indication of the general form of the crystallization (or melting) curve to be expected of pyrolite. The mineral assemblage to be expected in the earth's mantle, if it is composed of pyrolite, has been discussed in considerable detail by Ringwood (1962,1963). At low pressures and at

temperatures near the melting range, such as those discussed above, the minerals to be expected are olivine, pyroxene, and plagioclase. In all three systems examined above the olivine precipitates first, followed later by pyroxene together with re-solution of olivine. In the third system, the albite, the third solid present at the ternary eutectic, is the low temperature melting point component of plagioclase. Thus, we believe the shape and the temperature ranges covered by crystallization curves for these three component systems provide good evidence of the behavior of the multi-component system pyrolite.

More detailed consideration of the temperature of initial precipitation in the multi-component system is now required. In the first two systems considered the melting point of forsterite was changed about the same amount by considerably different quantities of FeO and Al_2O_3. In addition, iron is incorporated in solid solution in one case whereas Al_2O_3 is not. Some way of estimating the combined effect of the FeO, Al_2O_3, CaO and Na_2O is therefore needed.

For an ideal solution the liquidus curve near the melting point of the solute may be calculated from

$$\ln X_s = \frac{\ell}{R}\left(\frac{1}{T_m} - \frac{1}{T}\right) \qquad (2.13\text{-}1)$$

where X_s is the mole fraction of solute

R is the gas constant

ℓ is the heat of fusion

T_m is the melting temperature.

The liquidus curve for a non-ideal solution can be fitted with this equation, to a first approximation, by changing the value of ℓ. We will attempt to use an equation of the form

$$\log(X^2_{MgO} \cdot X_{SiO_2}/.148) = Q\left(\frac{1}{T_m} - \frac{1}{T}\right). \qquad (2.13\text{-}2)$$

To estimate the combined effect of the various components in our system the product $X^2_{MgO} \cdot X_{SiO_2}$ is an attempt to take into consideration the fact that in the solution the chemical potentials μ are related by

$$\mu_{forsterite} = 2\mu_{MgO} + \mu_{SiO_2}. \qquad (2.13\text{-}3)$$

Table 2.13-II shows calculated Q values for various "binary systems". Although Item 5 in the table indicates a very low Q value for the system forsterite - albite we find values in systems containing potassium and lithium listed as Items 6 and 7 which are more in line with other values. Results for the system listed as Item 8 seems to indicate that the low value in 5 is not due to an interaction effect of Na + Al. Based on these considerations we choose to adopt a Q value for FeO of 9.4 and an average Q value of 4.6 for the Na_2O, CaO, Al_2O_3. From these Q values we can calculate an effective value for the multi-component mixture, based on the relative mole fractions of the various oxides, to use to estimate the temperature of initial precipitation in the mixture.

$$Q_{effective} = \frac{.113}{.209} \times 9.4 + \frac{.087}{.209} \times 4.6$$

$$= 7.$$

Although the calculation using this Q value suggests that olivine precipitation will begin at 2050°K in the multi-component system this value is above the values shown in Figure 2.13-1 as obtained from the ternary system.

If we calculate Q values for the ternary systems we obtain the results shown in Items 9 and 10 of Table 2.13-II. The Q value obtained for $MgO-SiO_2-FeO$ is not as high as that calculated in Item 3. Figure 2.13-2 shows the data of Table 2.13-II in the form of average curves for the effect of FeO, Al_2O_3, and alkali metals on the crystallization temperature. The variation in the predicted crystallization temperature ranges from 2005 to 2060°K. From a consideration of these data and the previous calculations it appears that 2040°K ± 20 would be our best estimate of the temperature of initial crystallization of pyrolite.

We should now consider what more is known about the lower end of the melting curve. In pyrolite basalt would be expected to represent the low melting fraction. Figure 2.13-1 shows the ranges observed by Yoder and Tilley (1962) for the liquidus temperature, the solidus temperature, and the ternary eutectic temperature of several basalts. Yoder and Tilley also present the results of Kennedy (1948) in Table VIII of their paper. He reports a point for 70% solid at 1413°K with the first silicate appearing at 1470°K. These points are transcribed to Figure 2.13-1 assuming that

TABLE 2.13-II

"Q" VALUES CALCULATED FROM PHASE DIAGRAMS

	System	T(°K)	$T^{-1}(°K^{-1})$	$\log(X^2_{MgO}X_{SiO_2}/.148)$	$(T_m^{-1}-T^{-1})$	Q
1.	Mg_2SiO_4	2168	.463	-	-	-
2.	Mg_2SiO_4-Al_2O_3 (712)*	2073	.483	-.102	-.020	5.1
3.	Mg_2SiO_4-Fe_2SiO_4 (687)	2133	.470	-.066	-.007	9.4
4.	Mg_2SiO_4-$CaMgSiO_4$ (598)	2073	.484	-.088	-.021	4.2
5.	Mg_2SiO_4-$Na_2O.Al_2O_3.6SiO_2$ (856)	2073	.484	-.018	-.021	~1
6.	Mg_2SiO_4-$K_2O.2SiO_2$ (399)	2073	.484	-.098	-.021	4.7
7.	Mg_2SiO_4-Li_2SiO_3 (443)	2073	.484	-.095	-.021	4.5
8.	Mg_2SiO_4-$K_2O.Al_2O_3.4SiO_2$ (811)	1873	.534	-.412	-.071	5.8
9.	MgO-SiO_2-Al_2O_3 (712)	2043	.490	-.154	-.027	5.7
10.	MgO-SiO_2-FeO (682)	2038	.492	-.215	-.029	7.4

* Numbers in parentheses refer to Figures in Levin, et.al.(1964)

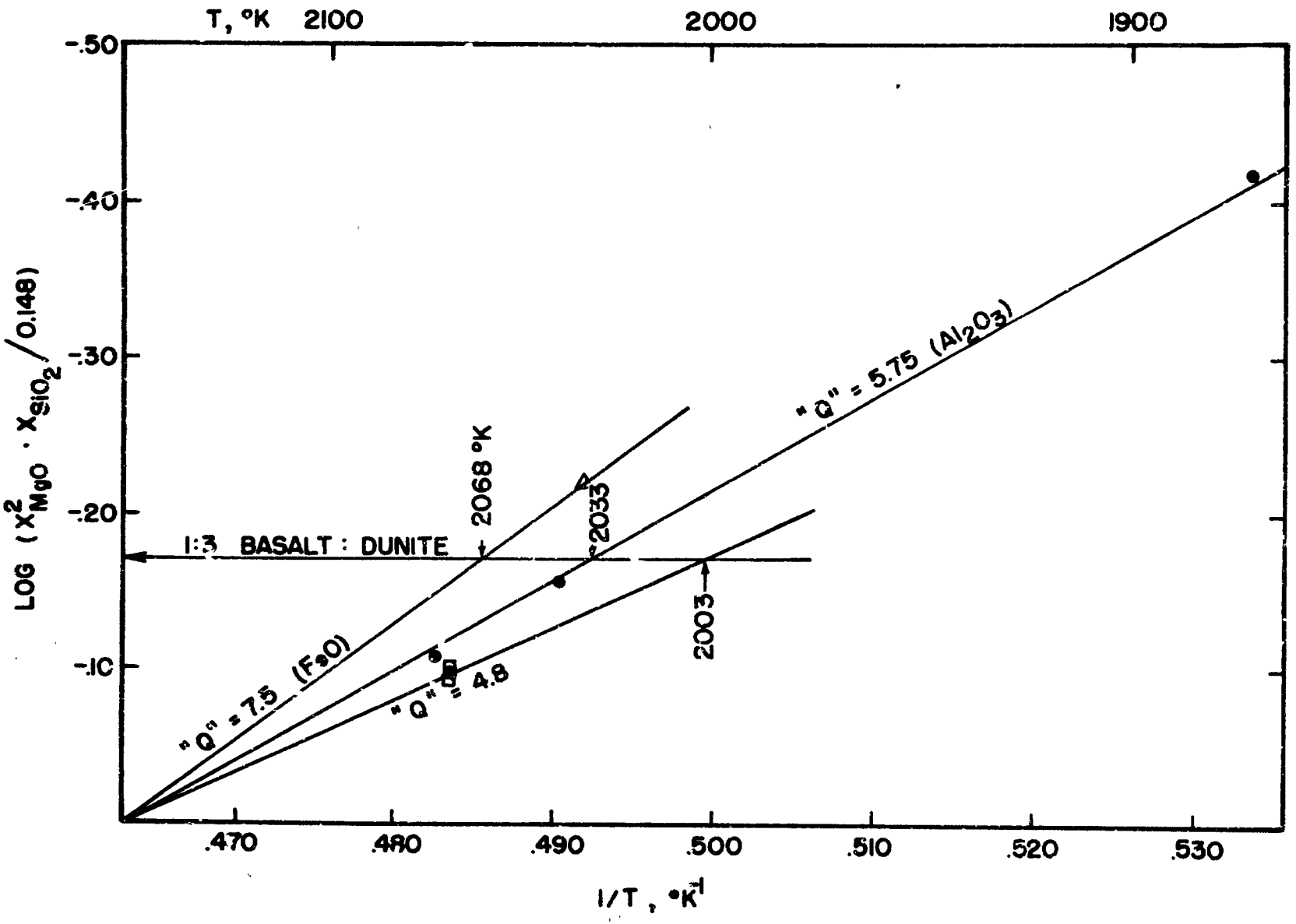

FIGURE 2.13-2 "Q" values calculated from phase diagrams.

basalt represents 25 percent of pyrolite. The temperature at which Kennedy reported both plagioclase and pyroxene were first present agrees well with Yoder and Tilley's results and is indicated by an arrow on the diagram. On the basis of these data for basalts the probable crystallization curve of basalt is drawn on Figure 2.13-1. This curve will also represent the final crystallization behavior to be expected of pyrolite.

Figure 2.13-3 shows a tetrahedron construction for the system diopside-forsterite-albite-anorthite after Yoder and Tilley (1962) which can be used to visualize pyrolite crystallization behavior. The pyrolite composition represents a point within the forsterite phase volume. On cooling, the olivine (forsterite) precipitates and the liquid composition moves toward the diopside-forsterite plane; when this plane is reached the pyroxene (diopside) commences to precipitate. The solution composition then moves along the plane until the line between the diopside-forsterite-plagioclase volumes is reached at which point plagioclase commences to precipitate. The liquid composition then moves along this line towards the albite corner of the tetrahedron with continuously changing composition of plagioclase until complete crystallization is achieved.

On the basis of all of the information presented above we predict a melting curve for pyrolite-1:3 at one atmosphere as shown on Figure 2.13-4.

2.132 The effect of Pressure on the Melting Curve

The effect of pressure on minerals and mineral mixtures leading to reactions, phase transitions, and changes in melting point is an active research area at this time (Boyd, 1964). While the limit of pressure explored in most studies of minerals has been about 50 kilobars lower than that in most of the earth's mantle, it is comparable to the pressure at the center of the moon.

The effect of pressure on the melting points have been determined for forsterite (Davis and England, 1964), enstatite (Boyd, et al, 1964), diopside and albite (Boyd and England, 1963). Of the data for forsterite, diopside and albite plotted in Figure 2.13-5 only that for forsterite has an essentially constant slope over the range of study. Davis and England in discussion of their data on forsterite believe the following qualitative conclusions can be drawn:

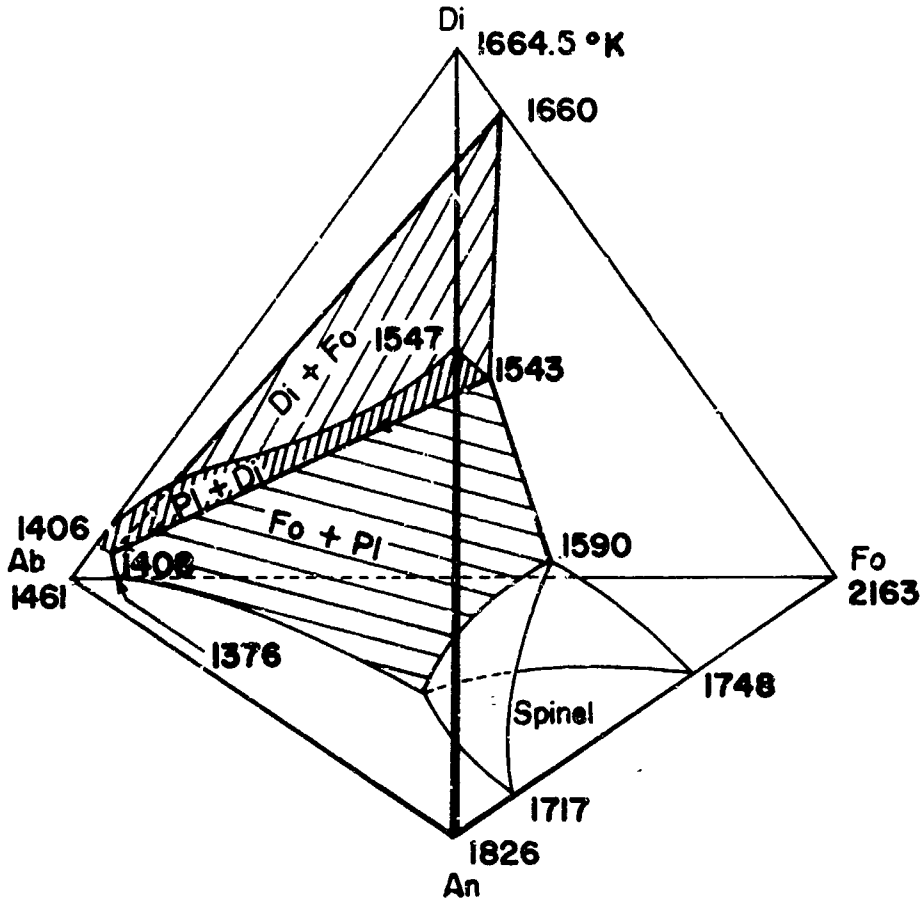

FIGURE 2.13-3 The diopside-forsterite-albite-anorthite system (after Yoder and Tilley, 1962).

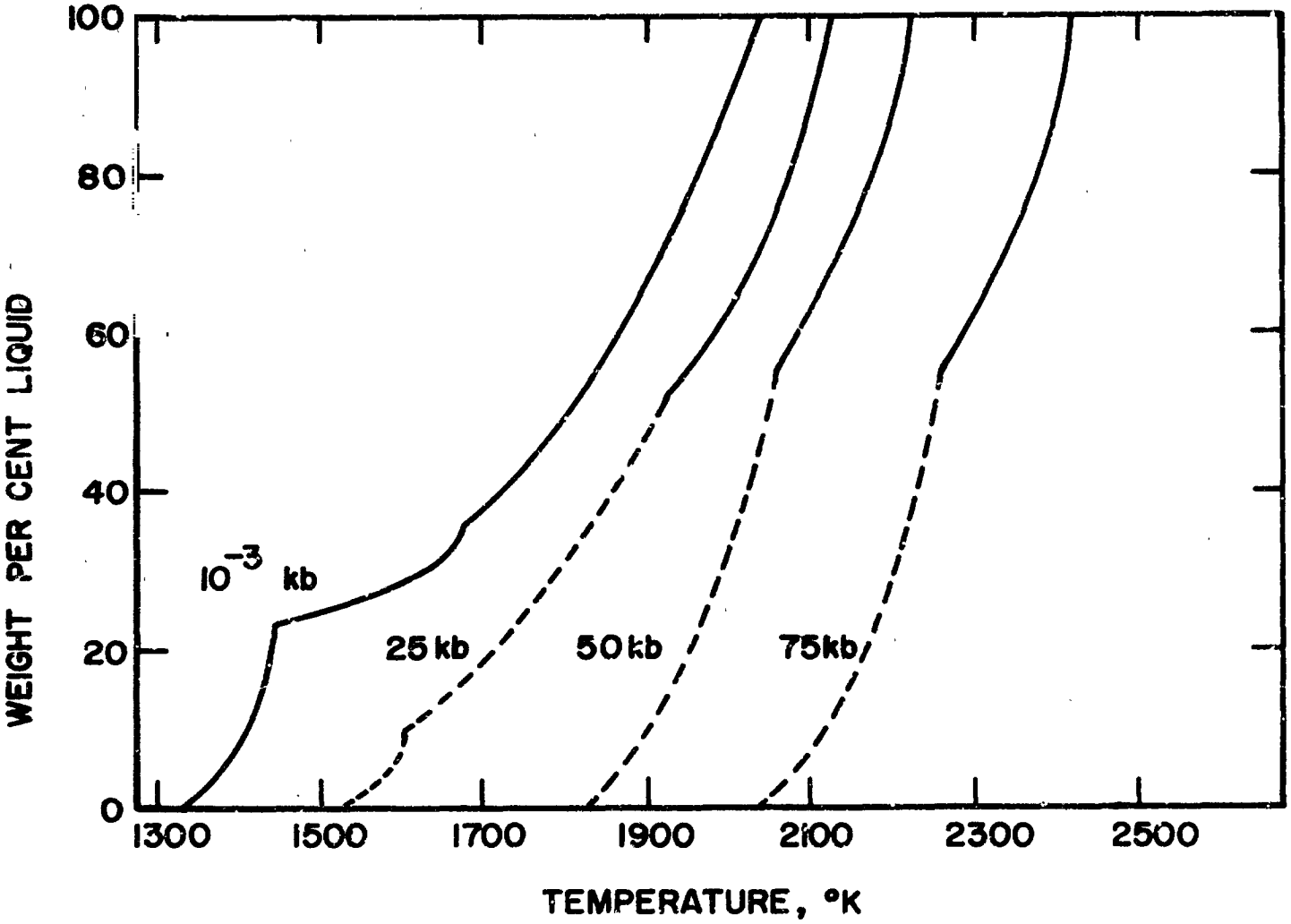

FIGURE 2.13-4 Predicted melting curves for pyrolite-1:3 at selected pressures.

"Because dT/dP of forsterite is much smaller than the initial dT/dP of any other silicate yet determined, eutectics in systems having forsterite as a component should shift toward Mg_2SiO_4 with the application of pressure; however, the approach of most silicate melting curves to dT/dP = 6 degrees per kilobar at 30 kilobars should confine this effect to lower pressures."

Forsterite behavior can be taken as equivalent to that of the olivine phase of pyrolite while diopside behavior can be taken as equivalent to that of the pyroxene phase. Thus the above comment of Davis and England, together with the dT/dP data for forsterite, can be used to indicate the effect of pressure on the upper portion of our melting curve for pyrolite.

The effect of pressure on the lower portion of the melting point curve is more obscure. Yoder and Tilley (1962) have studied the melting behavior of several basalts and eclogites at pressures up to 40 kilobars; the melting range and the basalt to eclogite transformation range reported by them are also indicated on Figure 2.13-5. The slope of the basalt melting curve in the lower pressure region is much less than that in the same pressure range observed for albite or diopside. This is surprising since one would expect the pyroxene and plagioclase components of the basalt to behave like diopside and albite. Ringwood (1962) discusses the experimental knowledge of the effect of pressure on the melting point of liquidus minima in terms of an entropy of mixing effect which would tend to decrease the dT/dP slope of the mixture as compared to the slopes for the pure components. This idea is based on a paper of Newton et al (1962) who invoked the entropy of mixing to explain the observed slower rate of change of the eutectic melting point with pressure in the Na-K system. For that system the effect can be significant because the entropy of fusion of sodium or potassium is about 1.7 e.u., approximately the same magnitude as expected for a mixing effect. However, the entropies of fusion of the silicate minerals appear to be on the order of 10-14 e.u. so any mixing effect should have very little effect on the melting curve of the eutectic.

It seems more likely that the lower dT/dP rate is attributable to shifts in the phase equilibria of the systems with pressure. Neufville, Clark and Schairer (1962) have studied phase relationships in the system

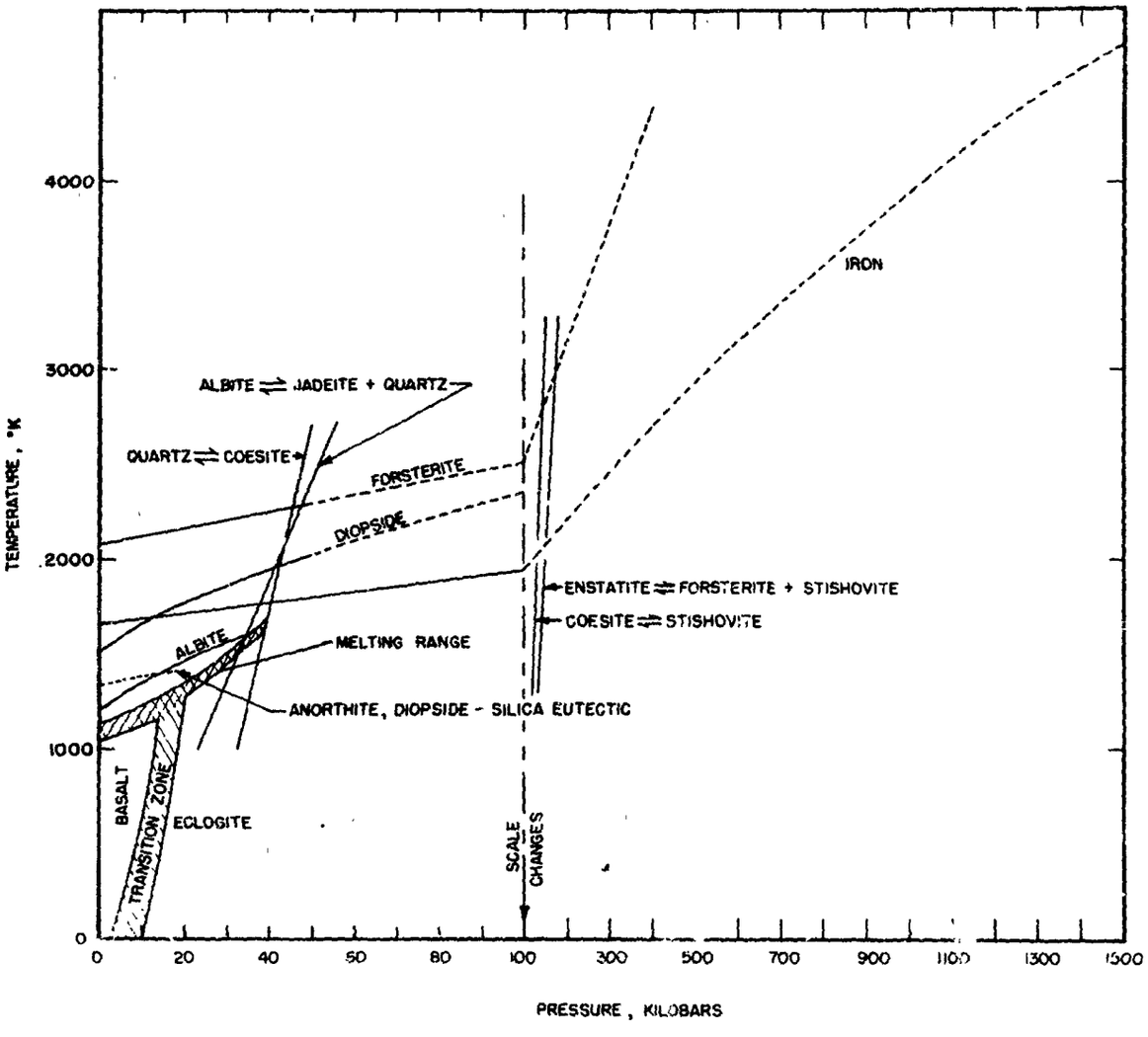

FIGURE 2.13-5 Melting temperatures as a function of pressure for various minerals and rocks.

diopside-anorthite-silica at one atmosphere and at 20 kilobars total pressure. They find that the system is complicated by the incongruent melting of anorthite at 20 kilobars and that there is a considerable shift in the composition of the eutectic and an increase in melting point of the eutectic of about 100° from the value of 1495°K at one atmosphere. Their conclusions would indicate that for a mixture like pyrolite one can expect that the Al_2O_3 content of liquids forming by partial fusion of the same parent material should increase as a function of depth up to pressures at which plagioclase disappears from the liquidus.

Considerable change with pressure can be expected in the solid solution range of minerals anticipated in pyrolite. Boyd and England (1960) have measured the solubility of alumina in enstatite at 1670°K and 18.2 kilobars. They find that under these conditions from 14-19 percent Al_2O_3 will be dissolved. Clark and Neufville (1962) have reported finding continuous solid solution between diopside and $CaAl_2SiO_6$ at 20 kilobars indicating that the ability of diopside to accept Al_2O_3 in solid solution is more pronounced than the analogous behavior of enstatite mentioned above. It has also been established that albite is transformed to jadeite and quartz with increasing pressure (Birch and LeComte, 1960); the P-T line for this transformation is shown on Figure 2.13-5 somewhat higher than the basalt-eclogite transition reported by Yoder and Tilley (1962). Recent work by Boyd and England (1964) indicates that at still greater pressures high alumina content pyroxenes tend to break down into garnet and lower alumina content pyroxenes.

From these data it appears that the olivine-pyroxene-plagioclase assemblage characteristic of pyrolite at one atmosphere will gradually change with increasing pressure to an olivine-pyroxene mixture possibly containing some garnet. Because of changes in solid solution range it could be extremely misleading to think that the observed solidus behavior of basalt, eclogite, or the anorthite-diopside-silica system would represent that of pyrolite. One can understand why this may be so if one recognizes that the changing solid solution range of the pyroxene mineral means a changing distribution ratio between solid and liquid for components such as Al_2O_3 and thus the composition of the liquid at equilibrium can depend on such factors as the relative ratio of pyroxene mineral to plagioclase mineral in the initial composition.

It does not appear from the literature we have reviewed that there is any firm basis for predicting the change in initial melting behavior of pyrolite with increasing pressure. It is conceivable that the initial melting point curve may not vary smoothly with increasing pressure but may have maxima and minima as the number and composition of the phases present at equilibrium changes.

Figure 2.13-4 presents our best estimate of changes in melting point curves at 25 and 50 kilobars. The one atmosphere curve was discussed earlier. As pressure is increased from one atmosphere to 25 kilobars the melting point of the pyroxene phase will increase more rapidly than that of the olivine, thus the phase boundary between the two will be reached at a higher relative temperature as indicated by the higher break in the melting curve. The solid solution range of the pyroxene phase increases at the same time and much less plagioclase phase would be expected. This has been indicated by a lowering of the lower break in the melting curve. For pressures of 50 kilobars we have drawn a melting curve showing complete disappearance of the plagioclase phase and no change in relative position of the olivine-pyroxene phase boundary. Our present understanding is that the volume of any garnet phase which may be formed at these high pressures will probably be very small and we have chosen to ignore it.

In the absence of any definite knowledge as to the behavior of the initial melting point of pyrolite with increasing pressure these curves for 25 and 50 kilobars have been drawn showing some decrease in absolute temperature interval for complete melting on the basis of the behavior of eclogite reported by Yoder and Tilley.

Although pressures above fifty kilobars are not normally expected on the moon it is important to consider the melting behavior at these pressures in order to make comparisons with the earth. Pyroxene and olivine will likely remain the dominant phases to pressures above 100 kilobars and in Figure 2.13-4 we have indicated no change in the relative melting curve predicted for 50 and 100 kilobars. In Figure 2.13-5 we have shown the P-T boundary curves for the recognized transformations of coesite to stishovite and enstatite to forsterite + stishovite at pressures above 100 kilobars.

Ringwood (1962) has discussed a possible series of polymorphic transitions between 400 and 1000 kilometers which can result in a continuous increase in density. He proposes that these transitions lead eventually to a breakdown into a mixture of simple oxides of the elements. One should remember, however, that much remains to be learned about the behavior of these minerals at such high pressures and that other sequences of reactions providing increased densities may be recognized as our knowledge increases. We, therefore, see no basis at this time for attempting to predict a melting curve in this pressure range.

While we cannot logically extrapolate the melting point curve of minerals such as forsterite, because of possible polymorphic changes or reactions, an extrapolation of existing pressure-temperature data for iron would appear to be more reasonable (Gilvarry, 1956). Not only would a knowledge of the iron behavior yield estimates of the temperature in the earth's core, but it would provide a strong constraint on speculations as to why the moon does not also have a core.

Figure 2.13-5 shows the iron melting behavior as reported by Bundy and Strong (1962). From these curves it would appear that at pressures greater than 50 kilobars iron melts at a lower temperature than basalt, but in the moon where lower pressures prevail it would always melt at a higher temperature than basalt. If the temperature of the moon is never above that necessary for formation and extrusion of a basalt magma, any free iron which may be present can be included as part of the higher melting component. Extrapolation of Bundy and Strong's data to very high pressures would indicate a temperature at the earth's core-mantle boundary of at least 4500°K. However, Sterrett, et al (1965) have presented fairly convincing arguments for questioning the reported uncertainties of the temperature and pressure values on which such extrapolations are based.

2.133 The Effect of Aqueous Atmospheres on the Melting Curve

Our only direct evidence for water content in the pyrolite comes from measurements of water content of basalts and from the relative mass of the hydrosphere and crust. Jacobs, et al (1959) give estimates for the volume of the solid crust of 8.3×10^{24} cm^3 and for the hydrosphere of 1.4×10^{24} cm^3. The hydrosphere thus makes up roughly 5 weight percent of the total crust. If all of the material above the mantle has originated from a primary basaltic magma then this magma would have to contain at least 5 percent water. In contrast to the above argument, analyses of most basalts show a water content of the order of one percent or less by weight. If these values are more representative of the average water content of basalt they would seem to imply that not all of the earth's hydrosphere is a product of igneous activity as we know it today. For reasons discussed in Chapter 3 we believe that the latter alternative is more consistent with the available data and that the water content of basalts probably represents equilibrium water pressures on the order of half a kilobar or less.

Experimental studies of basalt have shown that high partial pressures of water have a marked effect on its melting behavior. In summarizing their results, Yoder and Tilley (1962, Figure 29) show that by increasing the water pressure from atmospheric to 10 kilobars the liquidus temperature is decreased from 1510 to 1360°K and that the melting range is more than doubled extending to 870°K. The stable phases and the order of appearance also changes. Amphibole is stabilized by high water pressures and may become the first silicate to appear at water pressures slightly above 10 kilobars. In the presence of excess of water the basalt composition is represented at relatively low temperatures by amphibolite or hornblende gabbro.

Markedly different results are obtained when water pressure is less than total pressure. Yoder and Tilley summarize their data on this behavior in their Figure 34. The liquidus temperature for the basalts under anhydrous conditions is increased about 6° per kilobar or about 60° for 10 kilobars total pressure. Recall that under 10 kilobars water pressure the liquidus temperature is reduced by about 150° from that at 1 bar, representing about 220° below 10 kilobar pressure without water. Now when water pressure is 7 kilobars out of 10 total the liquidus temperature is only reduced about

50° below that for the same total pressure without water. At the same time the effect of increasing pressure at constant partial pressure of water is to decrease the stability range of amphibole.

These observations are quite important. If the water content of a typical basalt does represent equilibrium water pressures on the order of one kilobar or less as we believe, then, when pressures are 10 kilobars or greater we find from Yoder and Tilley's work that the liquidus curve is little affected by this quantity of water. We shall assume similar behavior for the solidus.

2.134 Behavior Pattern Indicated for the Model

The anticipated melting behavior for pyrolite at pressures of 1 bar and 25, 50, 100 kilobars is sketched in Figure 2.13-4. The major assumption in developing the curve at one atmosphere is that total composition is equivalent to 25% basalt and 75% dunite. This assumption is used to position the experimental data on basalt with respect to the remainder of the curve.

If we had assumed that basalt represented a lower fraction of the total mantle composition, the predicted melting curve would change in the following manner. Since the total composition would now contain more olivine and pyroxene the first solid would appear at a slightly higher temperature. We would still predict the initial precipitation of olivine followed by pyroxene. The largest change would be observed in the low temperature portion of the curve. The behavior of the initial melting (basalt) fraction would now be compressed along the "weight % liquid" scale with no change in the temperature positioning of the ternary eutectic or solidus.

In Figure 2.13-4 the liquidus temperature is increased with pressure proportional to the behavior reported for pure forsterite. This is more readily seen on Figure 2.13-6. The solidus temperature variation with pressure is less certain. The values selected are based on the experimental behavior discussed for basalt, eclogite, and the diopside-anorthite-silica system.

At one atmosphere the principal mineral phases are olivine, pyroxene, and plagioclase. The experimental evidence discussed on page three indicates that plagioclase will tend to disappear with formation of more pyroxene phase as pressure increases. We show complete disappearance between 25 and 50 kilobars in Figure 2.13-4, but this is quite uncertain. Complete disappearance below 25 kilobars may be possible.

Above 100 kilobars the behavior is quite speculative at this time and we have not felt that further extension of these curves was warranted. If necessary a linear extrapolation parallel to the predicted behavior of forsterite is probably the best course while maintaining the absolute temperature range of melting constant.

If we are to select a discrete melting temperature for use in the computer simulation it seems to us to be most logical to choose that temperature where the basalt fraction of the mixture (25 percent in pyrolite-1:3) is molten. While at first glance this might appear to be too drastic an oversimplification it is not only in line with our policy of using the simplest possible model consistent with observations but it seems to be the only assumption which would always produce basalt melts from the earth's mantle. A third advantage of this choice is that it allows us to define a single melting temperature at each pressure by imposing the constraint that the melt fraction remains constant as the pressure changes.

We have, therefore, selected the melting curve for basalt, shown in Figure 2.13-6, for use in the computer simulation of the evolution of the moon. This curve starts at 1500°K at atmospheric pressure and increases linearly at a rate of 11.0 degrees per kilobar up to the maximum pressures encountered in the moon's interior.

2.14 Heat of Fusion

The heat of fusion plays an important role as an energy reservoir both in the generation and crystallization of magma. In this section we review the state of our knowledge for heats of fusion of silicate minerals as a function of temperature and pressure in order to determine appropriate values for use in the theoretical analysis.

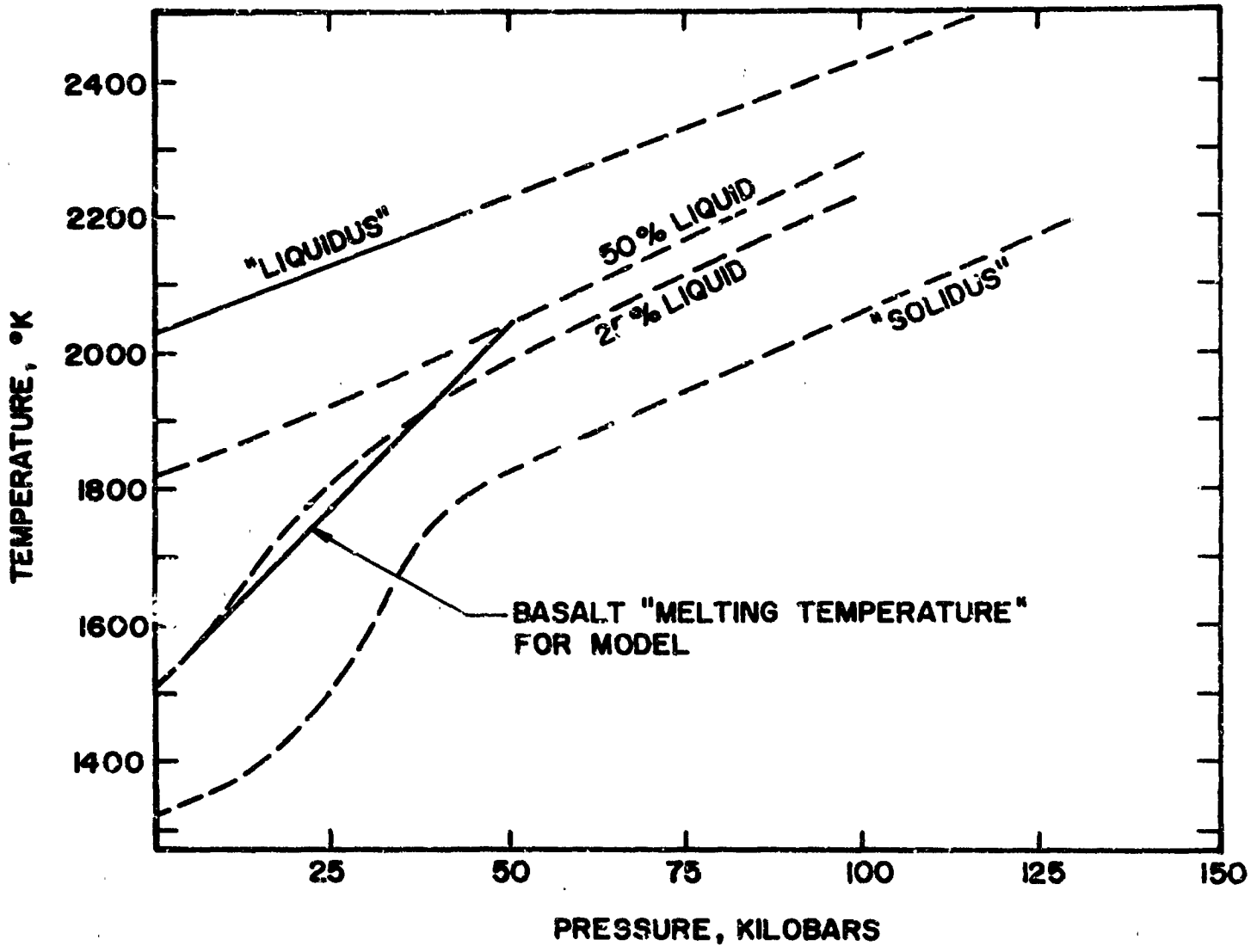

FIGURE 2.13-6 Postulated fractional melting behavior of pyrolite-1:3 as a function of temperature and pressure.

2.141 Heat of Fusion at Low Pressures

Heats of fusion are tabulated for many minerals but most are derived from the indicated freezing point lowering obtained in phase studies. MacDonald (1954) has pointed out that these values have very large uncertainties due to the generally low precision of the phase studies. In his review he presents data for four compounds which he considers to be good, including the only two calorimetric studies of which we are aware at this time. These data are presented in Table 2.14-I and represent a range of silicate composition.

Bradley (1962) has recently made some further calculations for the fayalite-forsterite system. By treating the system as an ionic solid and solution he derives heats of formation for fayalite and forsterite of 25,200 and 29,300 calories per mole respectively. These data are much higher than the values of about 14000-15000 previously calculated from the phase studies and are in much better agreement with the calorimetric value for fayalite given in Table 2.14-I and with our estimate for forsterite based on the entropy of fusion of fayalite.

TABLE 2.14-I

SOME EXPERIMENTAL HEATS AND ENTROPIES OF FUSION

Compound	T_m (°K)	ΔH of Fusion (cal/mole)	ΔS of Fusion (cal/mole-deg)	ΔH of Fusion (joules/gm)
Fe_2SiO_4 (fayalite)	1490	22,000±1000	14.8±0.6	453
Na_2SiO_3	1361	12,470±500	9.2±0.3	426
$NaAlSi_3O_8$ (albite)	1393	13,000±2000	9.3±1.5	208
$CaAl_2SiO_8$ (anorthite)	1823	18,000±3000	10.0±1.7	270

The entropy of fusion for inorganic compounds is not found to be as constant as the entropy of vaporization; however, it is generally the same for the same structural type of compound. Thus we can use the entropies calculated for the silicates listed in the first portion of Table 2.14-I to predict the heats of fusion for similar silicates. This is done for forsterite, enstatite and diopside in Table 2.14-II with due consideration for the structural relationships.

TABLE 2.14-II

SOME PREDICTED HEATS OF FUSION

Compound	T_m (°K)	ΔH of Fusion (cal/mole)	ΔH of Fusion (joules/gm)
Mg_2SiO_4 (forsterite)	2163	32,000	950
$MgSiO_3$ (enstatite)	(1830)	16,800	699
$CaMg(SiO_3)_2$ (Diopside)	1664	30,600	590
"Plagioclase"			225
"Pyroxene"			650
"Olivine"			900

The heat of fusion per gram of compound in joules is given in the last column of Table 2.14-I and 2.14-II. There is a greater than 4-fold difference in the values. Since pyrolite at atmospheric pressure can be considered to consist of three phases, (olivine, pyroxene, and plagioclase) we have shown estimated average values for the heat of fusion of each of these phases in the last section of Table 2.14-II. Plagioclase is a solid solution of albite plus some anorthite and we have chosen a value of about 225 joules per gram for this phase. The pyroxene phase may be considered as enstatite, diopside, and ferosilite; for this we have selected a value of 650 joules per gram. The olivine phase will be about 90%, forsterite-10%, fayalite giving an estimate of 900 joules per gram for this phase.

It is evident that one value per gram of pyrolite cannot be chosen. In addition, the estimation of a heat of fusion is further complicated by the different forms of melting behavior to be expected in different portions of the melting curve and the way in which these may change with pressure. For example, with reference to melting at one atmosphere, one would expect simultaneous melting of plagioclase (the primary phase melting) olivine, and pyroxene from the solidus to the ternary eutectic point (Figure 2.13-4). Melting of 25 percent of the pyrolite, a point reached slightly above the ternary eutectic, essentially represents the basalt fraction of pyrolite. Based on the relative proportions of the olivine, pyroxene, and plagioclase phases in basalt (Yoder and Tilley, 1962) we estimate an average heat of fusion for basalt of 450 joules per gram. In crystallization from the binary

to the ternary eutectic point at one atmosphere we expect the re-solution of olivine and precipitation of pyroxene to occur. Assuming the reverse to occur on melting the heat of fusion per gram of melt formed will fall well below that for pyroxene and may approach the heat of fusion of SiO_2 which is about 250 joules/gm. Above the binary eutectic only olivine will be melting and the heat of fusion will be 900 joules/gm.

2.142 The Effects of Pressure on the Heat of Fusion

There are two factors which must be considered when estimating the effects of pressure on the heat of fusion of pyrolite: changes in the heat of fusion of individual minerals, and changes in the mineral assemblage.

Bridgeman (1949) calculated the heat of fusion at pressures to 12 kilobars from the Clausius-Clapeyron equation utilizing experimental values for the change in volume at fusion and the change in melting point with pressure for some organic compounds. He found that in the majority of cases the latent heat increased by moderate amounts with pressure. We do not, however, have comparable data for the silicate minerals of interest. Another thermodynamic equation, first derived by Planck, relates the change in latent heat of fusion with changes in pressure and temperature along the melting curve. Consideration of this equation,

$$\frac{d\ell}{dT} = \Delta c_p + \frac{\ell}{T} - \ell\left(\frac{\partial(\ln \Delta v)}{\partial T}\right)_p$$

where ℓ is the latent heat of fusion

c_p is the specific heat at constant pressure

Δv is the change in specific volume

indicates that the major contribution to the change in latent heat as melting temperature increases with pressure is due to the second term. Integration and solution of this equation indicates increases in the latent heats of these silicate minerals on the order of only 10 percent at 50 kilobars. In effect this result shows that to a first approximation the entropy of fusion of the silicate minerals remains constant as pressure increases.

The effects of changes in the mineral assemblage with pressure appear to be much more significant. When pressure is increased the pyroxene phase changes from an incongruent to congruent melting behavior and, because

of differences in the relative change in melting point of olivine and pyroxene phases with pressure, we expect a considerable shift in the boundary curve between olivine and pyroxene phases. This will shift the binary eutectic point in our melting curve and may well change the melting behavior to be expected between the ternary and binary eutectic points to one of simultaneous melting of olivine and pyroxene. This would mean a heat of fusion per gram of melt formed of between 650 and 900 joules per gram. In addition we anticipate that the plagioclase phase will disappear at higher pressures resulting in an increase in the relative volume of pyroxene phase, probably with little change in the heat of fusion of the pyroxene phase. When and if both these changes occur the heat of fusion per gram from the solidus to the binary eutectic point will be somewhere between 650 and 900 joules per gram.

It is interesting to consider the consequences of the fact that we anticipace the presence of a point in the 15 to 30 kilobars pressure region at which a phase transition occurs over a few kilobar pressure interval representing the transformation of the high pressure pyrolite system consisting primarily of an olivine and pyroxene phase to the low pressure system consisting of plagioclase, olivine, and pyroxene. Now, if we assumed that the high pressure phase was partially melted (say 10%) when a sudden pressure release favored the transition, the result without any temperature exchange with the surroundings would be an approximate doubling of the liquid fraction of the pyrolite due to the changes in phase composition and their resultant heats of fusion. This would represent a simultaneous volume increase which might tend to further propagate any fracture which had allowed the sudden pressure release. In other words one might say that there is a certain pressure and temperature region in which pyrolite would react "explosively", i.e., with a sharp volume increase, to any pressure drop of a few kilobars. This type of behavior would seem to provide a sound theoretical basis for the popular hypothesis that magma generation results from a sudden decrease in pressure. As the mechanism involved is closely related to the problems of migration it is discussed in more detail in Chapter 3.

2.143 Heat of Fusion for the Model

From the above discussion it appears that the major uncertainty in choosing a heat of fusion arises not from changes in latent heat due to pressure but rather from changes in melting behavior associated with probable

pressure induced phase changes. Heats of fusion for melting the basalt fraction of pyrolite may range from 250 to 750 joules per gram depending on the pressure. We estimate that at one atmosphere the heat of fusion below the ternary eutectic is on the order of 300 joules per gram while that between the ternary and binary eutectic may be somewhat higher. At pressures above the transition zone, say 30 kilobars or greater, the heat of fusion below the binary is probably on the order of 750 joules per gram. Thus in any calculation where it plays a critical role a single value for the heat of fusion of the first quarter or similar fixed fraction of pyrolite independent of temperature and pressure cannot be recommended since a two-to three-fold change is expected with increase in pressure. On the other hand for those problems in which one value is sufficient 500 joules per gram would appear to be appropriate.

2.15 Specific Heats

A plot of specific heats for solids rises from low temperatures and tends to flatten out at high temperatures. Dulong and Petit's law states that the specific heat per gram atom for most elements is about 6.2 calories (26 joules) per degree at room temperature. This value increases further with temperature. Kubachewski and Evans (1957) point out that it may be taken as about 7.25 cal (30.3 joules) per degree at the first phase transition, frequently the melting point. The specific heats of compounds are frequently found approximately equal to the sum of the heats of the elements.

The specific heats of liquids do not differ greatly from those of their solid and a value of 7.25 cal (30.3 joules) per degree per gram atom may be used if experimental measurements are not available. Little is known about the temperature dependence for liquids and a constant value is usually estimated in the absence of experimental data. The effect of pressure is small (Partington, 1951).

Some specific heat values for appropriate minerals, glasses, and rocks are presented in Table 2.15-I, taken from Birch et al (1942). The data for diopside, albite, and fayalite are also plotted in Figure 2.15-1 and show clearly the trend with temperature. The glass data may be taken as representative of the cooled liquid and provide one measure of the very small differences between solid and liquid. We have also shown on Figure 2.15-1

more recent data on Mg_2SiO_4, Fe_2SiO_4, and $MgSiO_3$ taken from the tabulations of Kubachewski and Evans (1957). A tabulated value for liquid Fe_2SiO_4 is 10% greater than that for the solid at the melting point and is reported to be essentially constant for the temperature range studied (1490-1724°K). The olivine phase of pyrolite will represent about 90% Mg_2SiO_4 + 10% Fe_2SiO_4. A curve representing such a mixture can be visualized on Figure 2.15-1 as falling slightly below that for Mg_2SiO_4. The pyroxene phase will consist primarily of $MgSiO_3$ plus again a small amount of iron and calcium in place of magnesium. The diopside curve represents a 50-50 calcium-magnesium mixture. Again the curve for the pyroxene phase can be visualized as falling very close to that for $MgSiO_3$. The plagioclase phase consists of a solid solution of albite and anorthite but in the pyrolite will be primarily albite. A curve for albite is given on Figure 2.15-1. Combining these values we would postulate a specific heat curve for pyrolite as shown on the figure. We believe this curve should be accurate to within ± 5% and will be approximately linear from 800 to at least 1900°K.

For the numerical calculations we have chosen a single specific heat of 1.1 joules per gram to represent both liquid and solid over the entire temperature range of the planet. This value, which represents the average specific heat between 273° and 1500°K, may be in error by as much as ± 30 percent at any point within the range but it should yield estimates of the amount of heat necessary to raise the moon from its initial "cold" state to the predicted magma generation temperatures which are within 10 percent of the correct value.

2.16 Thermal Conductivity

Of all the thermal parameters which must be known to predict generation of magma on the moon the thermal conductivity is the most uncertain. Thermal conduction on a microscopic scale results from movement through the solid of various species which transport energy. Among the heat transporting species are: phonons (quantized lattice vibrations), free electrons (and/or holes), photons of radiation, and excitons. The fact that these species can travel only a finite distance before being scattered or absorbed results in a diffusional type process - if there were no scattering or absorption the thermal conductivity would be infinite.

TABLE 2.15-I

HEAT CAPACITY OF MINERALS AND ROCKS (joules/gm/°K)*

Temp (°K)	Pyroxene		Diopside		Wollastonite		Anorthite		Albite		Fayalite	Basalt	Gabbro
	xtl	Glass	xtl	Glass	xtl	Glass	xtl	Glass	xtl	Glass	xtl		
273	.752	.756	.69	.71	.67	.69	.70	.68	.709	.724	.55	.85	.72
473	1.03	1.02	.98	.98	.92	.92	.95	.96	.986	1.00	.79	1.04	.99
673	1.15	1.14	1.06	1.07	1.80	1.03	1.05	1.06	1.085	1.114	.91	1.14	1.10
1073			1.15		1.05		1.17		1.196	1.26	1.095	1.32	1.18
1473			1.20		1.10		1.27					1.49	

* Taken from Birch, et al (1942)

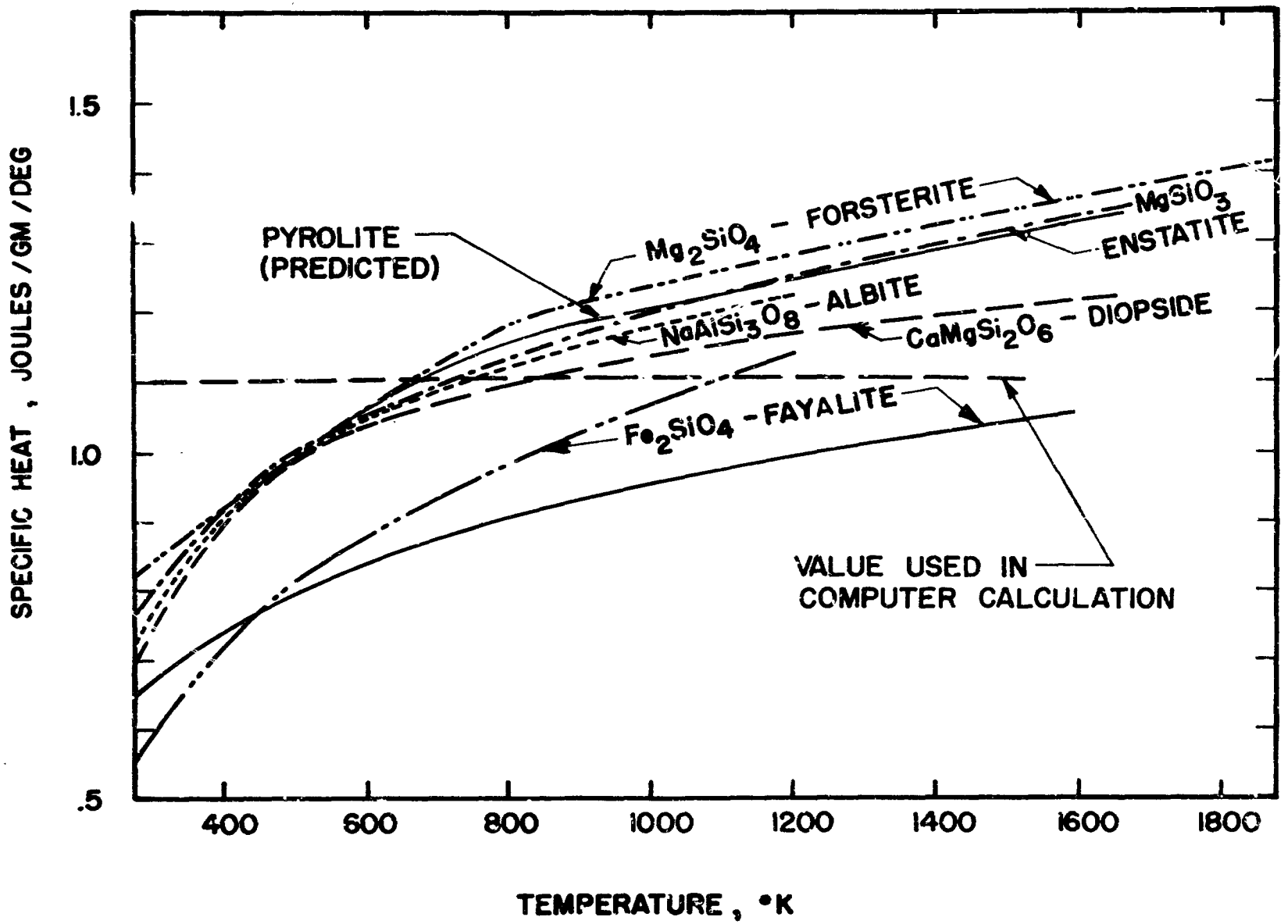

FIGURE 2.15-1 Specific heats as a function of temperature.

By considering the scattering and absorption mechanisms for each of the various species it is theoretically possible to determine the thermal conductivity, but the uncertainties are sufficiently great that at present one is often restricted to estimating limiting values.

If any one species is attenuated by several mechanisms the attenuation probabilities of the different mechanisms are additive; thus the total mean free path $\bar{\ell}$ resulting from the attenuation process for each species is given by

$$1/\bar{\ell} = 1/\bar{\ell}_1 + 1/\bar{\ell}_2 + 1/\bar{\ell}_3 + \ldots\ldots \qquad (2.16\text{-}1)$$

The most important attenuation mechanism is thus the one with the shortest mean free path. If any one $\bar{\ell}_i$ is very much smaller than the others the attenuation by the others does not contribute significantly to the total.

2.161 Phonon Conductivity

Most thermal conductivity measurements of rocks are made at atmospheric pressure and room temperature. At this temperature heat is primarily transported by ordinary lattice conduction; this may be considered either as the propagation of anharmonic lattice waves through a continuum or as the interaction between phonons (quanta of thermal energy).

Regarding the process as an interaction between phonons, for most solids satisfactory agreement between observation and theory may be obtained by writing the phonon conductivity k_p as

$$k_p = \frac{1}{3}\rho c v \bar{\ell}_p \qquad (2.16\text{-}2)$$

where ρ is the density

c is the specific heat

v is the velocity of phonons, which is essentially the velocity of sound in the material

$\bar{\ell}_p$ is an effective photon mean free path.

(See for example Lee and Kingery, 1960).

Above the Deybe temperature and at constant pressure the density, phonon velocity, and specific heat are relatively constant but the number of phonons increases, thus reducing their mean free path. The effective conductivity resulting from this process is inversely proportional to the

absolute temperature. Thus, the phonon conductivity above the Debye temperature may be estimated from

$$k_p = k_p(T_o) \times T_o/T \qquad (2.16\text{-}3)$$

As the phonon scattering is due to anharmonic terms in the lattice potential, a finite limit is placed on the length of the mean free path by the interatomic distances. When the temperature approaches the melting temperature the effective mean free path and hence the conductivity, is observed to approach a constant. Estimates of effective phonon mean free paths for silicate glasses using equation (2.16-1) and observed thermal conductivities yield values of about 7Å, approximately the dimension of a silica tetrahedron (see for example Kittel, 1956).

Other factors such as impurities and departures from stoichiometry have been observed to affect the phonon conductivity in simple systems at low temperatures. For our purposes they would appear to be irrelevant because the concept of impurity is no longer valid in the complex systems with which we are concerned. At the temperatures to be expected in the interior of the moon, such scattering would also be dwarfed by other scattering mechanisms.

Kingery et al (1954) have measured the phonon conductivity of forsterite. Their results which show clearly the temperature dependence of this type of conductivity are reproduced in Figure 2.16-1.

Little work has been done relating changes in thermal conductivity to the effects of high pressure on the dynamics of the crystal lattice. Lawson (1957) showed agreement between Bridgeman's (1945) results and the expression

$$k_p = A_o/3\gamma^2 T\kappa^{3/2}\rho^{1/2} \qquad (2.16\text{-}4)$$

where A_o is the lattice parameter

γ is Gruneisen's constant

κ is the compressibility

ρ is the density.

Differentiating (2.16-4) with respect to pressure and noting that $\partial\rho/\partial p = \kappa\rho$ yields

$$\partial k_p/\partial p = -A_o/6\gamma^2(\rho\kappa)^{1/2} \qquad (2.16\text{-}5)$$

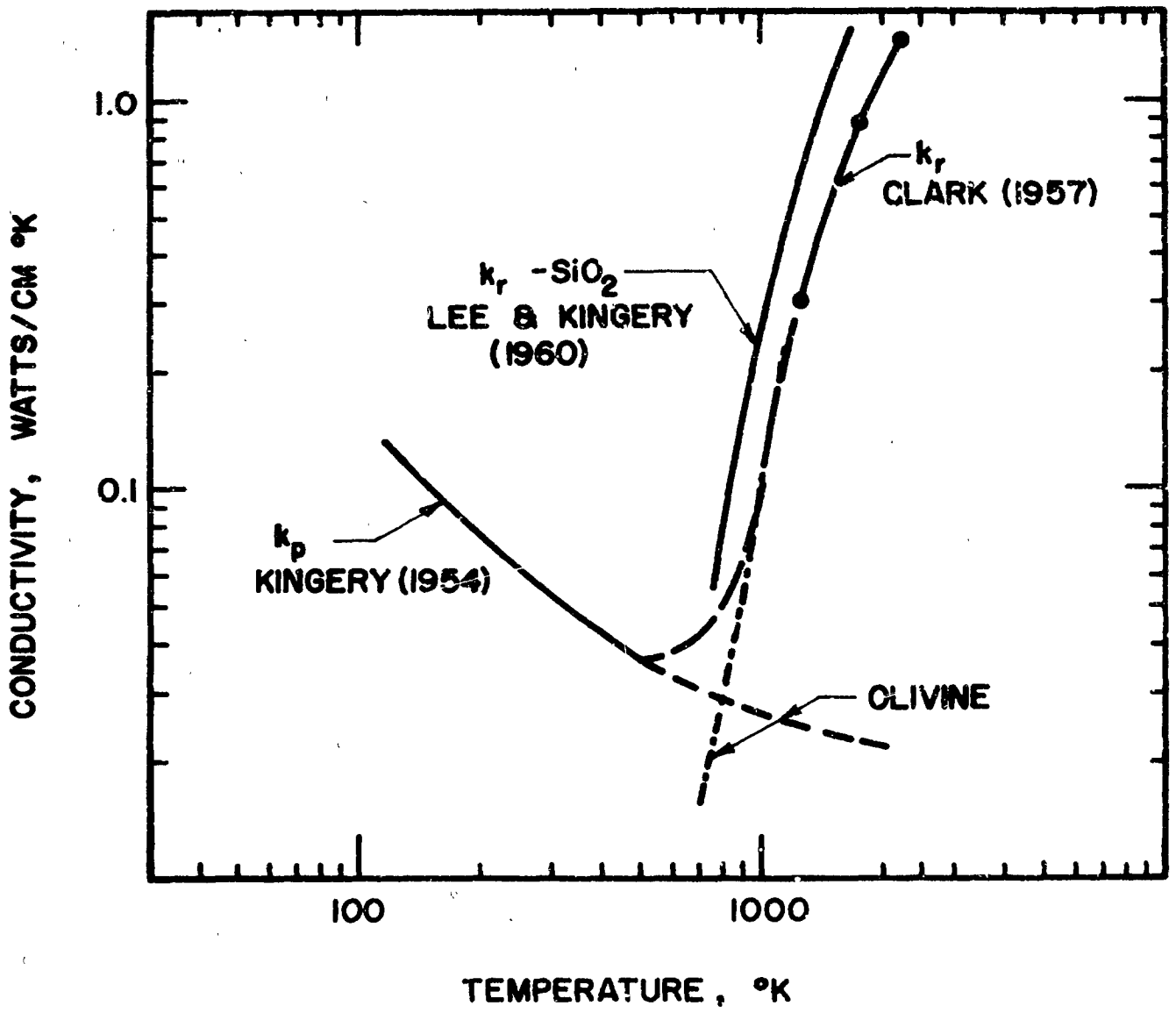

FIGURE 2.16-1 Thermal conductivity of olivine.

Now choosing $\Lambda_o = 7\times10^{-8}$ cm

$\gamma = 2$

$T = 1500°K$

$\kappa = .7\times10^{-12}$ dynes^{-1}cm^{-1}

$\rho = 3.4$ gm cm^{-3}

yields

$$\partial k_p/\partial p = -1.26\times10^{-6} \text{ sec}^{-1}°K^{-1}\text{cm}^2$$
$$= -1.26\times10^{-4} \text{ watts cm}^{-1}°K^{-1}\text{kilobar}^{-1}$$

Thus the effect of 50 kilobars pressure will be to decrease the phonon conductivity by about 0.006 watts cm$^{-1}°K^{-1}$, which is insignificant compared to the range of reliability of the radiative conductivity data to be discussed below.

2.162 Heat Conduction by Free Electrons or Holes

It is generally agreed that the transfer of heat by free electrons or holes is not important anywhere in the earth's upper mantle where temperature and pressure conditions resemble those likely to be encountered on the moon. As the thermal conductivity due to electronic processes k_e can be related to the electrical conductivity σ_e through the Wiedemann-Franz relationship:

$$k_e = \gamma (k_o/e)^2 \sigma_e T \qquad (2.16\text{-}6)$$

where k_o is Boltzman's constant 1.38×10^{-23} joules/degree

e is the charge on the electron 1.59×10^{-19} coulombs

γ is a constant equal to $\pi^2/3$ in the free electron model for metals (see for example Dekker, 1957) and lying between 2.5 and 4 in semiconductors.

While the electrical conductivity in the earth's mantle above 600 km appears to be everywhere less than 10^{-3}(ohm cm)$^{-1}$ even in the deep mantle it does not apparently have an average value greater than 1 (ohm cm)$^{-1}$. Taking the latter value as the worst possible case which could be expected in the moon would yield a value for k_e of 5×10^{-5} watts/cm°K which is negligible compared to the phonon conduction.

Lawson and Jamieson (1957) have suggested that excitons (bound electron-hole pairs) may contribute to thermal conductivity in the earth's deep mantle but they do not believe them to be important in the outer mantle where conditions most closely approximate the moon.

2.163 Photon Conduction

Heat may also be transferred through solids by transmission, or absorption and reradiation of electromagnetic energy. Although the possible geological significance of this photon conduction was first recognized by Birch and Clark (1940) it was not until the work of Clark (1956,1957), Lawson and Jamieson (1958), and Lubimova (1958) that serious attempts were made to estimate its role in the thermal history of the earth.

Clark has derived an expression for the radiative thermal conductivity in a body under planetary conditions of the form

$$k_r = \frac{4}{3} \int_o^\infty \frac{n^2(\lambda,T)}{\epsilon(\lambda,T)} \frac{\partial B(\lambda,T)}{\partial T} d\lambda \qquad (2.16\text{-}7)$$

where

$$B(\lambda,T) = \frac{2\pi c^2 h}{\lambda^5(\exp[hc/\lambda k_o T]-1)} \qquad (2.16\text{-}8)$$

n is the index of refraction

λ is the wave length

T is the absolute temperature

ϵ is the spectral extinction coefficient

c is the velocity of light

h is Planck's constant

k_o is Boltzmann's constant

The extinction coefficient $\epsilon(\lambda,T)$ is the sum of an absorption coefficient $\alpha(\lambda,T)$ and a scattering coefficient $S(\lambda)$.

Several simplifications of equation (2.16-7) are possible. For most materials in the approximation of weak absorption, n may be taken to be constant and k_r may be rewritten as

$$k_r = (16/3)\sigma n^2 T^3 \bar{\ell}_r \qquad (2.16\text{-}9)$$

where σ is the Stefan-Boltzmann constant,

$$\bar{\ell}_r = \frac{\int_o^\infty \{1/\epsilon(\lambda,T)\}\{x \exp(x)/[\exp(x)-1]\} B(\lambda,T)d\lambda}{4\int_o^\infty B(\lambda,T)d\lambda} \qquad (2.16\text{-}10)$$

and $x = ch/\lambda k_o T$

Comparison of equation (2.16-9) with (2.16-2) illustrates a formal analogy which is frequently drawn between radiative conduction and heat transfer in a gas by molecules or in a solid by phonons. Using this analogy in radiative transfer the transporting species are photons which travel with a velocity $v = c/n$, with a volume heat capacity $16\sigma n^3 T^3/c$ and an effective photon mean free path $\bar{\ell}_r$.

Unless the material has very high transmission in spectral regions remote from the bulk of the blackbody radiation curve the approximate relationship

$$\bar{\ell}_r(T) \simeq \frac{\int_0^\infty \{1/\epsilon(\lambda,T)\}\, \beta(\lambda,T)\, d\lambda}{\int_0^\infty \beta(\lambda,T)\, d\lambda} \qquad (2.16\text{-}11)$$

as used by Lee and Kingery (1960) holds.

We shall at first concentrate on the case where scattering is negligible and hence the extinction coefficient equals the absorption coefficient. Under this condition, the principal function to be evaluated is the magnitude of the spectral absorption coefficient $\alpha(\lambda,T)$ at the relevant temperatures and wavelengths. We feel that, while some general conclusions can be reached by theoretical discussion, there is no substitute for empirical data.

When considering radiative transfer in the moon, where we are interested primarily in temperatures below the melting temperature of olivine, the most important spectral region for radiative transfer is the near infrared. The temperature dependence of the blackbody energy is shown in Table 2.16-I.

TABLE 2.16-I

BLACKBODY ENERGY DISTRIBUTIONS

T°K	$\lambda^*_{2\%}$	λ_{max}	$\lambda_{98\%}$
300	5.3 μ	9.6μ	58.5μ
1000	1.6 μ	2.9μ	17.6μ
1700	.94μ	1.7μ	10.3μ
2000	.80μ	1.4μ	8.8μ

* $\lambda_X\%$ means that X% of blackbody flux falls at wavelengths less than λ.

In general for minerals the near infrared is a moderately transparent region, lying between the vibrational region of the infrared and the intrinsic "semiconductor" band gap region of the ultraviolet. It is most important to point out that while the peak absorptions for these two processes generally lie beyond the region where most of the blackbody energy is concentrated there is, particularly on the infrared side, a significant tail reaching into the region in question. This tail involving the wings of the fundamental vibrational absorptions, as well as combination tones resulting from them, should not be overlooked as a source of significant absorption. A general rule is that high temperatures will broaden these infrared absorptions leading to further increases in this tail at high temperatures. It can easily be seen that even if this absorption tail were unaffected by temperature and pressure the blackbody shift to high frequencies with increasing temperature increases the mean free path as the blackbody moves into a region of greater transparency. This type of infrared effect was observed by Lee and Kingery (1960) who saw an increase of photon mean free path with temperature in several ceramic materials. If the ultraviolet absorption edge were involved instead of the infrared absorption tail the effect would be just the opposite. Although it is generally recognized that the mean free path of photons is temperature dependent it has been customary in most calculations of the thermal history of planets to assume, for want of better data, that it is constant (see for example, MacDonald, 1959).

If absorption is the dominant process limiting radiative transfer in the moon, then the assumption of a mean free path which does not vary with temperature does not seem realistic. On the assumption that the absorption spectrum is independent of temperature Clark (1957a) was able to estimate the temperature dependence of k_r for olivine, diopside, pyrope, almandine, and grossularite. Mean free paths computed from the conductivities are shown in Figure 2.16-2 and the conductivities themselves have been reproduced in Figure 2.16-3. These values are illustrative of the previously mentioned point that even when the absorption spectrum is independent of temperature and pressure, the mean free path can still vary with temperature

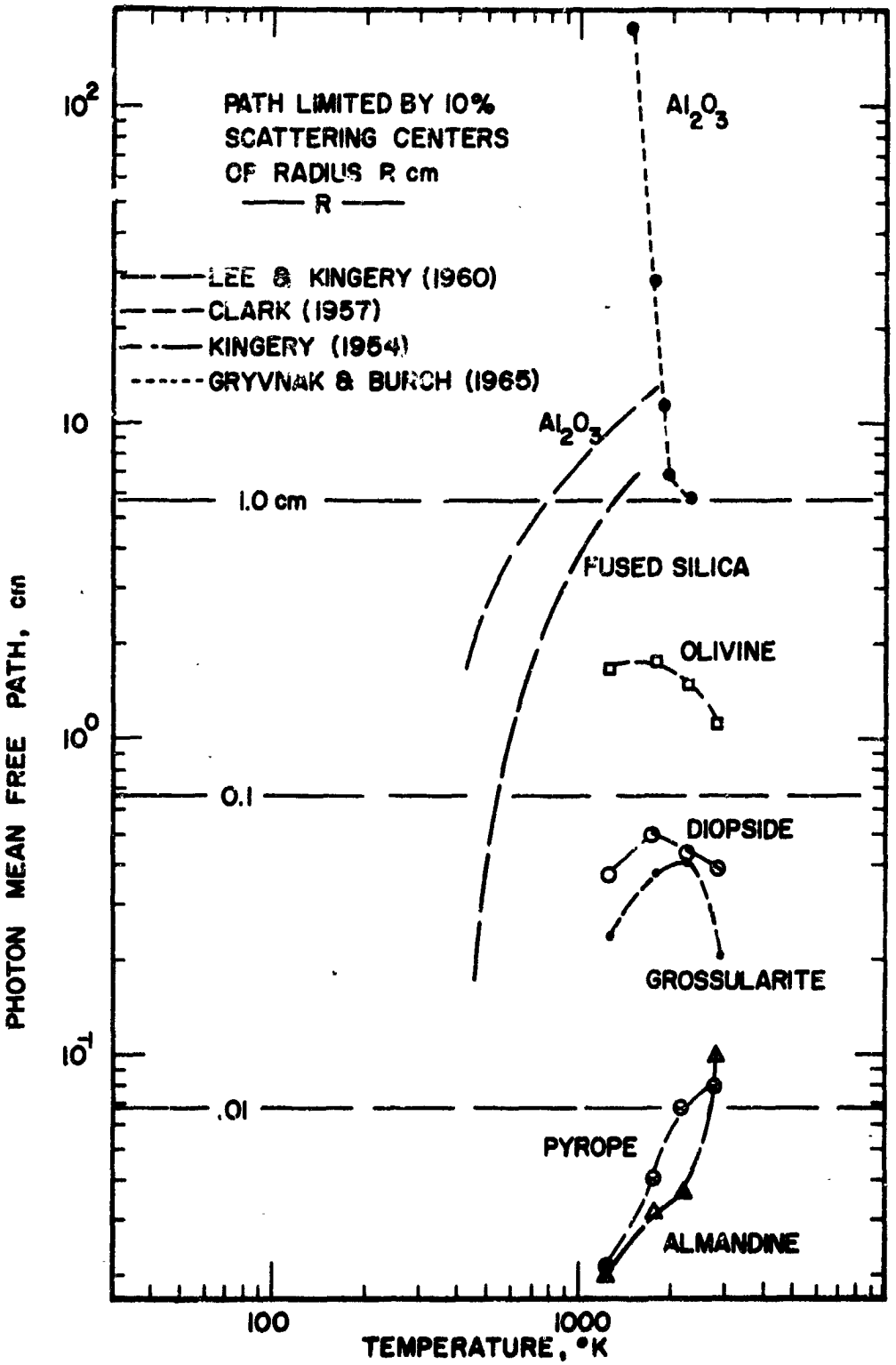

FIGURE 2.16-2 Computed photon mean free paths as a function of temperature.

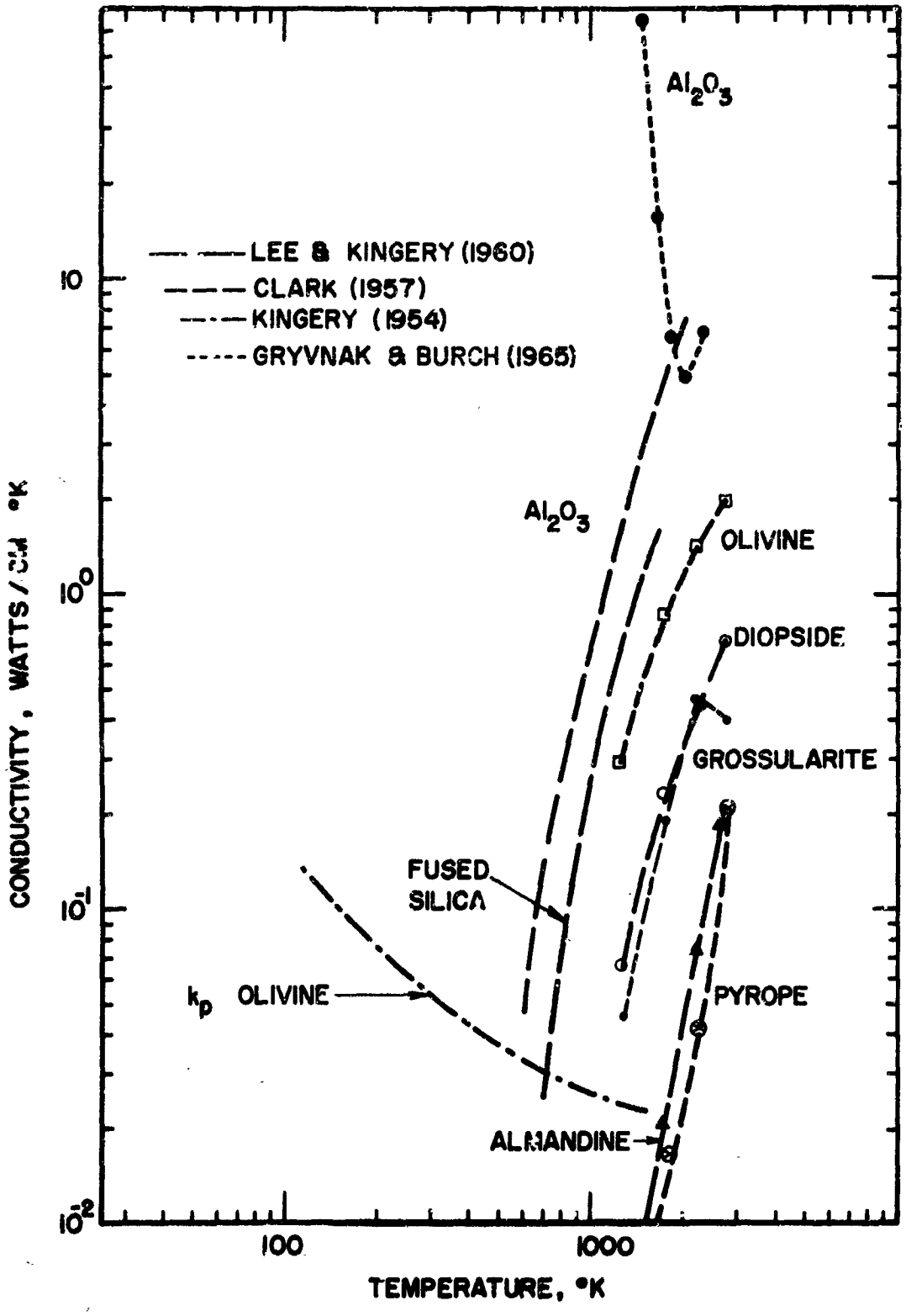

FIGURE 2.16-3 Computed thermal conductivity as a function of temperature.

because of shifts in the blackbody distribution when the absorption spectrum is wavelength dependent. It is also worth noting in conjunction with Clark's data that in a material composed of olivine plus relatively small amounts of very highly absorbing minerals, such as pyrope and almandine, the latter might lower the conductivity appreciably.

Clark's calculations indicate how thermal conductivites for a few minerals would be expected to vary with temperature if the spectra of the minerals do not change from their room temperature values. Unfortunately, data at various temperatures on the absorption over the entire spectral range necessary for thermal conductivity calculations for minerals is not available. The small amount of experimental data on other materials which has been reported indicates that high temperature may have a drastic effect on absorption coefficient and hence mean free path. In a very recent study of the absorption coefficient and refractive index of Al_2O_3 as a function of temperature up to 2300°K Gryvnak and Burch (1965) observed a large increase in the absorption coefficient, followed by a further discontinuous great increase on melting. The refractive index on the other hand only increased .05 up to 1970°K. Photon mean free paths computed from approximate numerical integration of their spectra between .5 and 5 microns using equation (2.16-10) are shown in Figure (2.16-2). The data used in the calculation as interpolated from the spectra are shown in Table (2.16-II) and the computed thermal conductivities in Figure (2.16-3). The increase in the photon mean free path of Al_2O_3 as a result of changes in α above 1500°K is so great that the conductivity decreases by over an order of magnitude within about 500°K.

There are also a few direct measurements which suggest the type of effects to be expected from pressure. Balchan and Drickamer (1959) have measured the effect of pressures up to 150 kilobars on the ultraviolet absorption edge of olivine and on the Fe++ electronic absorption in garnet. Lippincott et al (1960) have measured the effect of pressures up to 160 kilobars on the infrared absorption of several solids. The results of these experimental studies seem to show that while some distinctive effects are observed, in the absence of phase changes, changes in mean free path as a result of any pressures likely to occur in the moon would be insufficient to significantly affect the conclusions drawn as a result of ordinary pressure experiments.

TABLE 2.16-II

SPECTRUM OF ALUMINA (AFTER BURCH,1965)

INDEX OF REFRACTION 1.765

ABSORPTION COEFFICIENTS, CM**-1

	MICRONS	1473.K	1773.K	1873.K	1973.K	2293.K
1	0.50	0.0450	0.1100	0.2600	0.4000	0.3000
2	0.75	0.0140	0.0770	0.2000	0.3000	0.2500
3	1.00	0.0078	0.0550	0.1500	0.2500	0.2100
4	1.25	0.0052	0.0410	0.1100	0.2000	0.1900
5	1.50	0.0040	0.0320	0.0900	0.1700	0.1700
6	1.75	0.0034	0.0270	0.0730	0.1300	0.1400
7	2.00	0.0033	0.0230	0.0620	0.1100	0.1200
8	2.25	0.0034	0.0220	0.0590	0.1000	0.1200
9	2.50	0.0040	0.0220	0.0550	0.0930	0.1200
10	2.75	0.0050	0.0250	0.0570	0.0910	0.1200
11	3.00	0.0080	0.0340	0.0670	0.0990	0.1300
12	3.25	0.0220	0.0550	0.0900	0.1100	0.1700
13	3.50	0.0700	0.1100	0.1700	0.2000	0.2500
14	3.75	0.1900	0.2700	0.3600	0.4000	0.5100
15	4.00	0.4300	0.6000	0.7000	0.7900	1.0000
16	4.25	0.8100	1.1000	1.2000	1.4000	1.8000
17	4.50	1.5000	2.0000	2.3000	2.5000	3.3000
18	4.75	2.3000	3.3000	4.0000	4.2000	5.4000
19	5.00	3.7000	5.3000	6.5000	7.0000	8.7000
*	ABSORPTION1	5.75E-03	3.45E-02	8.64E-02	1.45E-01	1.68E-01
	MEAN PATH1,CM	1.74E 02	2.90E 01	1.16E 01	6.89E 00	5.96E 00
	CONDUCTIVITY1	5.23E 01	1.52E 01	7.16E 00	4.99E 00	6.77E 00
**	ABSORPTION2	4.54E-03	3.17E-02	8.36E-02	1.46E-01	1.69E-01
	MEAN PATH2,CM	2.20E 02	3.16E 01	1.20E 01	6.84E 00	5.93E 00
	CONDUCTIVITY2	6.63E 01	1.66E 01	7.40E 00	4.95E 00	6.74E 00

* Calculated by numerical integration of equation (2.16-10)

** Calculated by equation (2.16-11)

If room temperature spectra of the materials of interest were available one could attempt to extrapolate them to the high temperatures prevailing in the moon and in the earth. Because of the unfortunate dearth of such spectra, we can only indicate what factors are most likely to be important. A number of workers (Clark, 1957b; Lawson and Jamieson, 1958) have discussed these factors and attempted to make quantitative estimates of their contributions to total absorption. The mechanisms of absorption which must be considered are:

(1) Vibrational transition absorption (including lattice and internal vibrations);

(2) Free carrier absorption (free electrons, holes, etc.);

(3) Intrinsic semiconductor absorption (transitions from valence to conduction bands);

(4) Absorptions due to impurities (including extrinsic electronic transitions between bound states or to the conduction band) or transition metal ions where these are not impurities.

We have already mentioned that increasing temperature would be expected to broaden the vibrational bands resulting in some changes in α. The magnitude of free carrier absorption may be estimated from electrical conductivity measurements of the earth's mantle using the formula

$$\alpha = \frac{120\pi\sigma_e}{n} \qquad (2.16\text{-}12)$$

where σ_e is the electrical conductivity in $(\text{ohm cm})^{-1}$

and n is the refractive index.

While Lawson and Jamieson have disagreed with Clark on the magnitude of free carrier absorption in the earth's deep mantle, they are agreed that in the upper mantle, where conditions most resemble the moon, it is the principal limiting absorption mechanism.

Another mechanism, that of electronic absorption by transition metal ions, has also been considered by Clark, and Lawson and Jamieson. They conclude that, due to the position and intensity of such bands, this type of absorption is not very important in radiative transfer. The same arguments could be applied to exciton absorption which should be entirely unimportant.

From the above qualitative arguments it should be apparent that, while existing theory may be able to indicate what the significant absorption mechanisms are, there are so many complicating factors that prediction of detailed variation of the conductivity of most minerals at high temperatures and pressures is uncertain.

In addition to absorption photon transmission may be limited by scattering. Lee and Kingery (1960) have shown that in sintered polycrystalline oxides the major factor limiting infrared transmission is scattering by porosity but at the pressures encountered in the moon, porosity cannot be a factor. Clark (1957a) has pointed out that in the earth, scattering may be more important than absorption in materials such as olivine. When we remember that in our model the mantle does not consist of pure olivine the importance of considering scattering is at once apparent.

Neglecting absorption effects, the transmission of a transparent solid containing isolated scattering centers may be written

$$dI/dX = -KNsI \qquad (2.16\text{-}13)$$
$$= -SI$$

where I is the intensity of the radiation;
N is the number of scattering centers per unit volume;
s is the effective scattering cross section of the particles;
K is the total scattering coefficient.

K is a slowly varying function of the dimensionless parameter

$$p = \frac{4\pi r(m-1)}{\lambda} \qquad (2.16\text{-}14)$$

where λ is the wavelength in the matrix and m is the relative refractive index of the scattering center and the matrix.

Let us consider a rock consisting entirely of olivine, pyroxene and plagioclase feldspar in which the plagioclase makes up about 10% by volume of the rock. Following Lee and Kingery the scattering coefficient $S(\lambda)$ may be written as

$$3K(\lambda)V_s/4r \qquad (2.16\text{-}15)$$

where V_s is the volume fraction of the scattering material.
When $|p|$ is large.

$$K(\lambda) \sim 2 \qquad (2.16\text{-}16)$$

Neglecting effects of anisotropy we may take the index of refraction of plagioclase as approximately 1.56 and the combined olivine and pyroxene as 1.66 (Rodgers and Kerr, 1942). If the relative indices remain about the same in the infrared

$$m \sim .94$$

and $$|p| \sim .757\ r/\lambda. \qquad (2.16\text{-}17)$$

It is sufficient for our purpose to note that $|p| \gg 1$ when the radius of the particle is greater than several tens of microns. It would seem that because of the long times available for crystallization in the moon, the grain sizes of the major minerals would not be much smaller than this.

For a fixed volume percent of scattering centers, as long as the particle size is large compared to the wavelength the mean free path will be essentially independent of temperature and inversely proportional to the particle radius. Mean free paths for photon scattering of a mixture of 10% plagioclase and 90% olivine and/or pyroxene for several particle sizes have been estimated and are shown in Figure 2.16-2. These are of course independent of temperature. If the particle sizes of the plagioclase is of the order of 1 mm then the mean free path will be of the order of a centimeter. This is essentially the same order of magnitude as Clark (1957b) has estimated assuming crystal diameters the order of a centimeter and scattering by all the crystal boundaries. While the scattering estimates are by necessity quite crude they indicate that this may be the most significant factor in determining thermal conductivity.

2.164 Thermal Conductivity of the Model

Based on the above discussion we have adopted a standard phonon conductivity k_p which is equal to .055 watts $cm^{-1}°K^{-1}$ at 273°K and which is inversely proportional to the absolute temperature. This corresponds to the phonon conductivity for olivine reported by Kingery et al (1954). We have assumed any electronic contribution to heat transfer is negligible. Because of the uncertainty in the magnitude of the photon mean free path we have not selected a fixed value but rather have been forced to consider a variety of values. We have, however, imposed the condition that the photon mean free path is proportional to the temperature. This approximates

the form to be expected if absorption rather than scattering dominates and the mean free path is controlled by the movement of the blackbody function away from the infrared edge as the temperature increases. While a constant or a more rapidly changing photon mean free path might be more realistic we feel that the uncertainties in the data are potentially a source of much greater error than the choice of the temperature variation of the mean free path.

The standard total conductivity then is given by

$$k = k_p T_o/T + 16\sigma n^2 T^4 \bar{\ell}(T_o)/T_o \qquad (2.16\text{-}18)$$

Substituting an index of refraction of 1.7 which we have adopted as standard for the hypothetical moon model and the standard value of k_p at 273° into (2.16-18) yields

$$k = 0.055x273/T + 8.74x10^{-11} T^4 \bar{\ell}(273°K)/273 \qquad (2.16\text{-}19)$$

in watts/cm °K. Except when constant conductivities have been used to illustrate specific points this form has been used for all thermal calculations.

2.17 Standard Model Parameters

As a basis for calculations of volcanic history we selected a set of standard parameters to approximate the significant physical properties of a moon whose composition is equivalent to combinations of basalt and dunite in the ratios of 1:3, 1:4, and 1:5. The values of these parameters are summarized in Table 2.17-1. It should be apparent from the preceding discussion that each specific value chosen is only an attempt to provide a realistic first approximation to the average behavior of the material in the interior of the moon under the pressure and temperatures likely to be encountered. As our understanding grows each parameter will have to be refined until complete agreement between observations and theory is reached.

TABLE 2.17-1

STANDARD MODEL PARAMETERS

Radius	1700 km
Uranium content in basalt	0.2 ppm
Uranium content in dunite	0.0
Specific heat	1.1 joules/gm deg
Heat of fusion for basalt fraction	500 joules/gm
Melting temperature at 1 atmosphere	1500°K
Slope of melting curve	11.0°K/kilobar
Basalt density	3.0 gm/cm^3
Dunite density	3.42 gm/cm^3
Phonon conductivity at 273°K	.055 watts/cm °K
Index of refraction	1.7
Photon mean free path at 273°K	Variable
Basalt to dunite ratio	1:3 1:4 1:5
Uranium content in mixture, ppm	.05 .04 0.03
Mean density, gm/cm^3	3.33 3.33 3.34

2.2 MAGMA GENERATION ON THE MOON

We have assumed in our model that once magma is formed it is immediately transported from the region of generation to the surface. Magma generation, igneous activity, and volcanism thus become different aspects of the same phenomenon and for the purposes of this section we shall use the three terms interchangeably. The nature of magma generation can best be understood in terms of the way it should act to control the internal temperature distribution of the moon. We shall therefore look briefly at this aspect before proceeding with a discussion of the volcanic history.

2.21 Role of Volcanism in Thermal History

On a planet which is heating by radioactive decay two factors, thermal conduction and volcanism, compete to keep the planet from melting entirely. While thermal conduction has been intensively studied, the role of volcanism has been largely neglected because it contributes little to the total heat flow.

To isolate the effects of volcanic activity let us consider what would happen if the moon had all the properties of the standard model (Table 2.17-1) except for a constant thermal conductivity of .02 watts/cm °K. Such a conductivity is typical of rocks measured at the surface, but lower than that to be expected at depth. Figure 2.21-1 shows the predicted present temperature distribution under the following conditions:

a) Melting is neglected (Model 40)
b) Melting is allowed but the magma is not free to migrate (Model 41)
c) The magma can migrate to the surface where it cools but heat sources are not preferentially concentrated in the melt (Model 42)
d) Same as (c) but the heat sources are concentrated in the melt (Model 43).

For computational reasons so-called "present" temperature distributions actually represent the temperature 0.1×10^9 years in the future for a moon which was at 273°K 4.5×10^9 years ago.

Examination of Figure 2.23-1 shows that near the surface the temperature distributions for all four assumptions are very similar. Below about 500 kilometers, where the melting temperature is reached, the temperatures developed under assumption (b) gradually begin to fall below those for the assumption (a) until near the center the difference is about 80°. This is approximately the temperature difference which would be expected by allowing for the heat of fusion of 1/6 of the material. The temperature differences between (c) and (b) are similar but in (c) an additional temperature drop of several tens of degrees has resulted from the replacement of the extruded lava by cooler material from the layer above. Case (d) where the heat sources migrate with the melt differs considerably from the other three in that the temperature has stabilized itself along the melting curve of the "basalt" phase.

For simplicity in programming the model we have assumed that after magma is removed from a layer, material with the average composition and average temperature of the layer above it is mixed in to take its place. Magma extruded on to the surface will be mixed throughout the entire thickness of the uppermost layer. These assumptions will sometimes lead to an apparent diffusion of extrusive basalt downward into the mantle rather than the more realistic accumulation at the surface. As the computer program has been designed to keep track of the total thickness of material extruded, one is able to compare the basalt concentration for the mixing model with that resulting from surface accumulation alone. The present basalt distributions for Model 43 computed for each of the two different assumptions are compared in Figure 2.21-2. Both predict a concentration of this fraction near the surface, but the mixing assumption results in a distribution over a greater depth than is perhaps realistic. However, as long as this assumption does not result in the prediction of an unrealistic amount of remixing of the extruded lava into a region where it is remelted and re-extruded, and effect on the prediction of magma generation should be negligible.

The influence of thermal conductivity on volcanism can be illustrated by seeing how each of the four present temperature distributions, illustrated in Figure 2.21-1, would be altered by increasing the

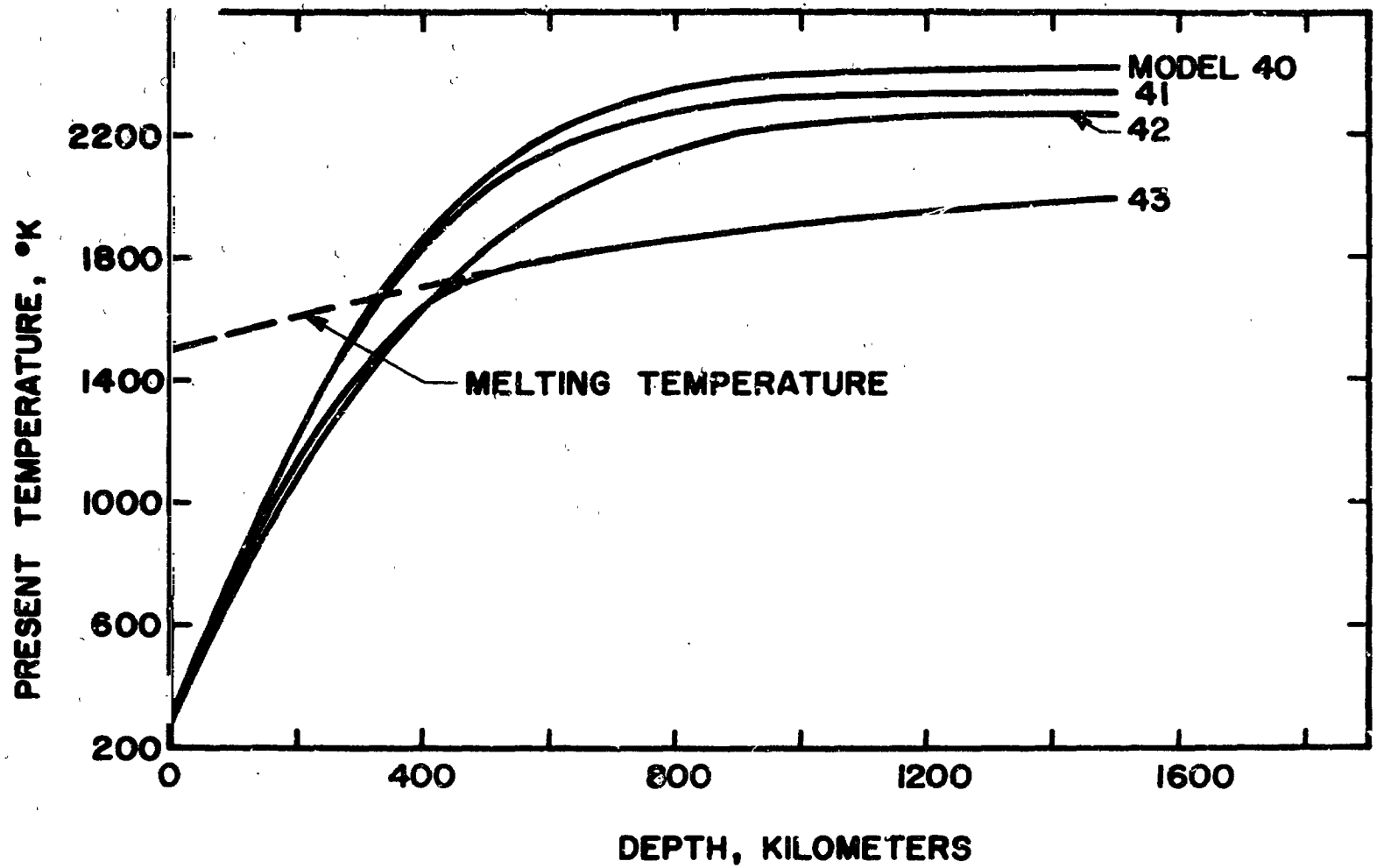

FIGURE 2.21-1 Present temperature distribution in moon composed of pyrolite-1:5, with constant thermal conductivity 2 x 10^{-2} watts/cm °K, for different conditions [melting is neglected (Model 40); melting is allowed but the magma is not free to migrate (Model 41); migration to the surface is allowed but heat sources are not preferentially concentrated in the melt (Model 42); magma can migrate and heat sources are concentrated in the melt (Model 43)].

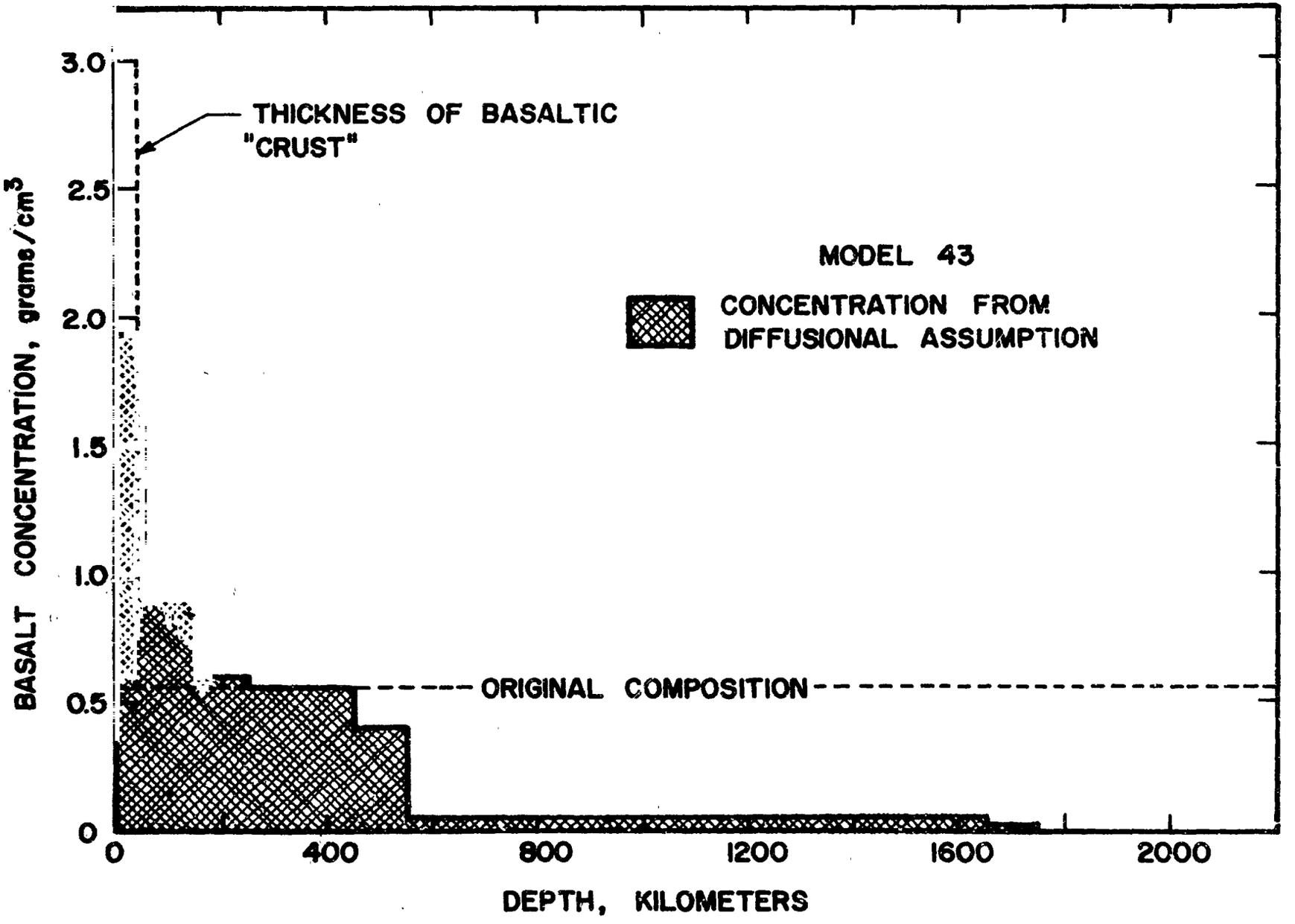

FIGURE 2.21-2 Comparison of concentration of basaltic fraction under mixing assumption with computed thickness of basaltic crust, for Model 43.

conductivity to 5.5 x 10^{-2} watts/cm °K. Present temperature distributions for Models 44 through 47, corresponding to 40 through 43 except for the greater conductivity, are plotted in Figure 2.21-3. When volcanism and differentiation of heat sources are assumed, the temperature remains below the melting temperature of the basalt as before, but because of the increased efficiency of conduction, magma generation has only been required below 1000 kilometers. Even below this depth less differentiation has been necessary to keep the planet from exceeding the melting temperature of the basalt phase (Figure 2.21-4) and so the resultant "crust" formation has been much less complete. The term "crust" in this sense has been used by analogy with the terrestrial oceanic crust whose seismic velocity is consistant with it being primarily basalt.

The above examples have been chosen to illustrate how volcanism acts as a safety valve when normal thermal conductivity alone cannot remove all the heat which is generated. Viewed this way many of the effect of changing various parameters become intuitively obvious. While a constant thermal conductivity has been chosen for simplicity in illustrating the safety valve analogy, the same affects are observed when the conductivity is assumed to be temperature dependent.

2.22 Volcanic Parameters

Satisfactory functions for the quantitative description of volcanism should be easily relatable to the volcanic features observable at the surface and to the thermal history of the planet.

To describe the intensity of volcanism we have selected two such functions, the rate at which heat is being brought to the surface per unit surface area $P_v(t)$, and the volume of lava being supplied per unit time per unit surface area $F_v(t)$. The two are approximately related by the expression

$$P_v = [(T_o - T_L)c + \ell]\rho F_v \qquad (2.22\text{-}1)$$

where

T_o is the surface temperature
T_L is the lava temperature
c is the average specific heat
ℓ is the latent heat of fusion of the melt
ρ is the density.

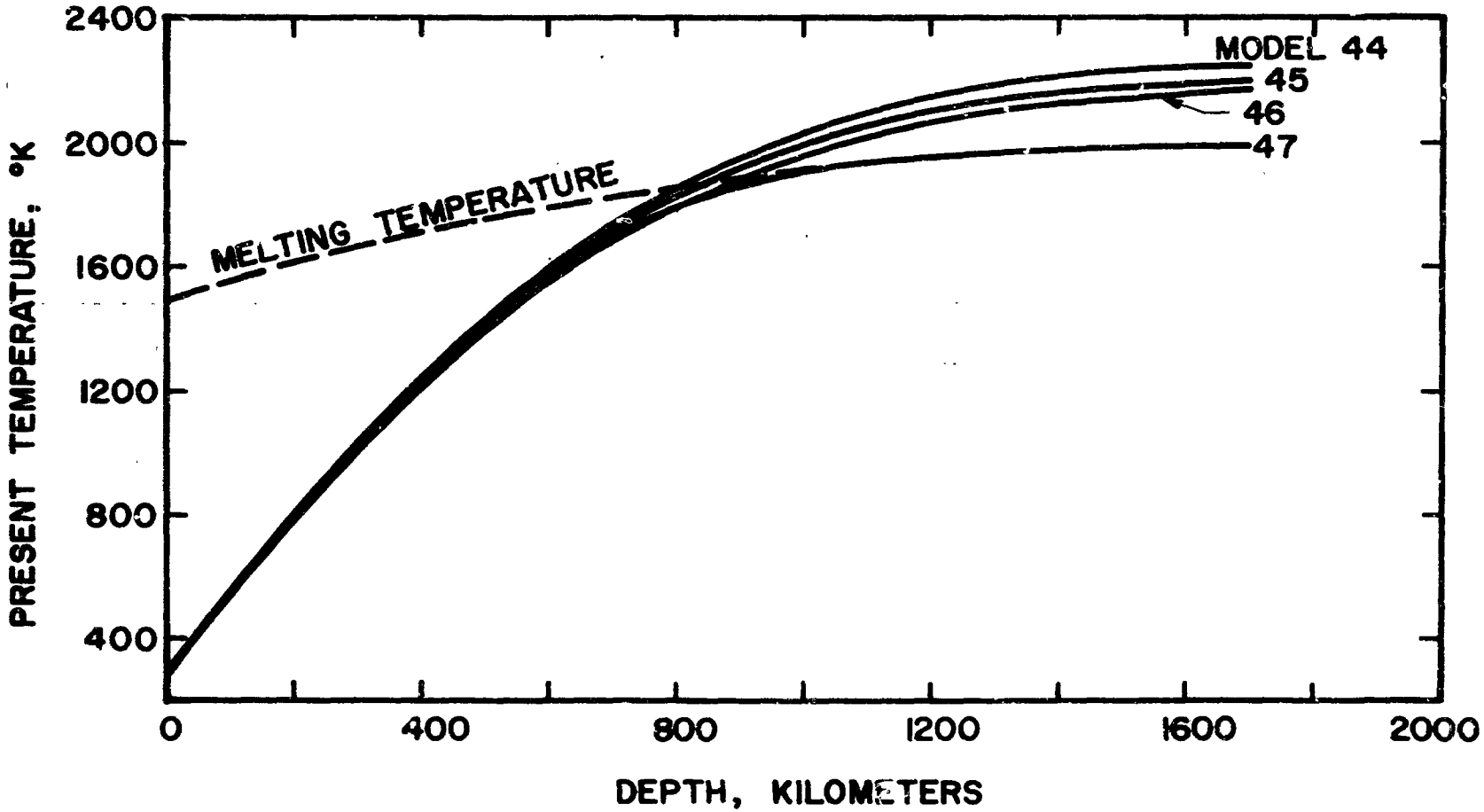

FIGURE 2.21-3 Present temperature distribution in moon composed of pyrolite-1:5 with constant thermal conductivity 5.5 x 10^{-2} watts/cm °K for the same conditions shown in Figure 2.21-1. [melting is neglected (Model 44); melting is allowed but the magma is not free to migrate (Model 45); migration to the surface is allowed but heat sources are not preferentially concentrated in the melt (Model 46); magma can migrate and heat sources are concentrated in the melt (Model 47)].

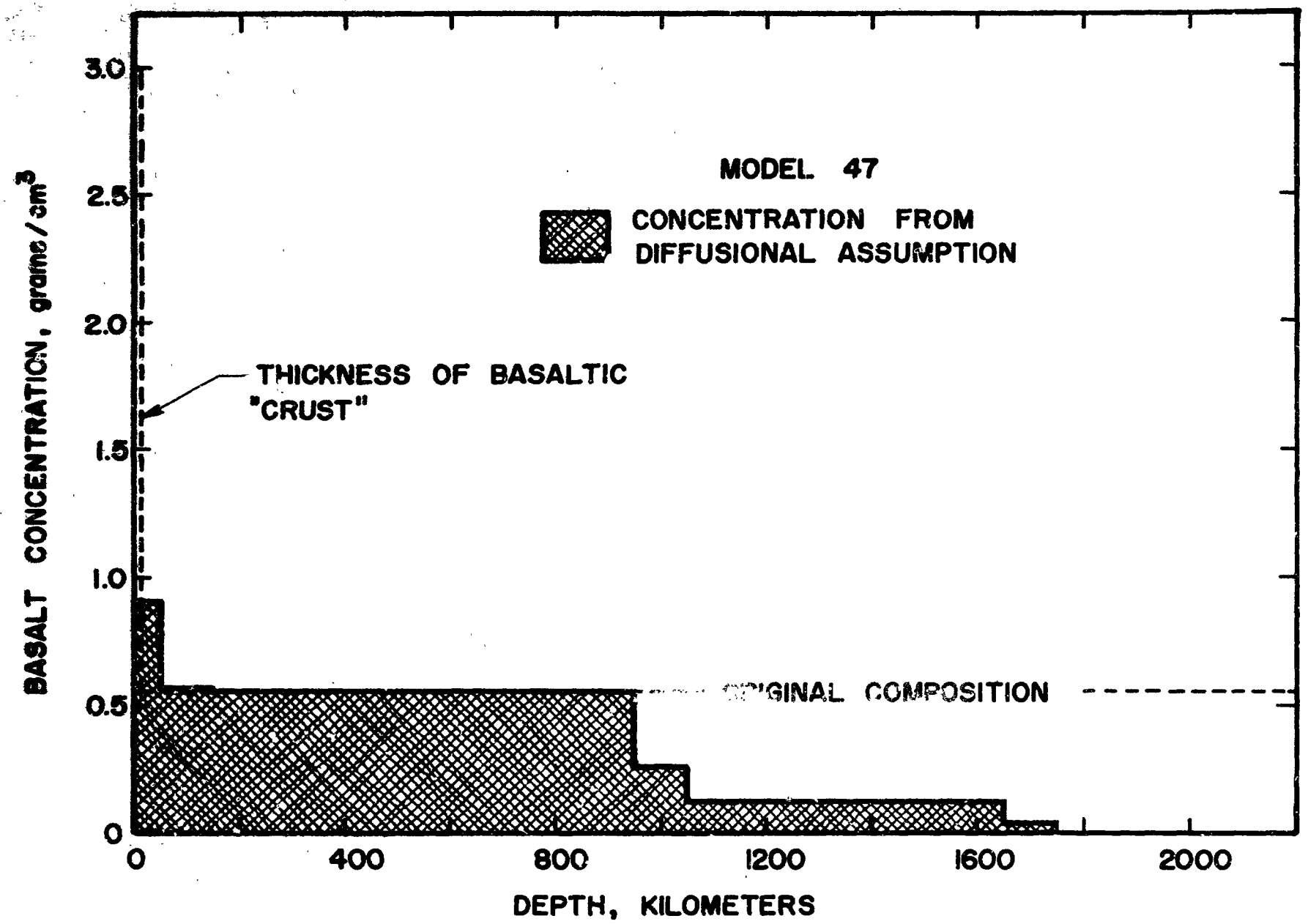

FIGURE 2.21-4 Comparison of concentration of basaltic fraction under mixing assumption with computed thickness of basaltic crust, for Model 47.

In the derivation of equation (2.22-1) and in the numerical simulation of generation we have neglected any possible interchange of mass and heat between the melt and the mantle through which it is moving. As discussed in Chapter 3, this interchange is probably very important in the mechanics of migration but neglect of it should not be expected to significantly alter the main conclusions of the study of generation.

By integration of the volcanic heat flow and the lava flow rate, one can derive the total volcanic heat energy $E_v(t)$ and the accumulated lava or "crustal" thickness

$$E_v(t) = \int_{t_o}^{t} P_v(t)dt \qquad (2.22\text{-}2)$$

$$L_v(t) = \int_{t_o}^{t} F_v(t)dt \qquad (2.22\text{-}3)$$

Combining (2.21-1), (2.21-2) and (2.21-3) yields

$$E_v = \{(T_o - T_L)c + \ell\}\rho L_v \qquad (2.22\text{-}4)$$

Use of equation (2.22-4) allows one to estimate the total volcanic heat flow from the total thickness of volcanic rocks present. For example, if we were to apply this to the earth's crust with standard model parameters (Table 2.17-1) the extrusion of 10 km of basalt should produce about 5.5×10^9 joules / cm^2. If this extrusion were uniformly distributed over the life of the planet it would have resulted in an average volcanic heat flow of 4×10^{-8} watts per square centimeter, which is far less than the present rate of terrestrial conductive flow, 6×10^{-6} watts per square centimeter.

Before attempting to answer the question, "When did the volcanism take place on the moon?" it is convenient to identify several times associated with significant stages in the development of the function $F_v(t)$. With no apriori knowledge of the behavior it seems appropriate to consider what might happen on a hypothetical undifferentiated planet, whose initial temperature is everywhere below the melting point of the potential volcanic phase (Figure 2.22-1).

Before the time t_s when volcanism starts $F_v(t)$ will be zero.

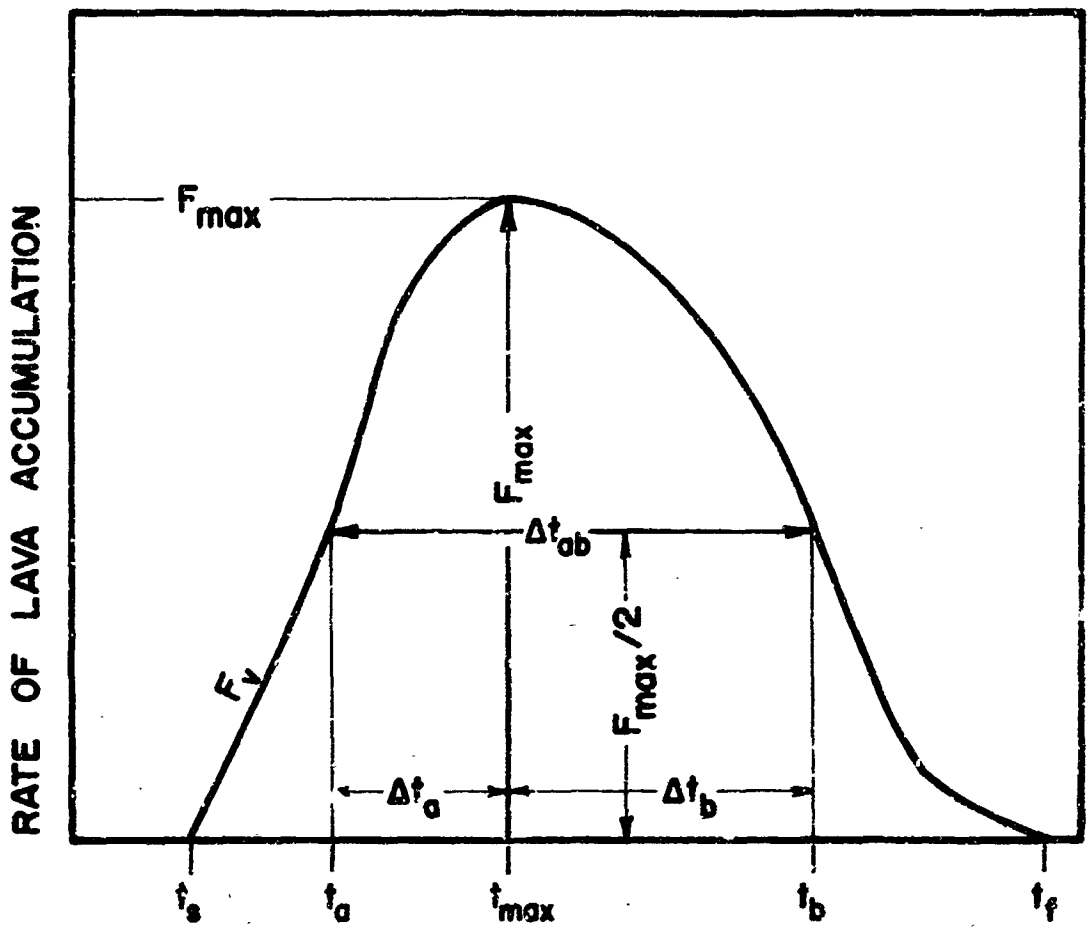

FIGURE 2.22-1 Significant times in the volcanic history of a planet.

After t_s, $F_v(t)$ will increase until it reaches a maximum $F_{v\ max}$ at a time we shall call t_{max} after which it decreases and finally ceases at time t_c. The times at which $F_v(t) = F_{v\ max}/2$ we shall define as t_a for F(t) increasing and t_b for F(t) decreasing. The three parameters

$$\Delta t_a = t_{max} - t_a \qquad (2.22\text{-}5)$$

$$\Delta t_b = t_b - t_{max}$$

$$\Delta t_{ab} = t_b - t_a$$

provide a measure of the duration of the most significant part of the volcanism.

Because of the ease with which an approximate correlation may be made between the two functions P_v and F_v, we shall normally refer below only to F_v recognizing that much of the discussion below is equally applicable to P_v.

There will be, of course, small differences between t_a, t_b, and t_{max} as defined with reference to F_v and the corresponding times defined with reference to P_v, but the differences are small enough that we may neglect them.

2.23 The Onset of Volcanism

We shall first consider the starting time of volcanism t_s. Although the use of a computer is useful for understanding fine details of the volcanic history many of the features are predictable from a much simpler model.

A portion of the moon with density ρ and specific heat c which is far enough from the surface that conduction has not yet begun to remove a substantial amount of heat from it will reach its melting temperature T_m when

$$\rho c(T_m - T_o) = \int_{t_o}^{t_s} q(t)\, dt \qquad (2.23\text{-}1)$$

where t_o is the time at which the planet's temperature was T_o,

$q(t)$ is the rate of heat production per unit volume.

Now q(t) may be written in the form

$$q(t) = (\sum_i m_i \, C_{Ui}) \, q^*(t) \qquad (2.23\text{-}2)$$

where C_{Ui} is the concentration of uranium in the i th component, m_i is the mass of the i th component per unit volume and $q^*(t)$ is the thermal power supplied by all the radioactive isotopes per unit mass of uranium remaining at the present time.

An algorithm for computing $q^*(t)$ in watts per gram for a material with the standard isotope ratios may be obtained by comparing equation (2.23-2) with (2.12-5). For convenience in later calculations we have plotted the function $q^*(t)$ as Figure 2.23-1.

Substituting equation (2.23-2) into (2.23-1) yields

$$\rho c(T_m - T_o) \; / \; \sum_i m_i C_{Ui} = \int_{t_o}^{t_s} q^*(t) \, dt \qquad (2.23\text{-}3)$$

$$= Q^*(t_s)$$

By comparing the function $Q^*(t)$, for the standard terrestrial isotope ratios (Figure 2.23-2) with the function on the left of (2.23-3) one can estimate the time at which generation should be expected to begin. For example, suppose a region of the moon with the standard isotope ratios and thermal properties contains a mixture of 0.557 grams of basalt per cm^3 and 2.278 grams of dunite per cm^3 for a total density of 3.34 grams per cm^3. If 0.2×10^{-6} grams of uranium are associated with each gram of basalt and the specific heat of the material is 1.1 joules/gm deg, the heat output per gram of uranium required to heat from 273°K to 1500°K will be

$$Q^* = \frac{3.34 \times 1.1 \; (1500\text{-}273)}{0.557 \times 0.2 \times 10^{-6}}$$

$$= 4.05 \times 10^{-10} \text{ joules per gram of uranium.}$$

From Figure 2.23-2 we see that this amount of heat has been generated about 1.9×10^9 years after the time of formation.

As t_s in equation (2.23-3) has been derived on the assumption that

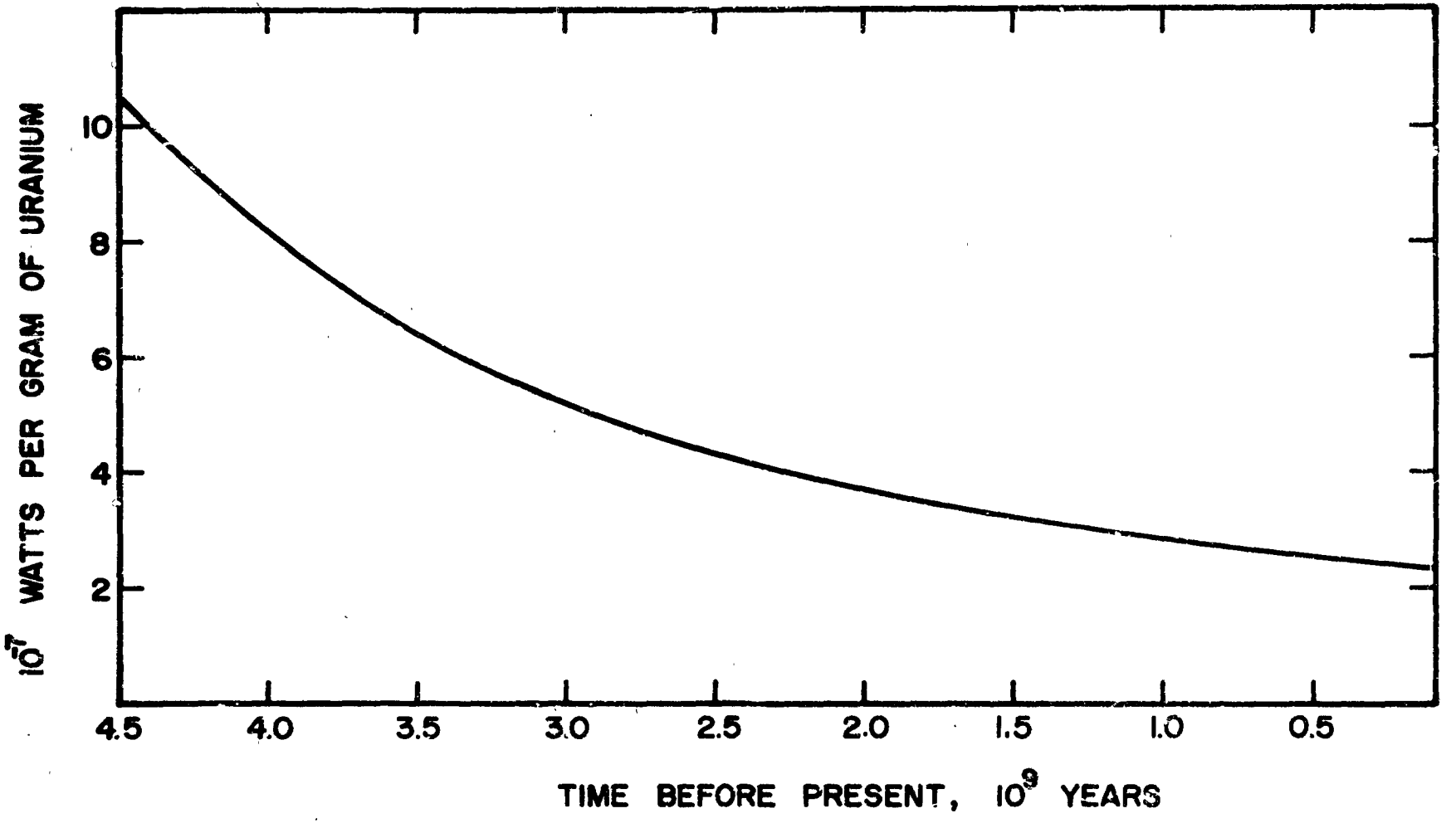

FIGURE 2.23-1 Rate of heat production, $q^*(t)$, per gram of presently contained uranium for material with terrestrial isotope ratios.

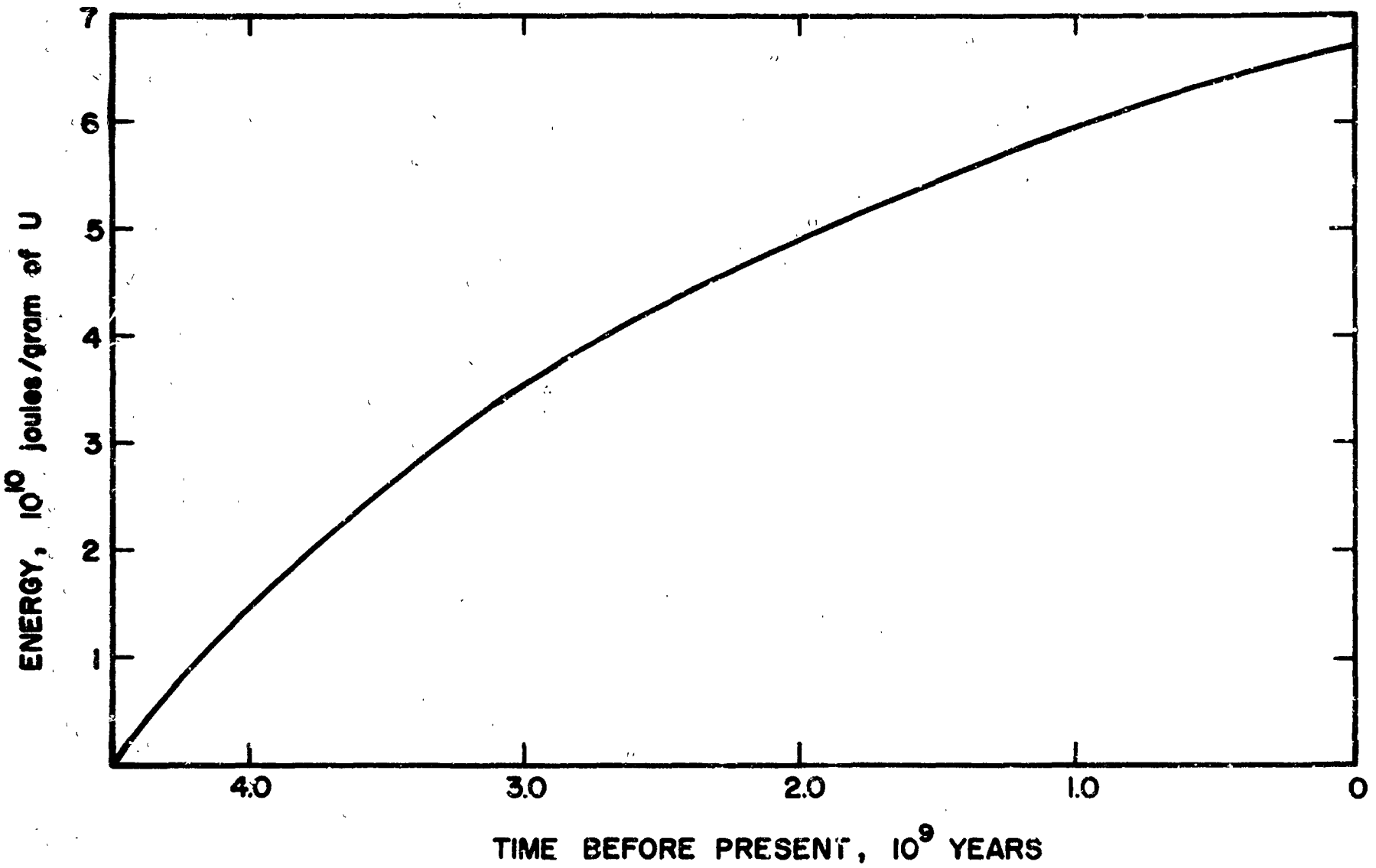

FIGURE 2.23-2 Total energy released, $Q^*(t)$, per gram of presently contained uranium for material which was formed 4.5×10^{-9} years ago with terrestrial isotope ratios.

no heat has been conducted away, use of it to estimate the starting time might not be expected to yield particularly accurate results. In fact, if the depth where the melting curve is first reached can be estimated, use of the melting temperature at this depth in conjunction with equation (2.23-3) and Figure 2.23-2 usually predicts values of t_s, which are very close to those given by the more sophisticated computer calculations, which allow for the effects of thermal conductivity.

2.24 Duration of Volcanism

There are two factors influencing the duration of volcanism: the time necessary to melt and remove all the basalt from a given depth, and the increase in the starting time of magma generation with depth as a result of the increased melting temperature. The actual duration of volcanism will be determined by whichever of these two effects dominates.

Let us first consider the time necessary to remove basalt from a given region. Once a region reaches the melting temperature, if no heat is being lost by conduction and if the basalt is removed as soon as it is melted and replaced by material which has no heat sources, the rate of generation of magma will be

$$- dm_B/dt = C_{UB} m_B q^*(t)/\ell \qquad (2.24\text{-}1)$$

where C_{UB} is the concentration of uranium in the basalt

m_B is the mass of basalt in each cc.

If the melting temperature does not change significantly with depth, equation (2.24-1) predicts that magma generation should commence abruptly

$$t_{max} = t_a = t_s \qquad (2.24\text{-}2)$$

and $$\Delta t_a = 0$$

If $q^*(t)$ does not change rapidly with time in the neighborhood of t_s

$$m_B = m_B(t_s) \exp[- C_u q^*(t_s) (t - t_s)/\ell] \qquad (2.24\text{-}3)$$

Equations (2.24-1) and (2.24-3) indicate that in the absence of significant conduction losses the rate of magma generation which will be proportional to the amount of basalt remaining and to the concentration

of heat sources in this basalt, should decrease exponentially with a relaxation time τ of approximately

$$\tau = \ell / C_{UB} q^*(t_s) \qquad (2.24\text{-}4)$$

For exponential decay the half-life, which would correspond to Δt_b defined in equations (2.22-5), is related to the relaxation time by

$$\begin{aligned} \Delta t_b &= .693\ \tau \\ &= .693 / C_{UB} q^*(t_s) \end{aligned} \qquad (2.24\text{-}5)$$

For standard isotope ratios and a uranium concentration in the basalt of 0.2×10^{-6}, if melting takes place 2×10^9 years after the time of formation, the relaxation time of magma generation should be about 120×10^6 years and Δt_b about 80×10^6 years. If melting starts either very early or very late in the moon's history, we would expect Δt_b to be decreased or increased, respectively, by about a factor of two.

We now turn to an examination of the effect that the increase of melting temperature with depth will have on the duration of volcanism. While in our model the melting temperature for the "basalt" fraction extends from 1500°K at the surface to nearly 2000°K at the center, most realistic assumptions for the conductivity imply initial magma generation at depths where the melting temperature is greater than 1800°K.

For the standard model with a total uranium concentration of 3.3×10^{-8} grams per gram in the pyrolite, the time necessary to heat to 2000°K is about 700×10^6 years longer than the time to heat to 1800°K. If the uranium concentration is increased to 4.0×10^{-8} or 5.0×10^{-8}, the heating interval decreases to 400×10^6 years or 300×10^6 years, respectively. These times are somewhat longer than those necessary to remove basalt from a given depth and might be expected to increase Δt_b considerably above the estimates predicted from equation (2.24-5). The change of time of initial melting with depth might also make Δt_a significant, although the decreasing volume of basalt with decreasing distance from the center of the planet combined with a relatively small melting temperature gradient might act to maintain Δt_a small. The manner in which the melting temperature gradient and heat conduction

combine to affect the volcanic history is best predicted by numerical simulation using the digital computer.

2.25 Computer Simulation of Volcanic History and Crust Formation

We have used the computer program to investigate the thermal history of a number of models of the moon of three different compositions. The different compositions were obtained by mixing basalt with a uranium content of 0.2 ppm, with different amounts of dunite containing no uranium. For each composition the phonon conductivity was assumed to be

$$k_p = 0.055\ 273/T \qquad (2.25\text{-}1)$$

the radiative conductivity was assumed to be given by

$$k_r = \frac{16}{3}\ n^2\ \sigma T^3 \bar{\ell} \qquad (2.25\text{-}2)$$

where

$$\bar{\ell} = \bar{\ell}_{273°} \times (T/273) \qquad (2.25\text{-}3)$$

The use of expression (2.25-3) is intended to approximate the form of the increase of the mean free path with temperature as a result of the shift of the black body away from the infrared edge of the absorption spectrum and implies that absorption rather than scattering provides the main limitation to the photon mean free path. The extreme uncertainties associated with this assumption have already been discussed in Section 2.16.

We have already pointed out that the starting time of magma generation in a moon of uniform composition should depend only on the total concentration of heat sources, the temperature at the time of formation and the thermal conductivity. Figure 2.25-1 shows the predicted times at which volcanic activity should begin in terms of the uranium concentration, and the photon mean free path at 273°K. It is apparent that if magma generation takes place at all, the starting time t_s will be much more sensitive to the uranium content than to the thermal conductivity. Thus, age determination on "early" volcanics, combined with uranium contents, determined either from sampling of the "pre-volcanic" lunar surface or from heat flow measurements, should make an almost unique estimate of the moon's temperature at the time of formation possible. If such a determination is considered to be important in the objectives

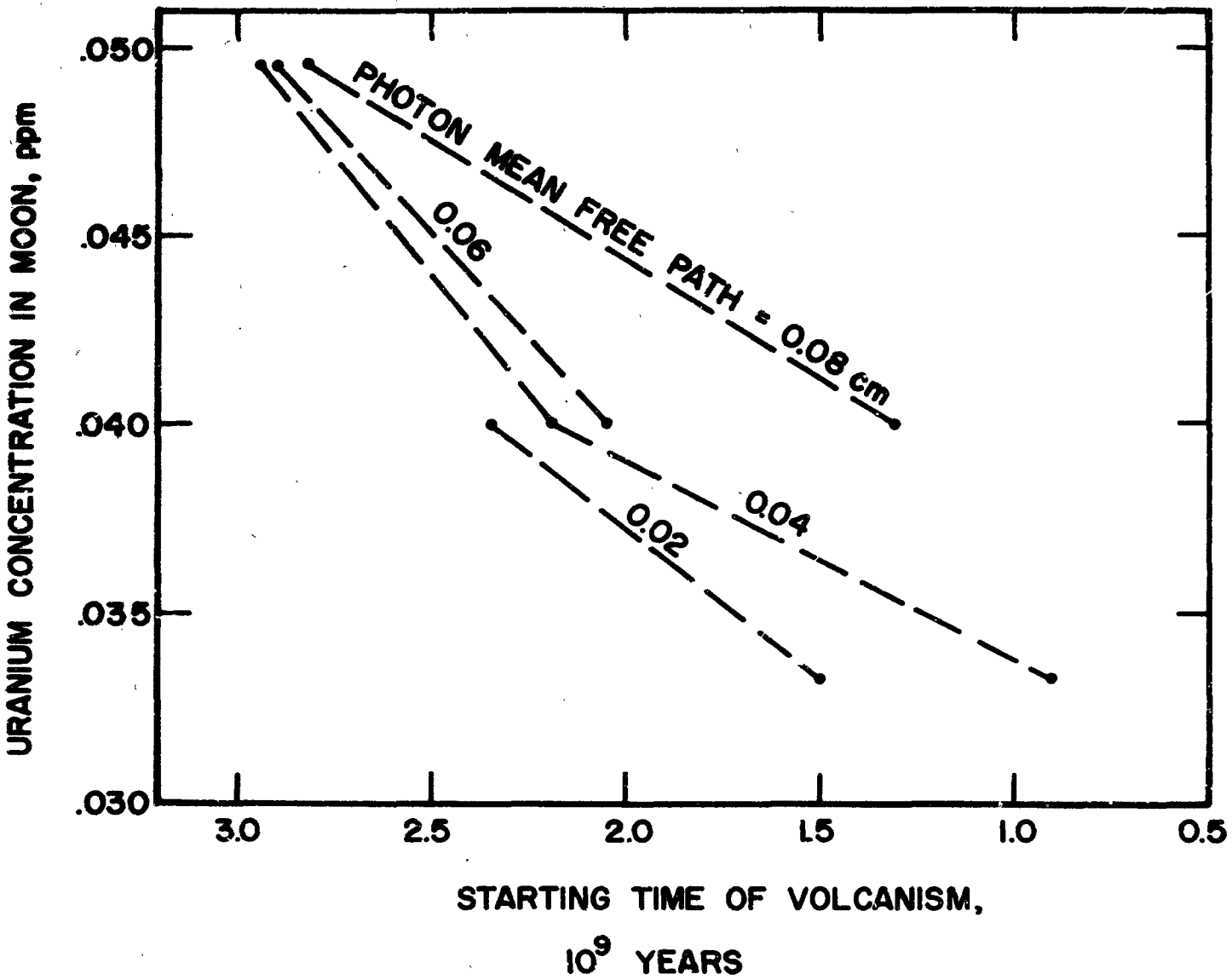

FIGURE 2.25-1 Beginning of volcanic activity as a function of uranium concentration and photon mean free path at 273°K.

of the Apollo, or subsequent programs, careful sample selection by the astronauts with regard to the stratigraphic relationships would appear to be required. In Figure 2.25-2 we have plotted the volcanic intensity function $F_v(t)$ for the same models whose starting times for magma generation have just been discussed. All the models show a sharp onset of volcanism with Δt_a so sharp that the computer output at intervals of 200 million years has shown a significant portion of the rise time only in two of the models with low uranium contents. It is interesting, but not surprising, to note that after generation begins all the functions $F_V(t)$ for a given composition decline very rapidly along almost identical curves. Δt_b for these curves is of the order of 3×10^8 years, confirming that the affects of the melting temperature gradient predominate. As would be expected, increasing the amount of basalt while keeping the uranium concentration in the basalt constant will both increase the intensity of volcanic activity and make it take place earlier.

The total thickness of basaltic extrusives and intrusives which remain on the moon's surface should provide another clue to the moon's thermal history. Figure 2.25-3 shows the predicted integrated thickness L_v of the igneous rocks as a function of composition and photon mean free path. It is interesting to note that for all the models investigated there is a rather simple, almost linear relationship relating the "crustal thickness" to the photon mean free path.

$$L_v(\bar{\ell}) = L_v(0) - 7.5 \times 10^7 \bar{\ell}$$

$$L_v(\bar{\ell}) \geq 0$$

where L_v and $\bar{\ell}$ are both measured in centimeters.

2.3 SUMMARY OF MAGMA GENERATION INVESTIGATION

On the basis of the above discussion we would predict that if the moon's composition is essentially the same as the earth's upper mantle then it is entirely likely that magma generation has played an important role in its thermal development by transferring radioactive heat sources along with basalt magma from the deep interior to the surface.

While lack of experimental data on the thermal conductivity of the rocks at high temperatures prevents prediction of the exact amount of

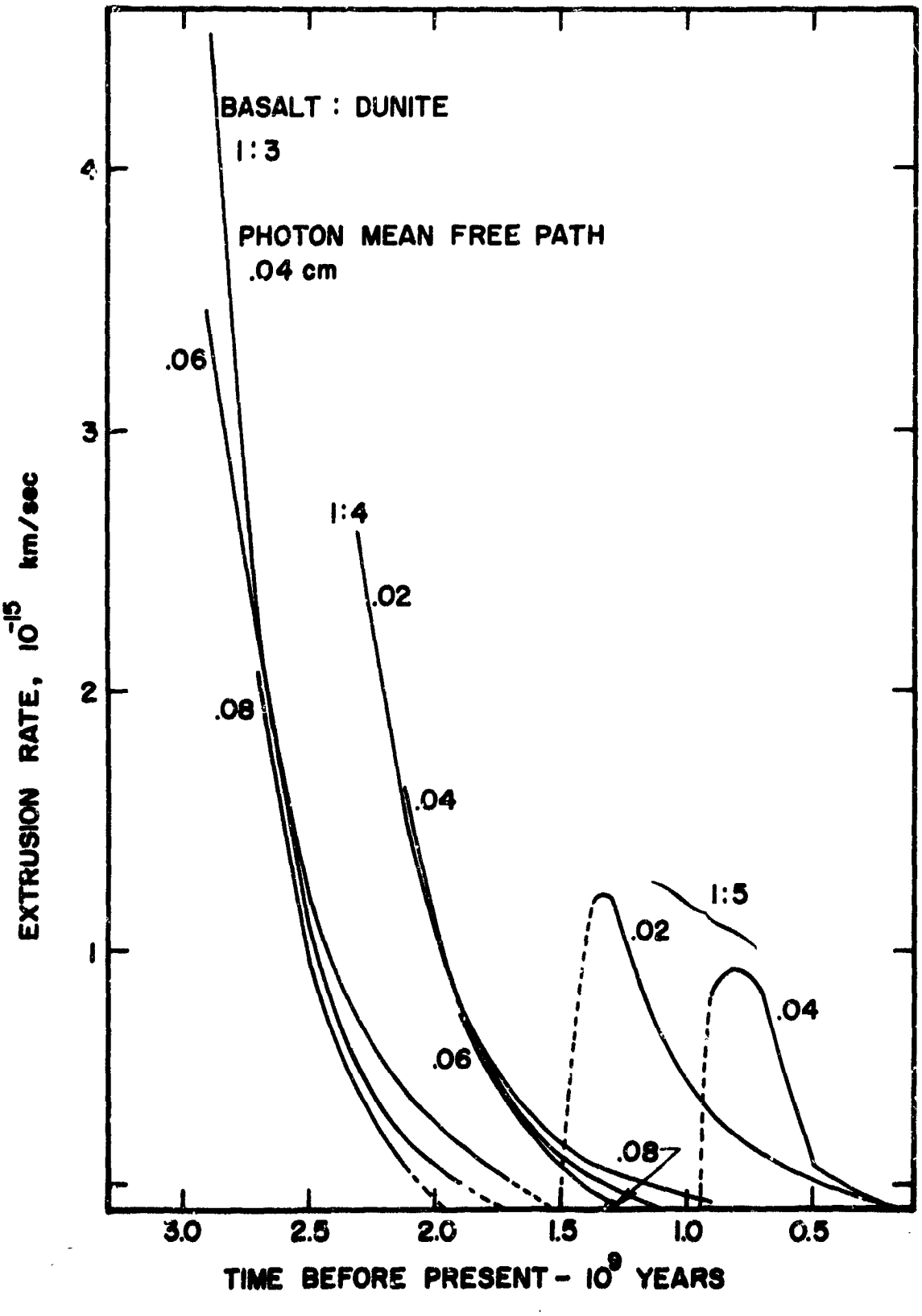

FIGURE 2.25-2 Rate of accumulation of volcanic rocks as a function of time for different photon mean free paths and basalt to dunite ratios.

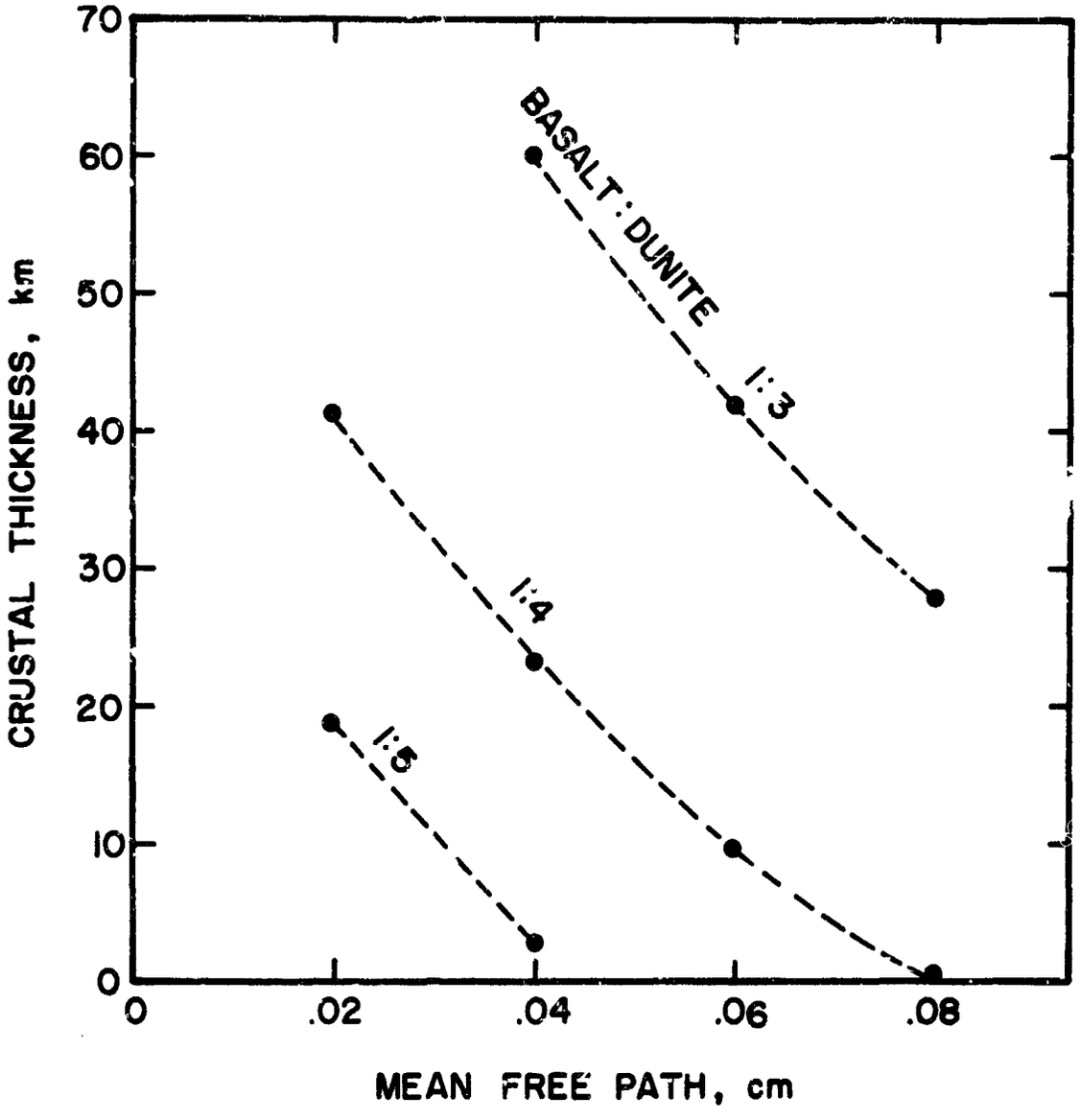

FIGURE 2.25-3 Integrated thickness of igneous rocks as a function of basalt to dunite ratio and photon mean free path, at 273°K for moon with standard parameters.

volcanic activity, we believe that if volcanism has taken place on the moon it reached its maximum intensity within less than 10^8 years and then declined approximately exponentially with a half life of the order of 3×10^8 years. It would appear that if astronauts can obtain a sample of the primeval surface material and an "early" volcanic rock an almost unique estimate of the moon's temperature at the time of formation should be possible.

We have not extended our calculations to a moon of either entirely basaltic or entirely granitic composition for several reasons. In the first place, both of these assumptions appear to us to be incompatible with the observed density. In addition, it would be necessary to predict the manner in which the radioactive isotopes will distribute themselves in various fractions of the basalt or the granite and then set this equivalent to the low melting fraction. This would involve a lengthy detailed study of the same magnitude as was necessary to determine the melting relationships of the "pyrolite" composition. If we recall that the main evidence for a granitic moon results from the hypothesis that tektites are fused samples of the moon's surface, then we believe that there is ample evidence that near-surface differentiation of the primary basaltic magma can form granitic or rhyolitic lavas. This evidence will be discussed in the following chapter.

We have also neglected tidal effects on generation. Kopal (1963) has shown that if the moon could maintain a viscosity of 10^{18} poises it could generate an appreciable amount of heat. The only regions of the earth's mantle where such a low viscosity might be approached is in the neighborhood of upper mantle low velocity zones (McConnell, 1963, 1965) where the melting point of basalt is probably approached. Thus, the only time we would expect the effective viscosity of the moon to drop as low as 10^{18} poises would be when melting was about to begin anyway. Any tidal heating at this time would probably just speed up the already rapid magma generation.

Kaula (1963) has discussed tidal dissipation of energy if the moon had a Q of 100 for distortion (Q is the ratio of the energy stored to the energy dissipated per cycle). He concluded that, compared to radio-

active heating, the rate of tidal heating for the present orbit should be insignificant. While we do not wish to speculate on the past orbits of the moon, it is possible that if the moon were partially molten at some time lower values of Q would cause an increase in tidal dissipation for the present orbit. Presumably, as mentioned above, any significant heating under these circumstances would only act to speed up the expulsion of the basalt phase after the melting temperature was reached.

3. MAGMA MIGRATION

In this chapter we shall be concerned with the mechanics of moving a melt from the "primary" magma chamber where it is generated to a "secondary" magma chamber near the surface of the planet, where it either cools as an intrusive or from which it is erupted as an extrusive.

3.1 EXPULSION OF MAGMA FROM PRIMARY MAGMA CHAMBER

In the discussion of magma generation we pointed out that if a small amount of melt were produced in a region where the pyroxene-olivene mineral assemblage is stable and then the pressure were suddenly decreased to a level where plagioclase, pyroxene and olivene were stable minerals the amount of melt should almost double. Although this behavior would seem to be in agreement with the popularly accepted theory that magma generation results from a sudden pressure release, it has been difficult to envisage how a large enough release can take place. Turner and Verhoogen (1960) have discussed this problem in some detail. Many of the difficulties of the pressure release hypothesis can be eliminated by postulating a local pressure increase prior to the decrease and expulsion of magma. It would appear to us that such a pressure buildup is a necessary result of partial melting of pyrolite at pressures of the order of 20 kilobars; the pressures under which Hawaiian magmas are likely formed (Eaton and Murata, 1960).

The type of process which we envisage taking place is portrayed in Figures 3.1-1 and 3.1-2. Consider a region which is initially below its "solidus" temperature. Upon heating above the solidus temperature, unless some of the liquid can escape, the pressure inside the region will increase rapidly as a result of the volume change on melting. If heating is localized in the neighborhood of the chamber the increase will continue until heating stops, until shear failure extends to the surface, or until an open fracture is formed in the wall rock allowing the melt to escape. Of these possible methods of stress relief the only one which is likely to permit a magma to move to the surface is the open tensile fracture.

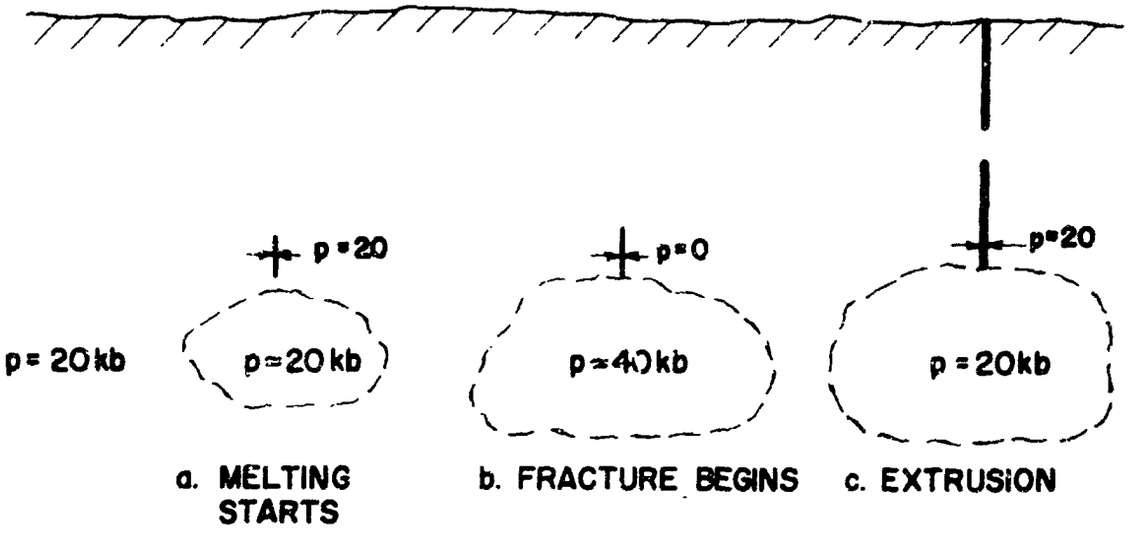

FIGURE 3.1-1 Stages in the generation and release of magma from primary chamber.

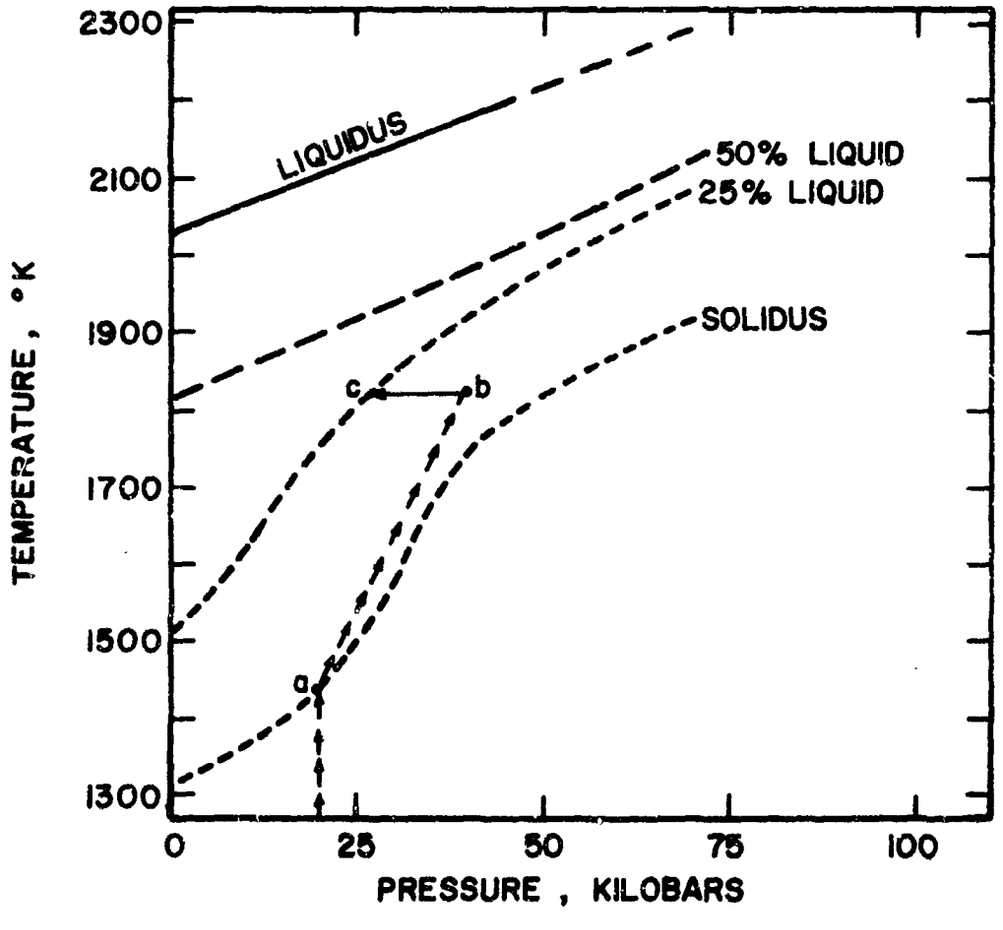

FIGURE 3.1-2 Postulated pressure variations within primary magma chamber during generation and release of magma.

In order to see how such a fracture could be produced let us consider the effects of a pressure increase within a cylindrical or spherical primary magma chamber which is small compared to its depth of burial (Figure 3.1-1). Assuming that the pressure in the chamber and wall rock is p before heating starts and that the walls are rigid enough that appreciable shear stress release cannot take place within the time necessary to cause melting, the stress acting across a radial plane in the wall rock at its contact with the melt will be zero when the pressure in the chamber is 2p (see for example, Sokolnikoff, 1956, p. 287, 395). Once initial fracturing has taken place the tendency for an increase of the melt with any decrease in pressure would be expected to maintain high pressure and cause the facture to continue to propagate toward the surface.

In Figure 3.1-2 we have reproduced part of Figure 2.13-6 showing the predicted melting behavior of pyrolite-1:3. We have indicated by the dashed line (a,b,c) how we would expect the pressure in the system to change as it is heated through its melting range. If the starting pressure were 20 kilobars, above the solidus temperature (point a) the pressure would increase simultaneously until the pressure is great enough to cause tensile fracturing in the surrounding region (b). As rocks are normally very weak in tension this pressure would not be expected to exceed 40 kilobars. As soon as a fracture forms, which is large enough that melt can flow easily into it, the high stresses caused by the melt at the tip of the fracture will cause it to enlarge. As the magma is expelled from the chamber the pressure will tend to drop, but a pressure decrease favors a rapid increase in the melt volume (c); thus the pressure tends to remain high and favors the propagation of the crack and eventual out-flow of magma.

3.2 MAGMA MIGRATION THROUGH DIKES

After leaving the primary magma chamber the movement of a melt is controlled by its viscosity, thermal properties and the pressure gradient. We shall first attempt to derive a simple theory illustrating how these factors interact to influence magma migration and then make

use of available data on the viscosity and other properties of basalt magmas to examine the implications of the theory.

3.21 Factors Influencing Migration Through Dikes

Consider an idealized vertical feeder dike of width 2w connecting a source of incompressible magma at depth with the surface (Figure 3.21-1). Let us choose the densities of the wall rock and the melt to be ρ_w and ρ_m, respectively, the z axis positive upward, and the x axis normal to the walls of the dike. If the magma deforms like an incompressible Newtonian liquid, and the flow is sufficiently uniform that accelerations may be neglected the equations of motion may be written

$$\frac{\partial}{\partial x}\left(\eta(x)\,\frac{\partial v}{\partial x}\right) = \rho_m g + \frac{\partial p}{\partial z} \qquad (3.21\text{-}1)$$

where

v is the velocity
η is the viscosity of the magma
g is the gravitational acceleration
p is the pressure normal to the z axis

To determine the pressure gradient we note that the pressure at a depth h outside the source region for the magma is $\rho_w gh$. If the source region cannot support shear stresses of the order $(\rho_w-\rho_m)gh$, which, assuming a 10 percent volume difference, will be about 10 percent of the total pressure, the hydrostatic pressure in the chamber will be $\rho_w gh$ and the pressure gradient in the column will be given by

$$\partial p/\partial z = -\rho_w g \qquad (3.21\text{-}2)$$

Equation (3.21-1) may then be written

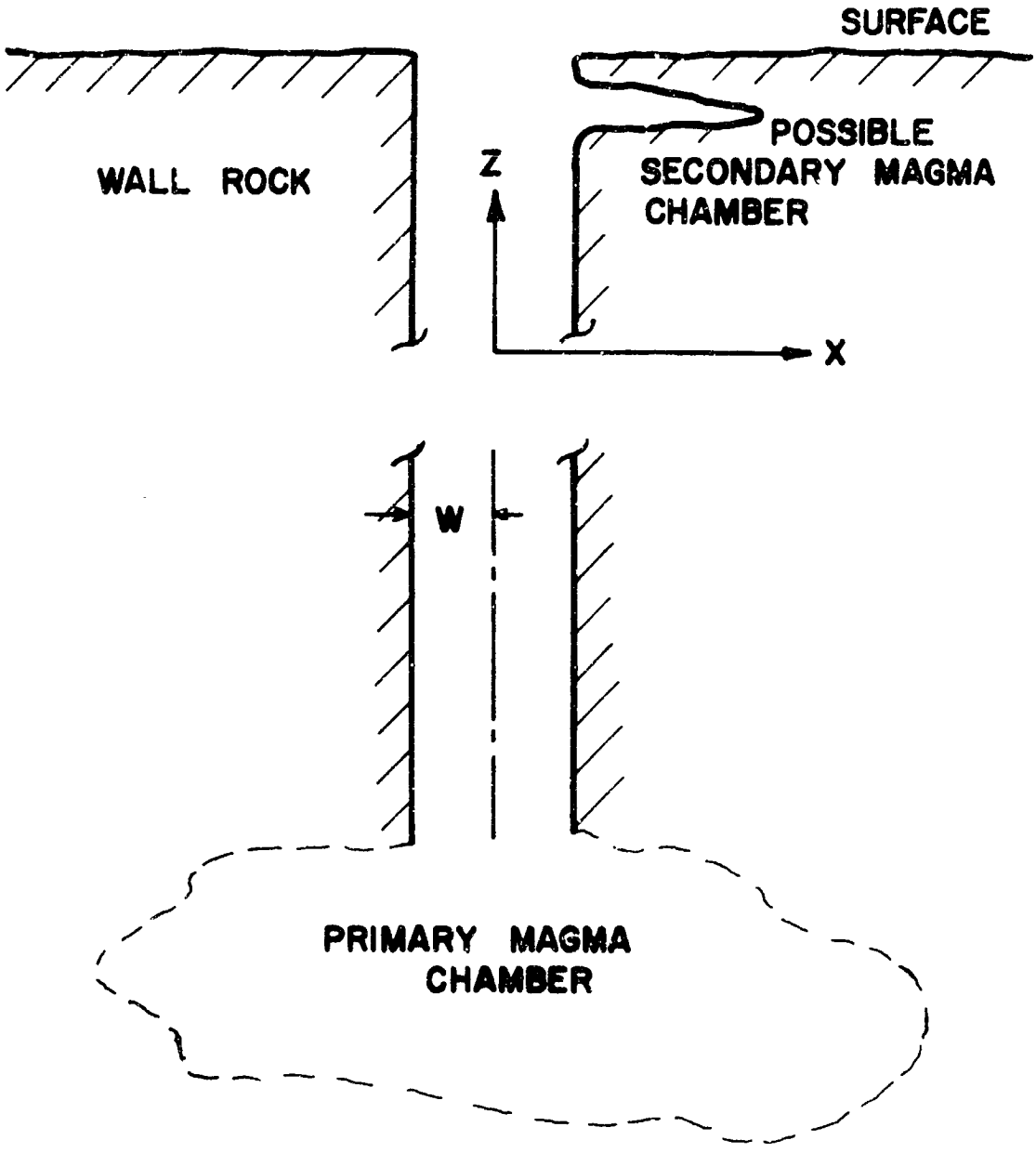

FIGURE 3.21-1 Model for simple dike propagation theory.

$$\frac{\partial}{\partial x}\left(\eta(x)\,\frac{\partial v}{\partial x}\right) = (\rho_m-\rho_w)g \qquad (3.21\text{-}3)$$

$$= \bar{p}_{,z}$$

where $\bar{p}_{,z}$ is then the effective pressure gradient driving the liquid.

Integrating (3.21-3) with respect to x we find that

$$\frac{\partial v}{\partial x} = \frac{\bar{p}_{,z}}{\eta(x)}\int_0^x dx \qquad (3.21\text{-}4)$$

$$= \bar{p}_{,z}\; x/\eta(x)$$

and the rate of heat generation per unit volume is given by

$$q(x) = \eta(x)\,(\partial v/\partial x)^2 \qquad (3.21\text{-}5)$$

$$= (\bar{p}_{,z})^2\, x^2/\eta(x)$$

Thus, if the viscosity is uniform over the width of the dike the greatest power generation will occur near the edges.

The total heat generated over the entire width of the dike is given by

$$Q_\eta(x) = (\bar{p}_{,z})^2\int_0^w \frac{x^2}{\eta(x)}\,dx \qquad (3.21\text{-}6)$$

if the viscosity is uniform everywhere

$$Q_\eta(x) = \frac{(\bar{p}_{,z})^2\, w^2}{3\eta} \qquad (3.21\text{-}7$$

The flow velocity v may be obtained by integrating (3.21-4) once more with respect to x yielding

$$v(x) = -\bar{p}_{,z} \int_0^x \frac{x\,dx}{\eta(x)} + v(0) \qquad (3.21\text{-}8)$$

If we impose the condition that v(x) is zero at the outer boundary, (3.21-8) may be rearranged to

$$v(x) = -\bar{p}_{,z} \int_x^w \frac{x\,dx}{\eta(x)} \qquad (3.21\text{-}9)$$

If the viscosity does not vary this reduces to

$$v(x) = -\bar{p}_{,z}(w^2-x^2)/2\eta \qquad (3.21\text{-}10)$$

If the viscosity is not uniform everywhere the equation (3.21-9) must be evaluated numerically.

The net flux of material, V, through the dike may be obtained by integrating (3.21-9) with respect to x yielding

$$V(w) = \int_0^w v(x)\,dx \qquad (3.21\text{-}11)$$

which for a constant viscosity reduces to

$$V(w) = -\bar{p}_{,z}\, w^3/3\eta \qquad (3.21\text{-}12)$$

Again, if the viscosity is not constant V(w) must be evaluated numerically.

Let us consider a dike whose temperature is sufficiently uniform that the viscosity and temperature do not change appreciably over the width of the dike. Then the total flow can be written

$$V = V(\bar{p}_{,z},\ \eta(T),\ w) \qquad (3.21\text{-}13)$$

and

$$\frac{dV}{dt} = \frac{\partial V}{\partial \bar{p}_{,z}} \frac{d\bar{p}_{,z}}{dt} + \frac{\partial V}{\partial \eta} \frac{\partial \eta}{\partial T} \frac{dT}{dt} + \frac{\partial V}{\partial w} \frac{dw}{dt} \qquad (3.21\text{-}14)$$

In view of our simplifying assumption of relatively uniform viscosity and temperature within the dike, we may write from (3.21-12)

$$\partial V/\partial \bar{p}_{,z} = -w^3\, 3\eta \qquad (3.21\text{-}15)$$

and

$$\partial V/\partial \eta = \bar{p}_{,z}\, w^3/3\eta^2 \qquad (3.21\text{-}16)$$

$$\partial V/\omega w = -\bar{p}_{,z}\, w^2/\eta \qquad (3.21\text{-}17)$$

Now under the assumptions of relative uniformity

$$dT/dt = Q_m/\rho c w \qquad (3.21\text{-}18)$$

$$= (Q_\eta - Q_w)/\rho c w$$

where Q_m is the heat being retained in the melt and Q_w is the heat being lost to the walls by conduction. If the temperature of the magma increases, the walls will begin to melt increasing the effective width. We may write

$$dw/dt = f^2 Q_m/\rho \ell \qquad (3.21\text{-}19)$$

where f is some function of the dike geometry flow rate, etc., which is equal to one if all the heat is used for melting and is zero if no melting takes place. Substituting equations (3.21-15) through (3.21-19) into (3.21-12) yields

$$\frac{dV}{dt} = \frac{-w^2}{3\eta}\left(\frac{d\bar{p}_{,z}}{dt} + \frac{\bar{p}_{,z}}{\rho}\left(\frac{3f^2}{\ell} - \frac{1}{\eta c}\frac{\partial\eta}{\partial T}\right)(Q_m - Q_w)\right) \qquad (3.21\text{-}20)$$

As long as the function γ defined by

$$\gamma = \frac{d\bar{p}_{,z}}{dt} + \frac{\bar{p}_{,z}}{\rho}\left(\frac{3f^2}{\ell} - \frac{1}{\eta c}\frac{\partial\eta}{\partial T}\right)(Q_\eta - Q_w) \qquad (3.21\text{-}21$$

is negative the flow rate will increase.

Let us first consider a fissure through which magma is being driven by a fixed pressure gradient. As long as

$$\left(\frac{3f^2}{\ell} - \frac{1}{\eta c}\frac{\partial\eta}{\partial T}\right)(Q_\eta - Q_w) > 0 \qquad (3.21\text{-}22)$$

the flow rate will increase with time. As the heat of fusion is positive and, except for one important case which will be discussed later, $\partial\eta/\partial T$ is usually negative under constant pressure gradient conditions, the condition for maintaining dike propagation reduces to

$$(Q_\eta - Q_w) > 0 \qquad (3.21\text{-}23)$$

Now we may take as a rough estimate

$$Q_w \sim k(T_m - T_w)/w \qquad (3.21\text{-}24)$$

where T_m and T_w are the temperatures of the melt and wall, respectively. Substituting (3.21-7) and (3.21-24) into (3.21-23) and setting the latter to equal zero yields

$$w^4 \sim \frac{(T_m - T_3)\,3\eta}{(\bar{p}_{,z})^2} \qquad (3.21\text{-}25)$$

If the viscosity is known this should give a rough estimate of the

minimum size fissure through which a magma can move under the effective pressure gradient $\bar{p}_{,z}$. As the wall rock begins to warm less heat will be conducted away and $(Q_\eta - Q_w)$ will tend to become more positive and, once established, the width of the fissure will grow indefinitely until the flow rate is limited by the rate at which magma can be supplied by the reservoir depth.

Let us now consider what will happen when the flow rate is fixed. Then $\gamma = 0$, and

$$\frac{d\bar{p}_{,z}}{dt} + \frac{\bar{p}_{,z}}{\rho}\left(\frac{3f^3}{\ell} - \frac{1}{\eta c}\frac{\partial \eta}{\partial T}\right)(Q_\eta - Q_w) = 0 \qquad (3.21\text{-}26)$$

For the normal decrease in viscosity with increase in temperature the pressure gradient will adjust itself until the heat generated is just equal to the heat lost from the sides, that is until

$$(Q_\eta - Q_w) = 0 \qquad (3.21\text{-}27)$$

If heat is being produced faster than it can be conducted away the temperature of the melt will increase causing the viscosity to drop and the walls of the fissure to melt away. Both these effects will act to make $(Q_\eta - Q_w)$ more negative while decreasing magnitude of the pressure gradient. Thus if a migrating magma encounters a construction or barrier which locally increases the pressure gradient the rate of heat production will increase until the obstruction is assimilated and the gradient returns to its normal value. This process would appear to provide a possible explanation for the extremely uniform widths observed in intrusive dikes. To see whether the predicted effects are of the right order of magnitude we must first consider the viscosity of basalt magmas.

3.22 The Influence of Viscosity on the Migration of Basalt Magmas

3.221 Viscosity as a Function of Temperature

The available data on the viscosity of basalts which we

consider most reliable is summarized in two papers: in the first of these Mackenzie (1957) has presented his own and previously reported work by Bockris, Mackenzie, and Kitchener (1955) on binary mixtures of alkali and alkaline earth metal silicates. These studies showed that there is a small viscosity difference between an alkali metal silicate and an alkaline earth silicate, and that viscosity varies with the silica to metal oxide ratio. They also showed that each of the alkali metals is equivalent in its effect. Similar behavior was found for the alkaline earth metals. Mackenzie has developed an empirical method for calculating the viscosity of an M_2O-MO-SiO_2 system.

In the second paper Turkdogan and Bills (1960) have presented a critical review of work on the CaO-MgO-Al_2O_3-SiO_2 system by Machin and Yee (1948), Machin, Yee and Hanna (1952) and by Kozakevitch (1959). They have also developed in their paper an empirical method of calculating viscosity for a given composition in this four component system.

We have used the data from these two papers to estimate the viscosity variation of the standard basalt component of the pyrolite. For purposes of our estimation, we have simplified the composition of this basalt (Table 3.22-1) to that given in Table 3.22-11. Mackenzie (1957) discussed the discrete ion theory of silicate melts and accounted for the difference between alkali and alkaline earth metal silicates and the equivalency of different alkali metal or alkaline earth cations on the basis of the cation charge. On this basis, and since we believe that iron exists in basaltic magma primarily as ferrous ion, we have lumped the FeO, MgO, and CaO contents of the basalt as MO in Table 3.22-11. The Na_2O and K_2O contents reported in Table 3.22-1 are presented as M_2O in the simplified composition. We will first assume a water free melt and will ignore the minor constituents of basalt such as MnO, P_2O_5, and TiO_2. It is evident from the values in Table 3.22-11 that the MO/M_2O ratio is better than 10/1. The data presented by Mackenzie indicates that this amount of M_2O would decrease the viscosity which we would have calculated assuming the metal oxide content as all MO by only a few percent. Therefore we have made this assumption and used the correlations of Turkdogen and Bills (1960) to estimate the silica equivalent of alumina based on the

TABLE 3.22-1

Standard Basalt Composition

Oxide	Wt %		Moles/100g
SiO_2	48.3		.805
MgO	7.86		.195
FeO	8.89	11.59	.162
Fe_2O_3	3.02	as FeO	
Al_2O_3	14.35		.141
CaO	10.58		.189
Na_2O	2.43		.039
K_2O	.88		.009
MnO	.19		
P_2O_5	.31		
H_2O	.83		
TiO_2	2.33		

TABLE 3.22-11

Simplified Basalt Composition

	Moles	Mole Fraction
SiO_2	.805	.523
Al_2O_3	.141	.091
M_2O	.048	.031
MO	.546	.354

molar ratio $Al_2O_3/M_2O + MO$.

From data in their paper we have drawn the curve given in Figure 3.22-1 as our estimate for the variation of the viscosity of a typical "dry" basalt in the temperature range from 1200° to 2300°K. We have also shown on this figure some curves taken from Eitel (1965) representing work by Euler and Winkler (1957) who compared their own measurements of viscosities of silicate melts with much earlier studies. While we cannot assume that these melts were volatile free the agreement with our estimate for a "dry" melt is good.

3.222 Viscosity as a Function of Pressure

We have found no references to the quantitative effect of high pressure on the viscosity of liquid siliates, but Steele and Webb (1963) have recently reviewed the existing high pressure studies on liquids in general. The viscosity of most substances increases with pressure at constant temperature. The rate of change of viscosity generally increases with increasing pressure. This behavior is the opposite of that observed for most properties as pressure is increased.

Although many empirical relationships have been reported (Partington, 1951) for the variation of viscosity with temperature and pressure, we have found no reasonable basis for applying these to our situation. Several attempts have also been made to develop relationships on a theoretical basis (see for example the work of Glasstone et al., 1941, and of Macedo and Litovitz, 1965).

Theoretical developments utilize the concept of free volume in a liquid. One view of a liquid is that the essential difference between it and a solid can be regarded as the introduction of holes; the volume change on melting is then taken to be proportional to the number of holes and is frequently called the free volume.

Now we do know the changes in melting temperature with pressure for several silicates, and these are related to the volume change on melting by the relationship

$$\frac{dT}{dP} = \frac{\Delta V}{\Delta S}$$

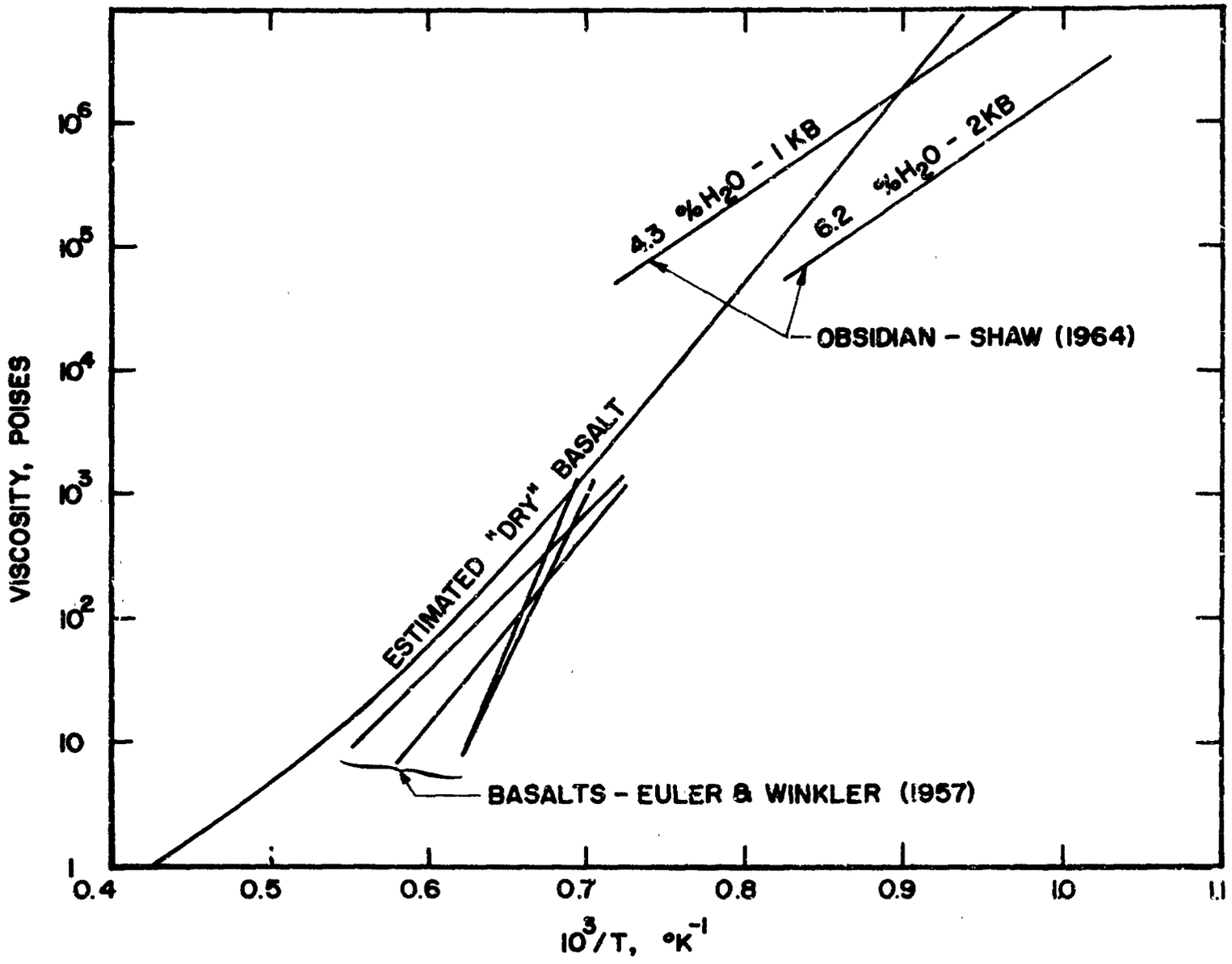

FIGURE 3.22-1 Viscosity of basalt as a function of temperature.

Thus, if we assume that the entropy of melting remains constant with change in pressure we can calculate free volume as a function of pressure. We have tried to make use of this information together with the theoretical equations of Eyring et al. and of Macedo and Litovitz to estimate the change in viscosity of a silicate liquid in going from 1 atm to 50 kb pressure at constant temperature. As our estimates differ by orders of magnitude, we conclude that no useful value can be derived by this means at the present time.

3.223 The Effect of Dissolved Volatiles on Viscosity

Of the numerous volatiles present in basalt lavas, water is generally recognized as the major species and is therefore the one with which we shall concern ourselves. Representative extrusive basalt analyses show less than one percent water, but the amount present prior to eruption is not yet well established.

It has recently been reported by Engel and Engel (1964) that basalt flows dredged from the deep ocean do not show the vesicular character generally found in surface flows. Apparently as a result of the pressure under which the flow occurs no gas bubbles are formed. This might be interpreted as evidence for a total volatile content corresponding to a vapor pressure of less than 0.5 kilobars, since this represents the pressure under 5 kilometers of water.

With this pressure as an upper limit it is possible to estimate the water content of basalt based on laboratory studies of water-containing silicates. Friedmen, Long and Smith (1963) have studied the viscosity and water content of rhyolite glass. In their Figure 13 they present water pressure vs. temperature curves for various weight percent water. By extrapolation we find that at 1500°K a pressure of 500 atmospheres corresponds to about 0.7 weight percent water. Shaw (1964) has recently reviewed the data on water solubility in silicate melts in conjunction with preparation of a theoretical paper. From his Figure 7a which summarizes experimental data of several workers on the albite-water system, we find that 500 atmospheres pressure correspons to about 0.05 mole fraction of water or roughly 0.4 weight percent water at 1300°K.

Again in his Figure 7e for the system $CaAl_2Si_2O_6$ - SiO_2-H_2O in the temperature range 1000 - 1600K we find that 500 atmospheres corresponds to about .07 mole fraction or about 0.5 weight percent.

We conclude from these data that the actual water content of basalt before penetrating the earth's crust is less than one percent by weight. A similar conclusion is voiced by Einarson (1949) based on the explosive behavior of magmas and on a critique of analytical errors which can favor high analytical results on glasses.

The water content can affect viscosity in two ways: either as dissolved water or an entrained gas bubbles. The effect of dissolved water is to decrease the viscosity. Friedman et al., (1963) studied rhyolite to water contents of one weight percent and at temperatures of 770-1070K. They observed that the change in viscosity decreases with increasing water content and temperature. At 1060°K their data indicate a viscosity decrease of 2-3 orders of magnitude with addition of one weight percent water. Extrapolation of their data to 1500°K indicates a change in viscosity of much less than one order in magnitude on addition of the one weight percent water. Recall also that the loss of volatiles will represent only a fractional change in the total volatile content. We conclude from these data that at temperatures of 1300-1500°K corresponding to temperatures observed in basalt flows, the basalt viscosity will increase with loss of volatiles by only a few hundred percent at most. We do not expect that any order of magnitude changes in viscosity are likely due to changes in volatile content of the basalt.

We show on Figure 3.22-1 some recent work of Shaw (1964) on obsidian at relatively high water content which indicates an order of magnitude change in viscosity for two weight percent change in water content.

3.23 Comparison of Predicted Dike Widths with Field Evidence

Using the dry basalt curve of Figure 3.22-1 as a reasonable approximation to the viscosity of the basalt magmas, we may determine whether the simple theory developed for the flow of magma through a fissure predicts dikes of the size actually seen on earth.

As the viscosity decreases with increasing temperature, we may make use of equation (3.21-25) to estimate the minimum stable dike width.

At 1500°K the viscosity would be 4.5×10^2 poises.

Choosing $T_w = 300°$

$p_{,z} = .3 \times 10^3$ dynes/cm^2

$k = 5 \times 10^{-2}$ joules/cm °K

$= 5 \times 10^5$ ergs/cm

and substituting into (3.21-25) yields

$$w^4 = 9 \times 10^6 \text{ cm}^4$$

$$w = 55 \text{ cm.}$$

As w is the half width of the dike, this would indicate for a melt of this temperature and this viscosity, the narrowest fissure which could persist for a long distance would be about one meter wide.

At 1300°K the estimated viscosity would be about 1.8×10^4 poises and the calculated minimum width would be about 2.6 meters. For Icelandic basalt flows, whose viscosities are normally estimated to be around 10^4 poises, Th rarinsson (1965) has estimated "4 $\pm$ 2 meters as a reasonable width for eruption fissures 100 meters below the surface." Bodvarsson and Walker (1964) computed the average width of 1000 dikes in East Iceland to be around 3 meters, and the average of 450 dikes further south to be 3.7 meters. Thus the agreement of the theory with field observations would seem to establish the validity of the former.

3.24 Termination of Migration by Exsolution of Volatile.

In our above discussion of viscosity we pointed out that formation of gas bubbles and vesiculation begins at pressures of less than 500 atmospheres. In our opinion bubbles may be expected to have a profound effect on the viscosity and ultimately may bring about termination of the dike. Let us first consider the effect of the bubbles on the viscosity.

The effect of entrained gas on viscosity was examined by Einarsson (1949) in the laboratory in an attempt to interpret apparent order of magnitude differences observed in lava flows. He studied the viscosity

of an air-glycerine mixture and found that viscosity markedly increased with air content providing the air was well dispersed. The air bubbles were of a diameter of 0.1 - 0.2 mm and apparently surface tension was such that the bubbles did not deform appreciably during flow. Now it is well known that solid particles dispersed in a liquid will tend to increase viscosity. For spheres of nearly equal size, relative viscosity (η_r) is related to concentration of the spheres in volume fraction C by the expression (Roscoe, 1953)

$$\eta_r = (1 - 1.35c)^{-2.5} \quad (\text{for } C > 0.10)$$

For a suspension of spheres of very diverse sizes

$$\eta_r = (1 - C)^{-2.5}$$

representing a slightly less rapid increase in η_r with increasing concentration of spheres. The latter equation indicates a five-fold viscosity increase for C = 0.5 and 32-fold for C = .75. This indicates very rapid rise with increasing gas content providing the gas bubbles behave as solid spheres and are of unequal size. Possibly the nucleation and growth process may yield a more equal size distribution of particles and thus a more rapid change with gas content.

If we assume a one weight percent concentration of volatiles, this content represents water sufficient for over a 1000 fold increase in magma volume at atmospheric pressure. Thus a 2-3 fold volume increase at a hundred atmospheres or so pressure is easily visualized without large changes in water content of the magma. These data indicate that an evolution of finely dispersed gas in a viscous magma might readily increase viscosity of the magma by an order of magnitude or more.

It was mentioned above that if an increase in temperature resulted in a large increase in viscosity the flow would not be able to take place. If a melt enters a region where the pressure is low enough that the volatiles begin to come out of solution, viscous heating will increase, this will tend to increase the bubble content. Thus the stable flow theory should break down. For the average basaltic magma we would expect this to happen under pressures of the order of half a kilobar, corresponding

to depths of a couple of kilometers on the earth. With its upward motion being resisted, the melt would probably move laterally lifting the overlying rock and forming a sill, lacolith or "secondary" magma chamber.

We conclude from the above discussion that the primary effect of volatiles on viscosity of basalt will most likely be found as the basalt reaches a depth which is shallow enough that it suddenly finds itself "super heated" with respect to its volatile content. Bubble formation should occur rapidly throughout the viscous mass leading to almost an exponential rise in viscosity with increasing volume fraction of gas and possibly complete stoppage of the flow. In the viscous melt one can imagine that coalesence of the bubbles would be relatively slow thus requiring long times for the magma and gas to separate. As the gas bubbles coalesced and grew, they would become more deformable and the mass might again decrease in viscosity causing further migration and perhaps a volcanic eruption.

3.3 COMPARISON OF TERRESTRIAL AND LUNAR MAGMA MIGRATION

From the above arguments we would conclude that there is not likely to be any major difference in the mechanism of removing magma from a primary chamber on the earth or on the moon.

The stable width of a fissure is governed by the pressure gradient, and the temperature dependence of the viscosity. From equation (3.21-25) it appears that as a result of the lower pressure gradient a melt on the moon with the same temperature and viscosity as on the earth will require a fissure which is $\sqrt{6} \sim 2.5$ times as wide, to continue flowing. From equation (3.21-12) we would predict that the greater width of the dike would more than make up for the lower pressure gradient and would result in a flow in the early stages which is 2.5 times as great as a comparable one on the earth.

As termination of migration due to exsolution of volatiles is controlled mainly by pressure and volatile content, a melt on the moon would be expected to form a magma chamber and begin crystallization about six times deeper on the moon than similar magmas on the earth. This could have a very significant effect on the mechanics of subsequent eruption and on the shape and size of the volcanic features at the surface.

4. MAGMA CRYSTALLIZATION

4.1 INTRUSIVE CRYSTALLIZATION

If the hypothesis about termination of upward migration by exsolution of volatiles is correct, it would appear that the entire subsequent history of intrusion and extrusion of melts may be controlled by their volatile content. Once an upward flowing basalt magma encounters pressures low enough , the water and other volatile gases begin to nucleate in small bubbles, thus tending to plug the upward flow. Now the magma might be expected to spread horizontally forming what could be called a sill, lopolith, or "secondary" magma chamber. The volume of the intrusive would be accomodated by lifting the overlying rocks and causing the phenomenon known as tumescence to be observed at the surface. On the moon, formation of horizontal intrusion would be expected to begin at the same pressures as on the earth and therefore at depths six times as great: (i.e. on the order of tens of kilometers). It would appear that the dimensions of this horizontal intrusion would be controlled by the amount of melt available and the strength of the overlying rocks. At the present time we do not have any firm grounds for predicting whether such an intrusive would be larger or smaller than a similar feature on earth. This problem would require further study.

As crystallization of the melt progresses, the volatiles will become concentrated more and more in the residual liquid. As crystallization will act to supply heat to the system keeping the temperature high, the pressure in the chamber will continue to increase until one of several events takes place.

One possibility is that wall rocks are strong enough to contain the pressure build up, and when low enough temperatures are reached, the gas volume will decrease again. This is most likely to occur in a relatively small, deep intrusive.

A second possibility is that if the volatiles are able to collect near the roof of the chamber, the overlying rocks will be permeable enough to allow them to escape through fumaroles. This is likely to occur in low viscosity melts which cool very slowly.

If the pressure builds up enough to cause tensile fractures large enough for a stable dike configuration to be maintained, a low viscosity melt may become mobile again and either form a new chamber closer to the surface or be extruded as a flow.

If the viscosity of the residual liquid is so high that the bubbles cannot agglomerate and so high that the stable dike configuration requires a large fracture and a very large pressure gradient for flow to take place, any fracture formed will become, in effect, self-sealing. In this event the pressure will continue to build up until the strength of the overlying rock is insufficient to contain it and violent explosive eruptions will result. This type of eruption is the more likely if cooling has proceeded to such an extent that the remaining liquid is relatively acidic. All other factors being equal, it would appear that under lunar conditions the lower gravity should result in slightly less efficient bubble agglomeration and a larger stable dike size, both of these factors may cause more explosive activity than on the earth. The greater thickness of the overlying rocks might also act to contain the melt slightly longer, resulting in a more acidic residual melt and a greater tendency towards explosive activity.

It should be emphasized that while the above speculations appear to be qualitatively consistent, both with our models of magma behavior developed in the preceeding chapters and with observational evidence, it has not been possible within the scope of the program to extend the detailed mathematical analysis to a study of the dynamics of eruptions in order to either confirm or refute them.

4.2 COOLING OF EXTRUSIVES

As we now are convinced that the nature of the actual volcanic eruption is controlled more by conditions existing in the secondary magma chamber rather than deeper in the mantle, we see no reasonable grounds for predicting the detailed form of extrusives without first developing an adequate quantitative model to describe the interaction between the cooling melt within the secondary chamber, its volatile constituents, and the surrounding rocks.

As the composition and degree of vesiculation is controlled by the

events within the secondary chamber, we would expect a similar spectrum of mineral assemblages to be formed from the differentiation of basalt magmas on the moon as are formed on the earth. Simple preliminary calculations of the surface cooling of an extrusive has indicated that a lava flow on the moon, which can only lose heat from its surface by radiation, will not cool much more slowly than a similar flow on the earth. Thus any significant mineralogical changes as a result of the high vacuum should be confined to the uppermost few centimeters of the flow.

Because of the absence of an atmosphere, we would not expect as wide a variety of surface textures on lunar extrusives as their terrestrial counterparts. Some minor differences such as the degree of vesiculation and welding may exist, but we believe that it would be premature at this time to claim that lava flows on the moon are either more or less vesicular than those on the earth. More efficient bubble agglomeration and hence greater loss of volatiles resulting from a larger volume cooling more slowly might offset the increased vesiculation due to the high vacuum on the surface.

4.3 VOLCANIC ELECTRICITY

Electrical activity is another facet of volcanism which may exert some control on deposition of volcanic material. It has long been appreciated that the clouds formed as the result of volcanic eruptions are often highly electrified and that they can sometimes produce almost incessant lightning, comparable with the most violent thunderstorms.

Our understanding of the mechanism primarily responsible for the electrification of both the thundercloud and the volcano cloud has been quite limited. It has, however, been generally assumed by scientists that in both kinds of clouds the principle electrical charging process arises from the falling of charged particulate matter.

In the case of the thunderstorm it has been assumed that heavy, fast falling particles such as rain, sleet, or hail acquire one sign of electricity while small cloud particles acquire an equal and opposite charge. This initial charge separation process is then followed by a subsequent large scale charge separation process in which the fast falling

particles fall away from the slower falling particles, thus doing electrical work and creating an electric field.

Until the present time the prevailing view of the cause of electrification of the volcano cloud has been quite similar to the assumed mechanism for thunderstorm electrification. In the past, it has been assumed that big 'ash' (tephra) particles acquire an electric charge of one polarity while the smaller particles acquire an opposite charge and that as the result of their different terminal falling velocities they generate an electrical dipole.

If the generation of electrification in a volcano cloud depends on a process such as that described above, it seems quite clear that a volcano eruption on the moon could not generate charge. All evidence suggests that there is no atmosphere on the moon, and in the absence of a gas, big particles and little ones would all fall at exactly the same velocity and therefore no charge separation process would take place.

In a recent paper Anderson et al.(1965) describe atmospheric electrical measurements carried out from ships and from an airplane of the electrified cloud over the new volcanic island, Surtsey, off the south coast of Iceland. The observations and their interpretation shed some light on the nature of the electrification processes resulting from volcanic activity and shed considerable doubt on the mechanism of electrification that has generally been assumed. These new findings, therefore, have a considerable bearing on our speculations concerning the nature of electrification in different environments and it appears worth considering how these new observations affect our thinking about the possible electrical processes of volcanos on the moon.

The recent observations at Surtsey are of particular interest in connection with volcano electrification on the moon for they show that in the case of this volcano, the gases have a high density of space charge as they issue from the crater and that the differential settling of charged particles plays a small or negligible role in electric charge generation. The observations at Surtsey shed considerable doubt on the previously assumed mechanism of volcano charge generation and suggest that even though there is no atmosphere, volcanos on the moon could be

strongly electrified.

The conclusion that volcanos on the moon would necessarily generate charge is of course by no means warranted by the observations on Surtsey. As the article makes clear, it is possible that the strong electrification observed at this volcano may well arise because of subterranean interactions between the hot lava and the sea water such as Blanchard (1964) has observed in the laboratory. If the electrification at Surtsey is being caused by the sea water, it is quite possible that a volcano on the moon might be neutral, for certainly no sea water is present.

If we are to draw conclusions concerning the possibility of volcano electricity on the moon, it appears desirable to improve our knowledge of the mechanism by which volcanos on the earth produce their charge. At the present time we know that volcanos on earth far removed from the ocean are also electrified but we do not know whether these volcanos produce charge from a charge separation process taking place in the atmosphere or below the surface of the earth Accordingly, it appeared desirable to carry out further measurements on land volcanos such as Irazú, which was recently active in Costa Rica. During February, 1965, we attempted to obtain such information from the volcano Irazú in Costa Rica which had been erupting intermittently up until several days before our party arrived. Although no eruptions took place during the ten day field study, several commercial photographs were obtained which appeared to show electrical activity taking place within the crater. While the evidence presented by these photographs is not conclusive, it would seem to indicate that here also the particles were already charged as they left the crater. It would appear than that particles expelled from lunar volcanos are likely to be electrified and the key to understanding this electrification will have to come from a better understanding of the mechanics of eruption.

4.4 CONCLUSION REGARDING MAGMA CRYSTALLIZATION

We conclude on the basis of the above arguments that horizontal sills or lopoliths are to be expected on the moon at depths of the order of tens of kilometers. These sills are likely to serve as secondary magma chambers which can supply volcanos with more acidic melts upon partial crystalliza-

tion. While this prediction would seem to be in line with the views of O'Keefe (1963), Lowman (1963), and others who believe that tektites represent fused samples of the lunar maria, we must point out that to make this prediction more quantitative, extension of the type of analysis we have used in the previous chapters to the study of the interaction between volatiles, melt, and surrounding, rock is required. Such a study could also shed light on the mechanism of electrical charge separation which apparently takes place within the vent of volcanos.

5. BEHAVIOR OF VOLATILES AT THE SURFACE

We have already discussed the manner in which volatiles might affect the rheological properties of the melt and mentioned their role in explosive eruptions. To consider the transition between the magma chamber and the surface, a better understanding of the interaction between the volatiles and the melt is required in order to have any reasonable grounds for predicting the difference between lunar and terrestrial phenomena. Once the volatile elements become separated from the melt, it is somewhat easier to predict their subsequent behavior and to determine whether they are likely to remain at or near the present lunar surface. We shall first consider those substances such as H_2O and CO_2 which exist as gases at relatively low temperatures and are normally reported in analyses of terrestrial volcanic gases. We shall then discuss the possible importance of such substances as metallic oxides and halides which vaporize at lava temperatures.

5.1 COMPONENTS WHICH ARE VOLATILE AT LOWER TEMPERATURES

If the content of volatile species in lunar magmas is of the same order of magnitude as the content observed in terrestrial magmas after cooling as intrusives or as extrusives, we would expect greater quantities of these species to be volatilized during volcanic activity on the moon.

If these liberated volatiles still remain on or near the surface, they will be valuable both as clues to the geologic history and as potentially valuable natural resources. Based on the assumption that differentiation on the moon is comparable to that on the earth several studies have been made to estimate whether appreciable quantities of water or other volatiles should remain just below or on the moon's surface.

Hapke and Goldberg (1965) have evaluated the possibilities of permafrost layers at shallow depths on the moon as a function of the permeability of lunar "soil". They concluded that the presence of permafrost is of marginal possibility in the equatorial regions. In the polar regions, however, they concluded that if juvenile water had diffused upward through a permeable soil there is a good possibility of finding permafrost

within a few meters of the surface.

Watson et al, (1961, a, b) considered the loss of water from the lunar surface to be limited by the rate of evaporation from "cold traps" formed by permanently shadowed areas having a temperature of 120°K or less. They concluded that ice should now exist in such areas but other magmatic volatiles such as SO_2, CO_2, H_2S etc. will not be trapped as solids by this process. In reaching this conclusion, however, they took account only of the vapor pressure of the pure solid phases and not of any gas hydrates which might be formed.

As it is known that the partial pressure of many gases over their hydrates is much less than the vapor pressure of the pure substance in solid form it appears worthwhile to re-examine the possibility of finding volcanic gases on the lunar surface in the form of their solid hydrates. Before considering these hydrates, however, it will be desirable to review the properties of the various forms of pure ice and their predicted stability on the lunar surface.

5.11 Properties of Ice at Low Temperatures

In making their estimate of the rate of evaporation of ice, Watson et al. have used a value of about 1.4×10^{-12} mm of Hg for the vapor pressure at 120°K. This estimate is based on the data of Washburn (1933) for the vapor pressure of hexagonal ice extrapolated from much higher temperatures. The validity of this extrapolation for hexagonal ice has been generally confirmed by Engelke (1965) who has made independent estimates of the vapor pressure from the calorimetric data of Giauque and Stout (1936). Their work further indicates that no phase changes take place in ice when it is cooled from 0°C to low temperatures under laboratory conditions. However, according to the model of Watson et al, the ice is not cooled from 0°C but is first formed at low temperature. Under these conditions, several investigators have found that a cubic form of ice is formed in the temperature range from about 150°K to 180°K and an amorphous ice is formed below 150°K. These results, based on electron-diffraction, X-ray diffraction, and calorimetric investigations, have recently been reviewed by Blackman and Lisgarten (1958) who point out that none of the calorimetric investigations give any

indication of the transition between cubic and hexagonal ice. The heat of transition between these two phases is therefore probably very small and the vapor pressure of cubic ice is probably close to the extrapolated value for hexagonal ice.

For the transition at about 150°K from amorphous to crystalline ice (probably cubic although this was not ascertained), various investigators have obtained values ranging from 2 to 16 calories per gram for the heat evolved. The lower values are considered least accurate because the ice being measured was not all in the amorphous form. However, even if a value of 16 calories per gram is accepted it is too small to make a significant difference in the extrapolated vapor pressures for the purposes of the present estimates.

5.12 The Clathrate Gas Hydrates

In reaching the conclusion that volcanic gases such as SO_2, CO_2, and H_2S will not be found on the lunar surface, Watson et al, (1961b) took account only of the vapor pressure of the pure solid phases and not of any possible hydrates which may be formed. Miller (1961) has measured the partial pressure of gas over several hydrates at low temperatures and has estimated the possibility of finding gas hydrates on a number of the planets and their satellites. He concludes that there is a good possibility of finding methane hydrate and similar hydrates on some of the other members of the solar system. He does not, however, specifically consider the case of the moon.

The chemistry of the clathrate gas hydrates has recently been reviewed by Barrer and Stuart (1957) and by van der Waals and Platteeuw (1959). The stability of various gas hydrates in the solar system has been discussed by Miller (1961).

Figures 5.12-1 and 5.12-2 show the vapor pressures as functions of temperature in the vicinity of 120°K for hexagonal ice, and for several volcanic gases and their hydrates. The values for hexagonal ice is extrapolated from the data of Washburn (1933). The lines for CH_4 hydrate CO_2 hydrate, and SO_2 hydrate are estimated from the vapor pressure equations given by Miller (1961). The line for H_2S hydrate is based on an equation given by Mellor (1930). The vapor pressure lines for pure

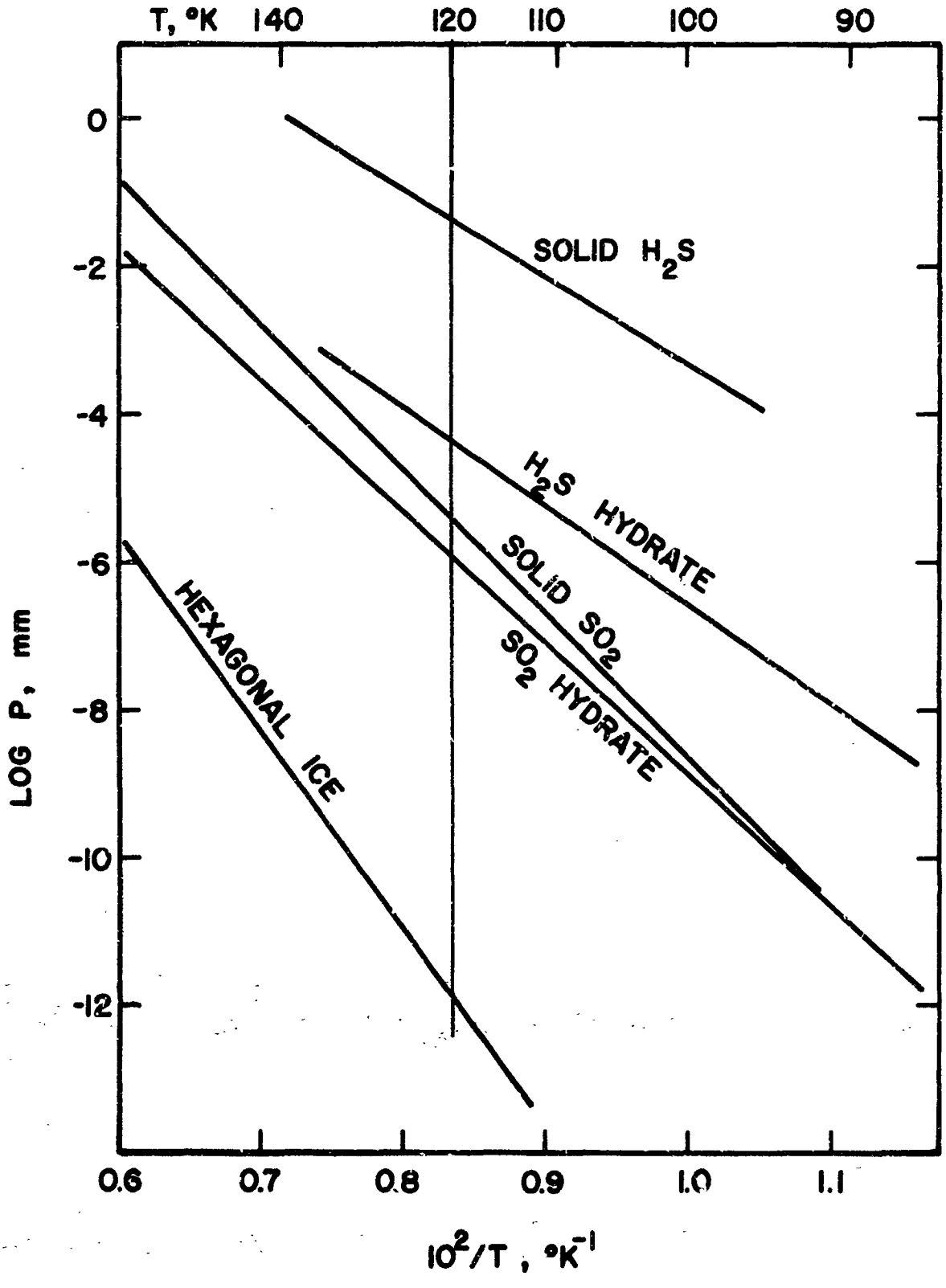

FIGURE 5.12-1 Vapor pressure as a function of temperature for SO_2, H_2S and their hydrates — compared with hexagonal ice.

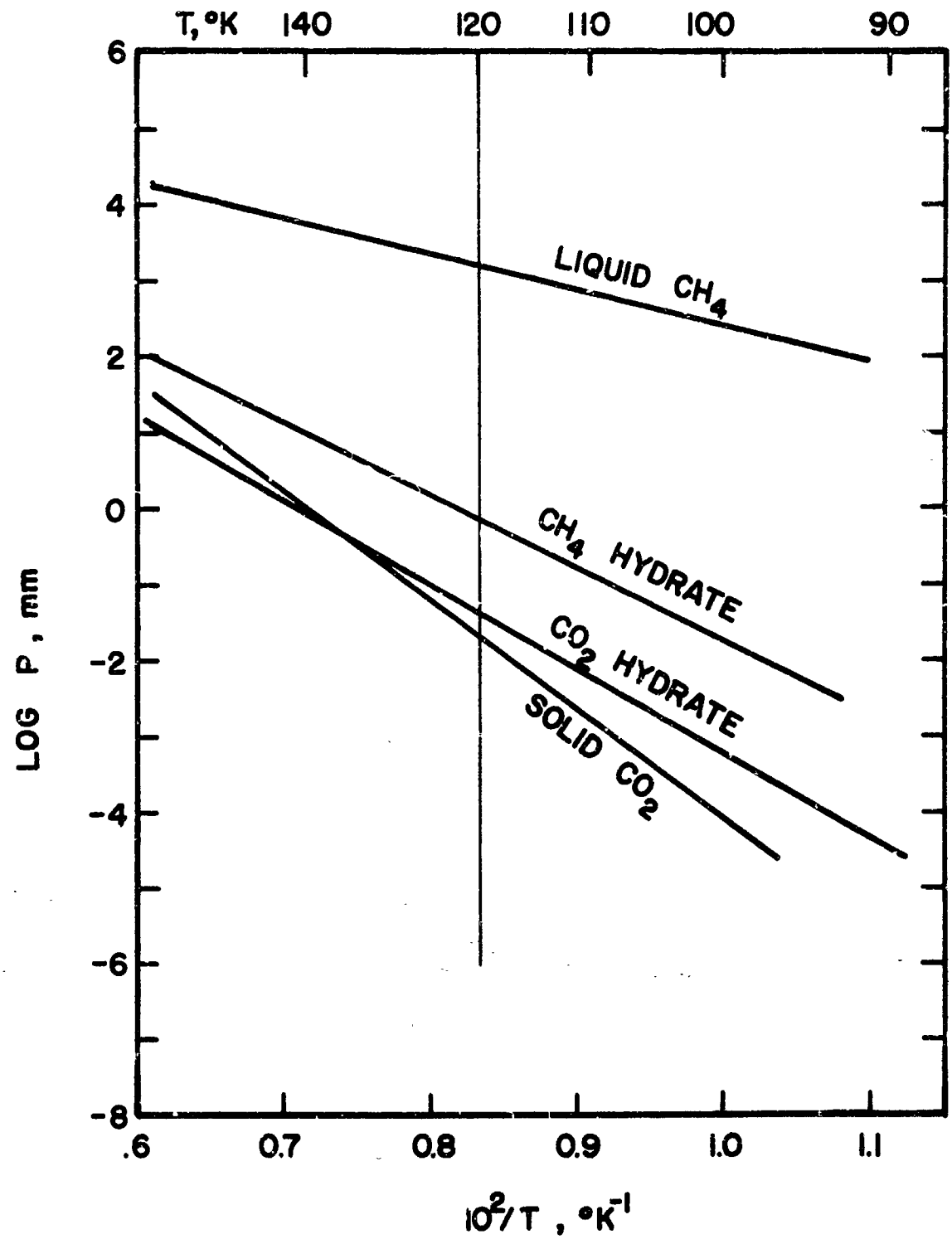

FIGURE 5.12-2 Vapor pressure as a function of temperature of CH_4, CO_2 and their hydrates.

SO_3, CO_2, H_2S, and CH_4 are based on the compilation of Stull (1947). It should be noted that all these lines involve a large extrapolation of the measured data to low temperature and pressure.

These results indicate that the degree of stabilization of these volcanic gases by hydrate formation is somewhat variable. The vapor pressure of CH_4 and H_2S hydrates at 120°K are approximately 1,000 times less than that of the pure substances. The vapor pressure of SO_2 hydrate is only slightly less than that of solid SO_2 and the curves appear to cross in the region of 90°K. With CO_2 the crossover occurs somewhat above 120°K. Because of the nature of the original data and the large extrapolations involved, however, the reality of these crossovers is highly questionable.

In any event it is evident from Figure 5.12-1 that the equilibrium vapor pressure of SO_2 hydrate, the most stable of those considered, is approximately six orders of magnitude higher than that of hexagonal ice. This indicates that hydrate formation has too little stabilizing effect on any of these gases to significantly affect the conclusion of Watson et al. that they will not be retained on the lunar surface.

5.2 SUBSTANCES WHICH VAPORIZE AT LAVA TEMPERATURES

There appears to be a considerable amount of evidence that vaporization of such substances as metallic oxides and halides may be responsible for many of the effects normally associated with volcanism.

5.21 Evaporation from Lava Fountains, Pools and Flows

Still and motion pictures of eruptions on the volcanic island, Surtsey, in February 1964 show that when fountains of molten lava are active, a dense cloud of dark smoke forms that is carried off by the wind (see Figure 5.21-1). More recent observations of this volcano reported by Bjornnson in the summer of 1964 describe a similar phenomenon in which a cloud of dark smoke was observed to form downwind of the quiet lake of molten lava that filled the crater.

These dark clouds, except for their color are quite similar in location and appearance to the clouds of white steam from erupting geysers and from heated pools in geothermal areas. Resemblance between the steam clouds and the volcanic clouds is so pronounced that they seem

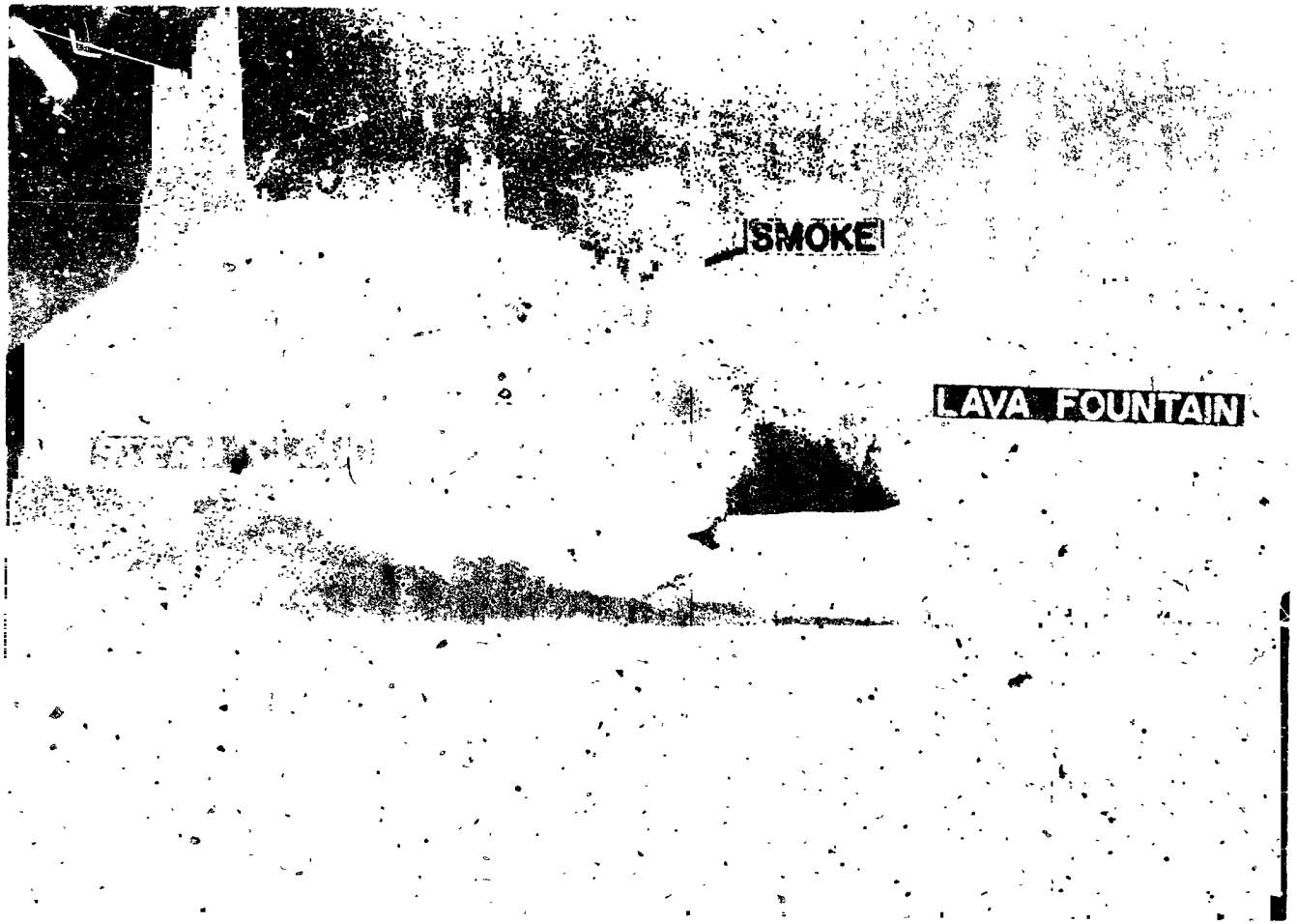

FIGURE 5.21-1 View of the new island Surtsey with cloud of dark smoke above lava fountain. White plume in foreground is steam cloud caused by contact of lava flow with sea water. (Photo by Sigurgeir Jónasson)

to be formed by a similar mechanism: i.e., the hot lava has a high enough vapor pressure for appreciable quantities of it to evaporate. Upon mixing with the much cooler atmosphere the vapor then condenses to form visible aerosol particles in much the same way that condensing water gas forms the visible aerosol particles called "steam". Since water and other substances condense this way to form aerosols, it seems reasonable that the lava vapors may condense in a similar manner either as vitreous droplets or as small crystalline particles.

To see whether significant evaporation would be expected from basalt, existing data on the vapor pressures and evaporation rates of the pure metal oxides found in basalt were examined. Some of these data are shown in Figures 5.21-2 and 5.21-3, respectively. Of the oxides, vapor pressures of Na_2O and K_2O are particularly high. At 1400°K the calculated rate of evaporation for pure K_2O into a vacuum would be of the order of 1 gram per square centimeter per second; for Na_2O the rate would be about .03 grams per square centimeter per second. These figures should not, in general, be extrapolated directly to a basalt lava. In an ideal solution the pressure of an oxide in a melt would be proportional to its concentration; on this basis, since K_2O only forms about one percent of our standard basalt, its initial evaporation rate in a vacuum would be estimated as 0.01 grams per square centimater per second. However, even this estimate is probably too high; one must recognize that these mixed oxides have a greater stability than their components due to chemical interaction. For example K_2SiO_3 has a vapor pressure three orders of magnitude lower than K_2O rather than the one-half one would predict from an ideal solution. In addition the evaporation rates would be further decreased as the surface becomes depleted in the high vapor pressure components and ultimately would be limited by the rates of evaporation of the less volatile species. The presence of appreciable pressures of the evaporating species above the interface would of course further decrease the rate of evaporation.

On the other hand some factors could act to increase the rate of vaporization above those shown in Figure 5.21-3. As water vapor will often accelerate the vaporization rate of oxides, the estimates provided

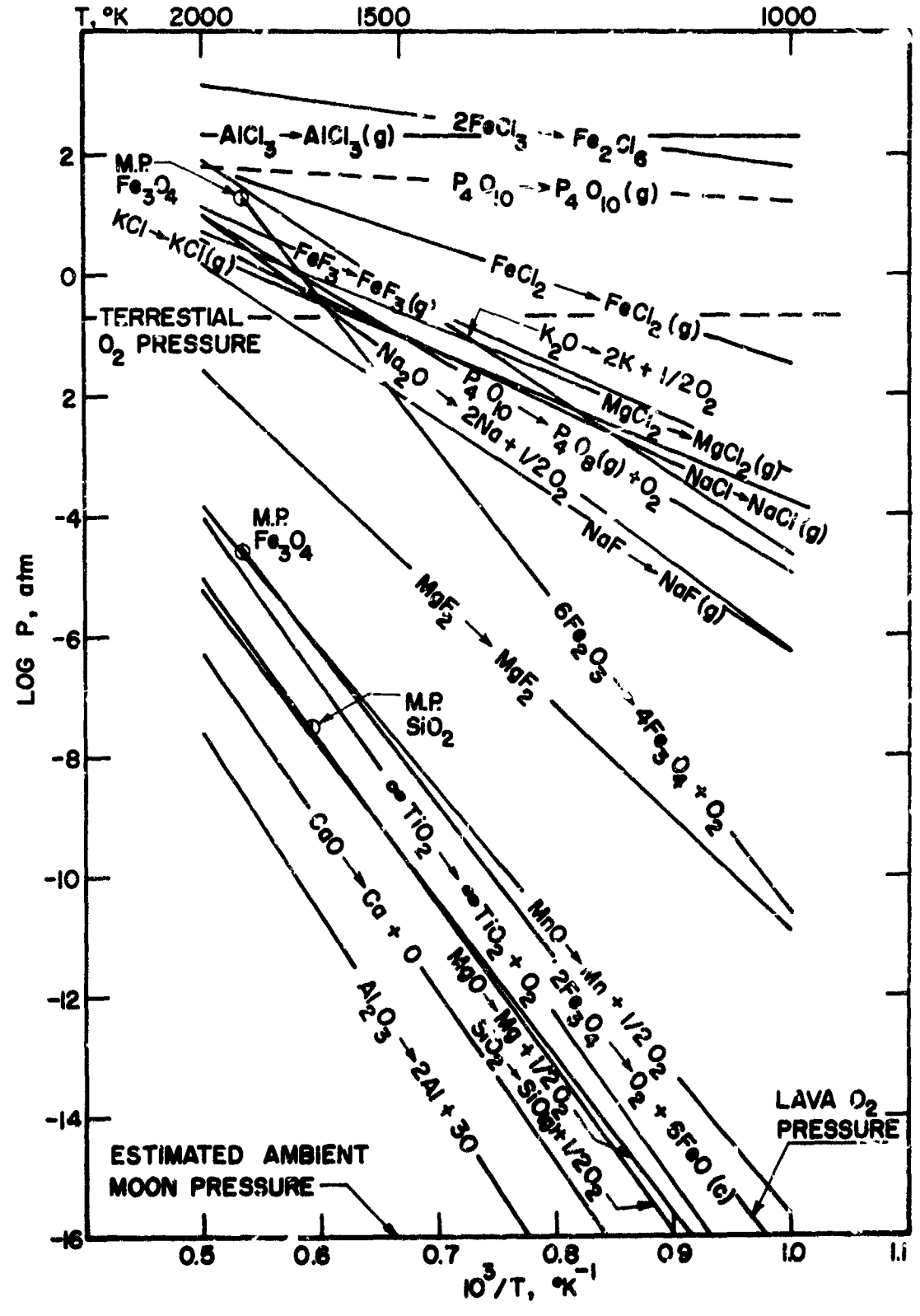

FIGURE 5.21-2 Vapor pressures of likely components of magmas.

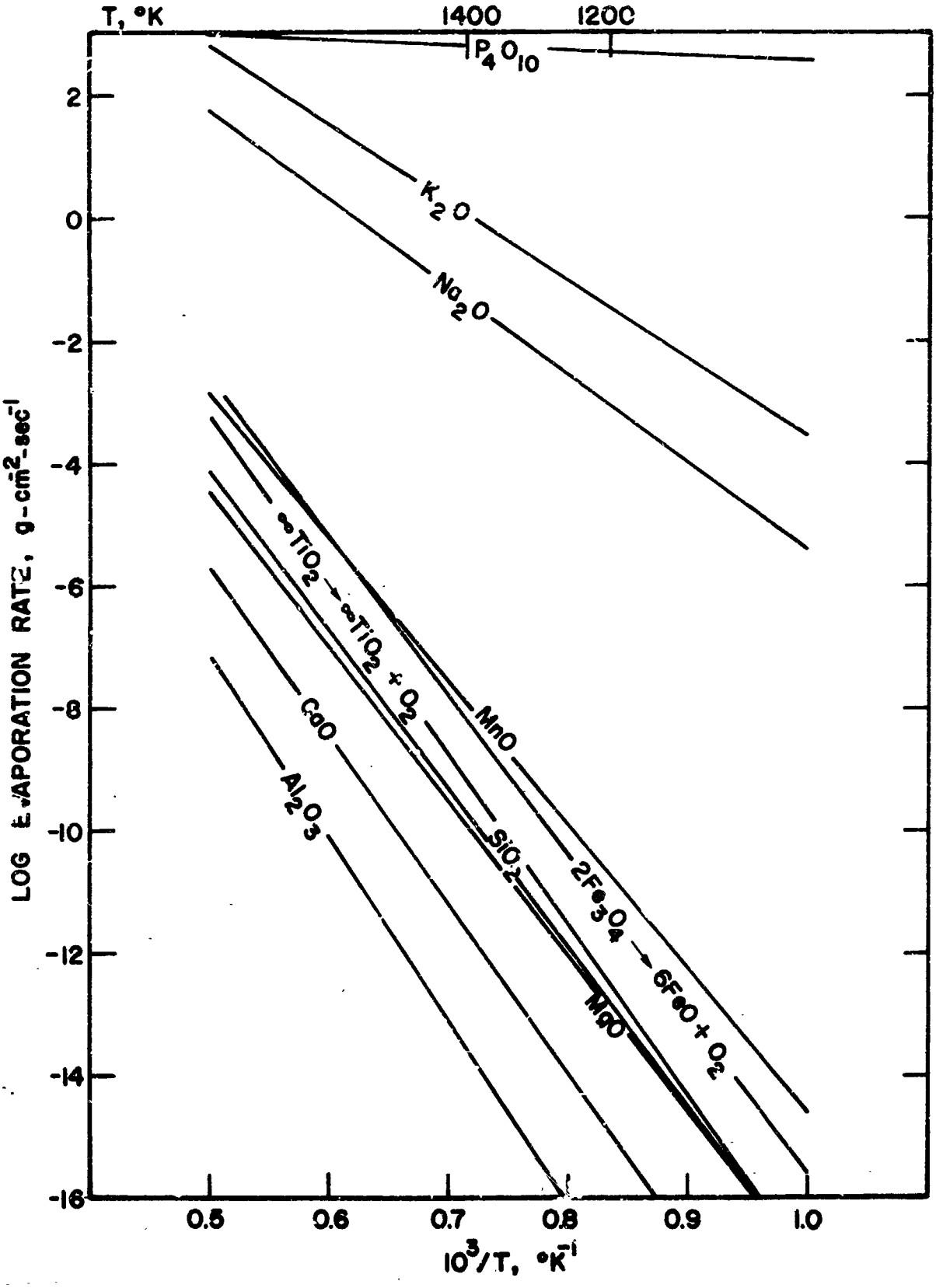

FIGURE 2.21-3 Evaporation rates of likely components of magmas.

by the pure oxide analyses may be in error by several orders of magnitude. For example, experiments performed on boron oxide at 1500°K show that in a dry system it has a vapor pressure of 10^{-5} atmospheres, but calculations indicate that a pressure of 10^{+5} atmospheres of HBO_2 would be in equilibrium with one bar of water vapor and liquid boric oxide. Other volatile gases such as H_2S could be expected to act in the same way as H_2O.

While mixed oxides frequently have greater stability than their components, mixed vapor species may also be formed which are more volatile than the separate oxides. While the silicates have not been experimentally studied, mass spectrometric studies of other systems we have investigated in the past have revealed many unexpected volatile molecules.

In order to confirm that hot lava could evaporate into the atmosphere producing aerosols, we carried out several simple experiments. We observed smoke to form when we melted basalts on an electrically heated wire filament and in a crucible. Basalt heated in air to around 1400°C in a platinum crucible produced a light brown condensate on a water cooled glass flask above the crucible (Figure 5.2-4). A mixture of basalt and dunite heated to about 1500°C under reducing conditions (in a graphite crucible in argon) produced a "smoke" containing dark brownish gray structures resembling cobwebs. X-ray diffraction of these "cobwebs" indicated the presence of Si, SiO_2, Mg_2Si and MgO. X-ray fluorescence of both deposits showed strong evidence of K, Ca, Fe and Si.

5.22 Vaporization in Phreatic Eruptions

If particles can condense from the gas phase over lava fountains and lakes, similar processes might take place in a phreatic eruption; some gaseous components from the hot lava may be present in the gas phase of the high velocity eruption that will condense to form an aerosol when cooling takes place by adiabatic expansion or by mixing with the atmosphere. While the larger particles of tephra in a volcanic eruption are undoubtedly formed by atomization and comminution of lava, it appears quite possible that some of the smaller tephra particles result from the condensation and growth of aerosol particles from the vapor phase.

It is well established that large numbers of very small particles are injected into the atmosphere from phreatic eruptions. All of the

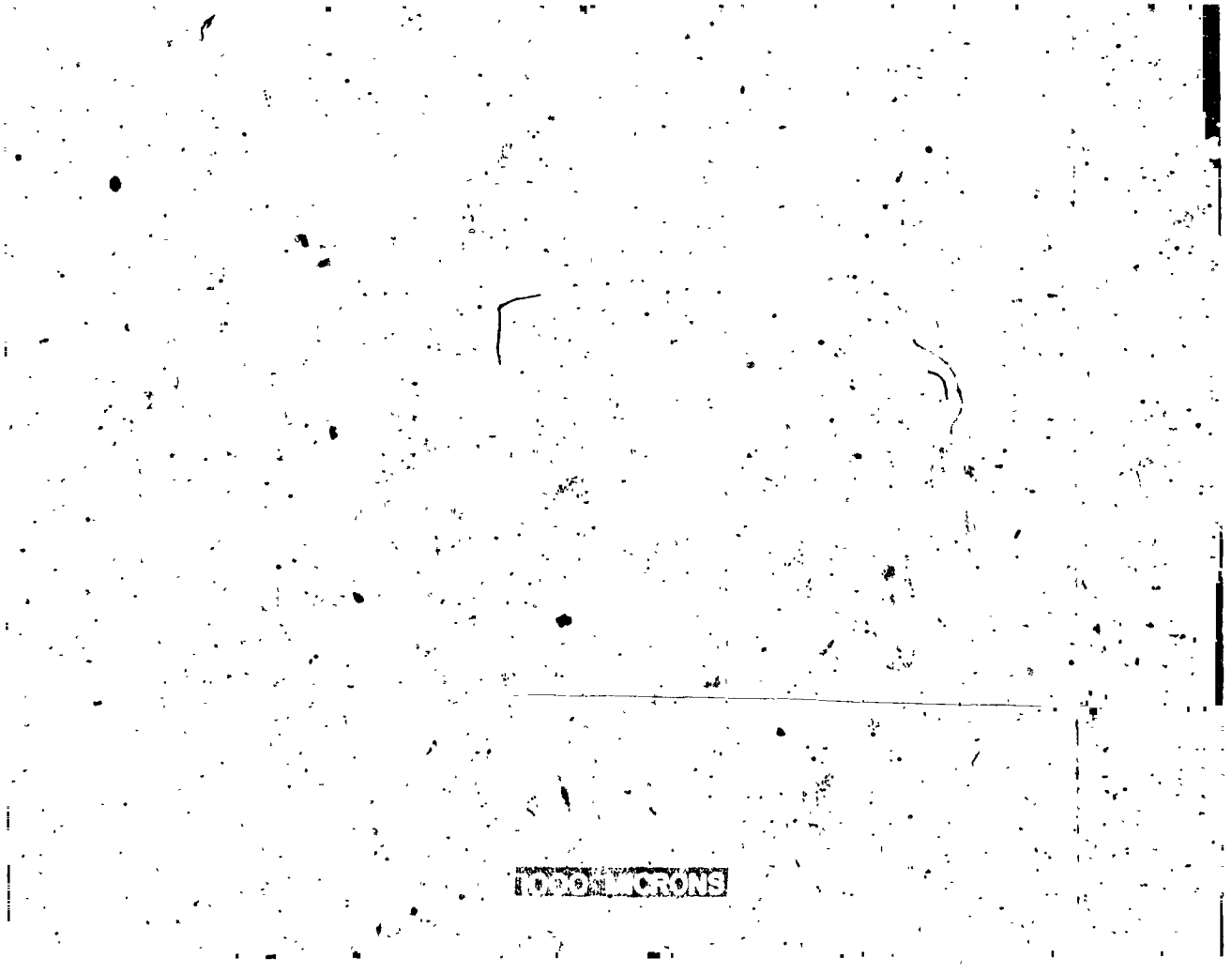

FIGURE 5.21-4 Photomicrograph of condensate formed on cold surface in air above crucible containing molten basalt at about 1400°C.

evidence suggests that the spectacular meteorological optical phenomena such as vividly colored sunsets and Bishop's rings associated with volcanic eruptions are the result of such particles. Since the optical phenomena extend over large portions of the globe and persist for months or even years (Burdecki, 1964) the particles must be so small that they settle very slowly. deBary and Bullrich (1959) state that in order to have Bishop's rings it is necessary to have:

a) an abnormally dense layer of aerosol particles with almost identical radii of 0.3-0.4 microns at a constant altitude;

b) a concentration of aerosol particles 5 to 10 times greater than usual.

These aerosol particles are so small and so uniform that it appears unlikely that they result from comminution or atomization; it seems far more probable to us that this class of particulate matter is the result of condensation from the vapor phase.

While we do not yet have a quantitative theory which can explain all the features associated with explosive eruptions we believe that some of the processes taking place in the eruption may be similar to those in the screening smoke generators developed by Langmuir and Schaefer (1948). Here a high boiling petroleum oil was vaporized along with water and then allowed to escape at high velocity into the atmosphere where it condensed as an aerosol.

Thus it seems likely that the formation and properties of the high temperature clouds of the volcano are in some ways similar to ordinary atmospheric water clouds. It would therefore appear worthwile to obtain quantitative information concerning the partial pressures of the components of the lava vapor during volcanic eruptions. If the vapor pressures are comparable to the partial pressures of water vapor in the atmosphere, a significant portion of volcano clouds and of the small tephra particles may be formed by a condensation and coagulation process similar to that which occurs in water clouds. Conceivably, if the partial pressure of the lava components is sufficiently high, the heat released by the formation of liquid or solid cloud particles may be of significance in the formation of nuées ardentes.

5.23 Vapor Deposition on the Moon

It is apparent that in the processes we observed to take place over Surtsey the ambient atmosphere is of dominant importance. The presence of an atmosphere affects the formation and deposition of aerosols in at least four ways:

1. It maintains a high enough concentration of the lava gas to allow sufficient supersaturation for particle formation by condensation.
2. It causes sudden quenching of the hot gases by mixing and expansion.
3. It prevents rapid falling of the particles.
4. It transports the particles by the wind.

Because of the atmosphere's great influence on the behavior of hot lava vapors, it is interesting to consider what sort of processes might take place in nature under the conditions of very low atmospheric pressure which exist on the moon. Here when silicates vaporize from volcanism or other causes the results will be different. At these very low pressures the mean free path of the molecules will be large and the chances of their coming together to condense to form a particle will be negligibly small.

Using the analysis of Watson et al. (1961) it can be shown that the average distance, $\bar{D}$, that a molecule liberated from a hot surface on the moon will travel before reaching the surface again is

$$\bar{D} = .886\ \bar{v}^2/g \qquad (5.23\text{-}1)$$

where

$\bar{v}^2 = 3RT/m$ is the mean square velocity

and

R is the gas constant

T is the absolute temperature

m is the molecular weight

g is the gravitational acceleration.

Values of $\bar{D}$ for a number of species as a function of temperature, calculated from this equation, are shown in Figure 5.23-1. It is apparent that the average distances a molecule will travel after liberation from

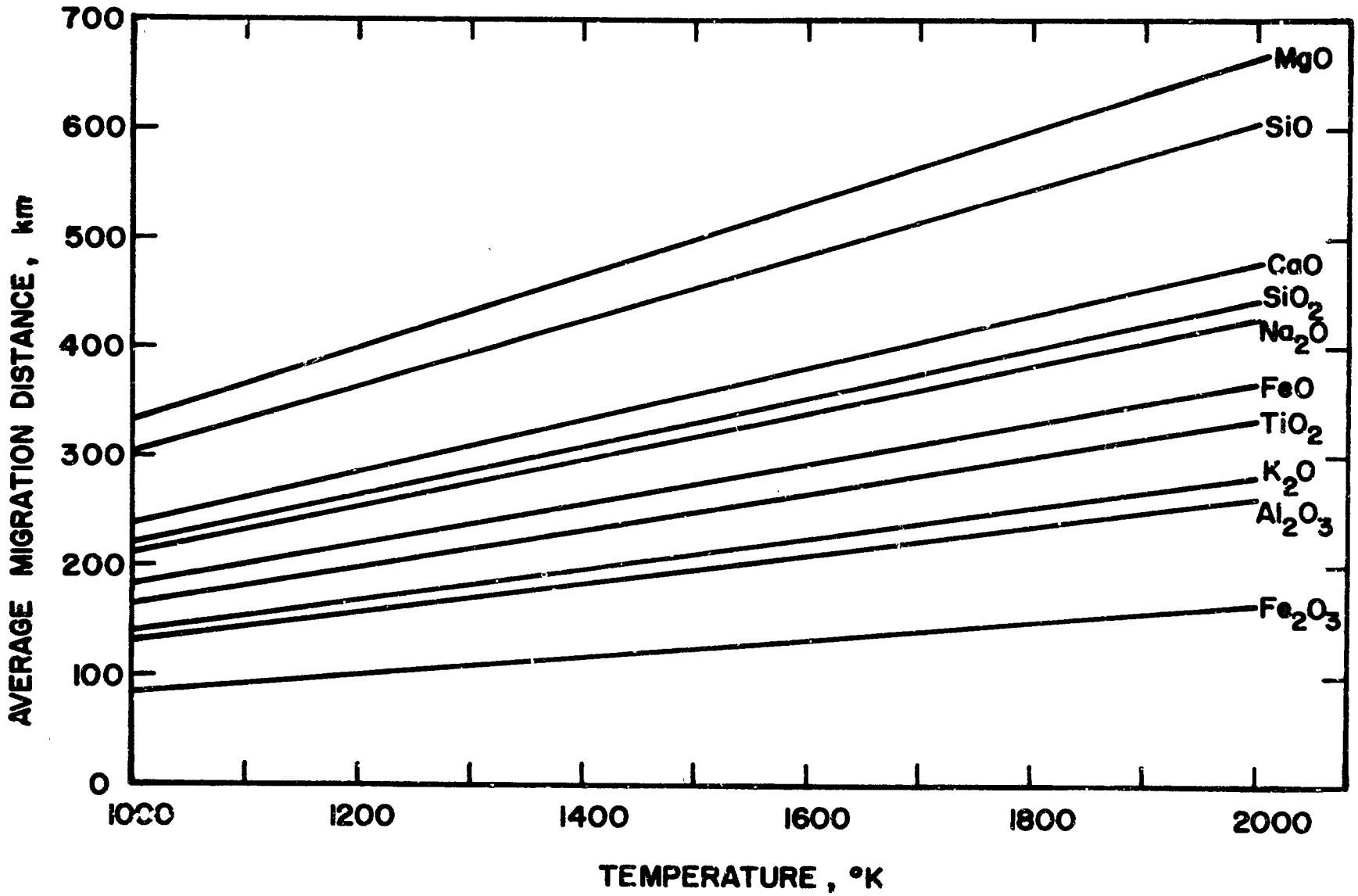

FIGURE 5.23-1 Average migration distance as a function of temperature for various species evaporated from molten lava.

the molten magma will be of the order of hundreds of kilometers. This will insure relatively uniform deposition over a substantial fraction of the moon's surface, even from a small area of melt.

To investigate effects of vacuum, we performed a simple experiment by heating about 1/5 gram of basalt to about 1200°C in a vacuum of 10^{-4} torr for a few minutes. This produced a dark brown film several microns thick on a microscope slide suspended above the melt. Again X-ray fluorescence showed strong lines of K, Ca and Fe. No good X-ray diffraction peaks were observed from the thicker parts of the deposit, but under the optical microscope small particles showing apparent crystalline outlines were observed on the thinner parts of the film (Figures 5.23-2 and 5.23-3). Dark field electron microscopy of thinner parts of the film from the slide showed the presence of crystals ranging in size from several hundred to several thousand angstroms.

The observed photometric properties of the surface of the moon are consistent with the idea that vapor deposition may have played a role in its formation. Hapke(1964) has summarized the photometric characteristics of the entire visible portion of the lunar surface in particular drawing attention to the low albedo, strong backscattering, unusual polarization properties, and brownish gray color. He concludes that the only materials that would be photometrically consistent with the observations are some types of vegetation, non-metallic whiskers and dark finely divided particles. There can be no vegetation because of the lack of atmosphere. He suggests that although whiskers might be formed by the combined effects of sputtering by the solar wind and condensation of material vaporized by micrometeorites, they are unlikely to survive under repeated meteorite bombardments. Hapke concludes that the surface must be covered with a layer of pulverized rock powder ten microns or so in size which has been "darkened by exposure to solar radiation or some other agent and arranged by micrometeorite bombardment into a porous material with a bulk density only one tenth that of solid rock." A comparison of Figure 5.21-4, Hapke, and Van Horn's (1963) photographs of a fine powder with the required "fairy-castle" packing shows a strong resemblance. Simple preliminary measurements indicate

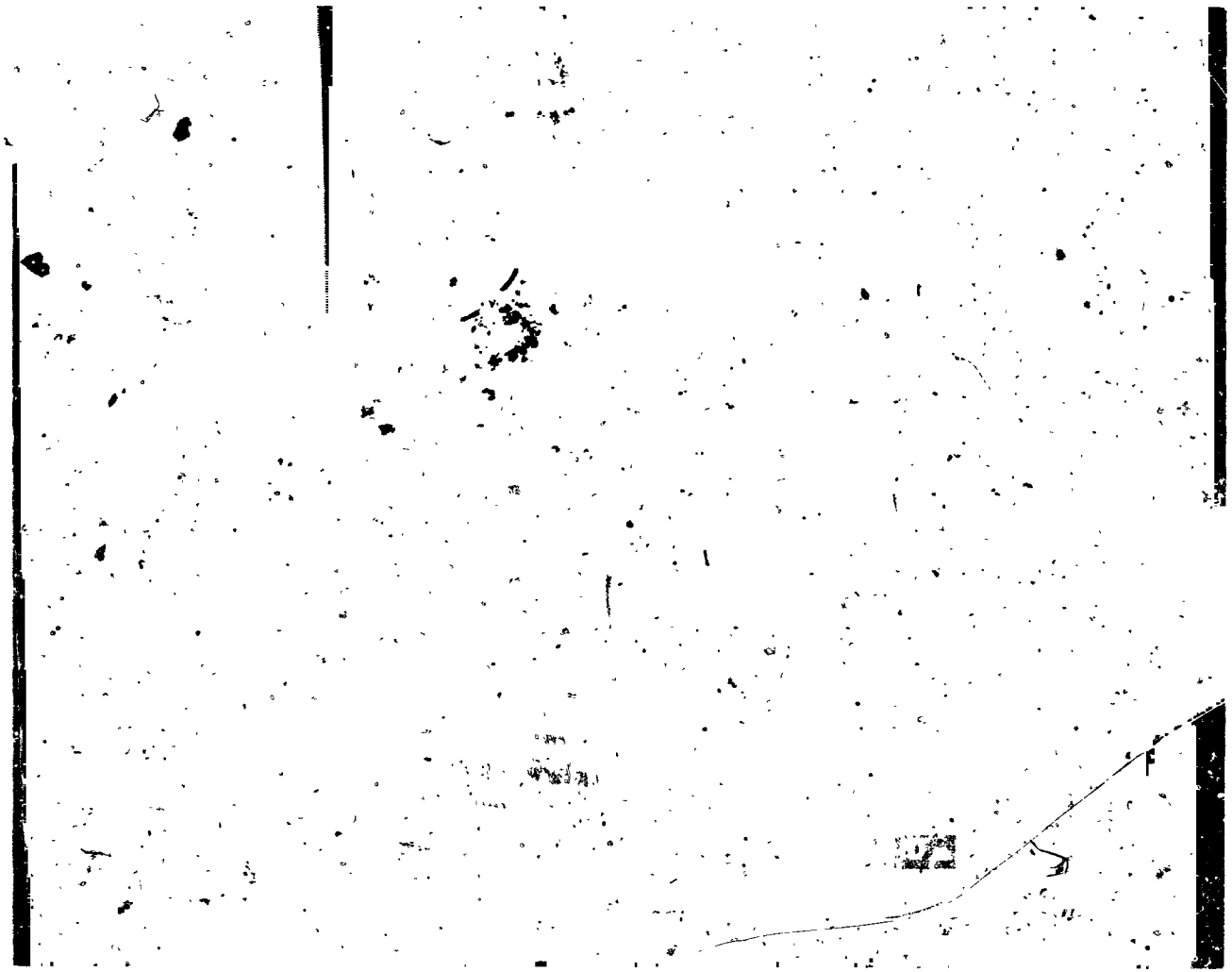

FIGURE 5.23-2 Photomicrograph of thin condensate film formed on glass held for several minutes in a vacuum above molten basalt at about 1200°C.

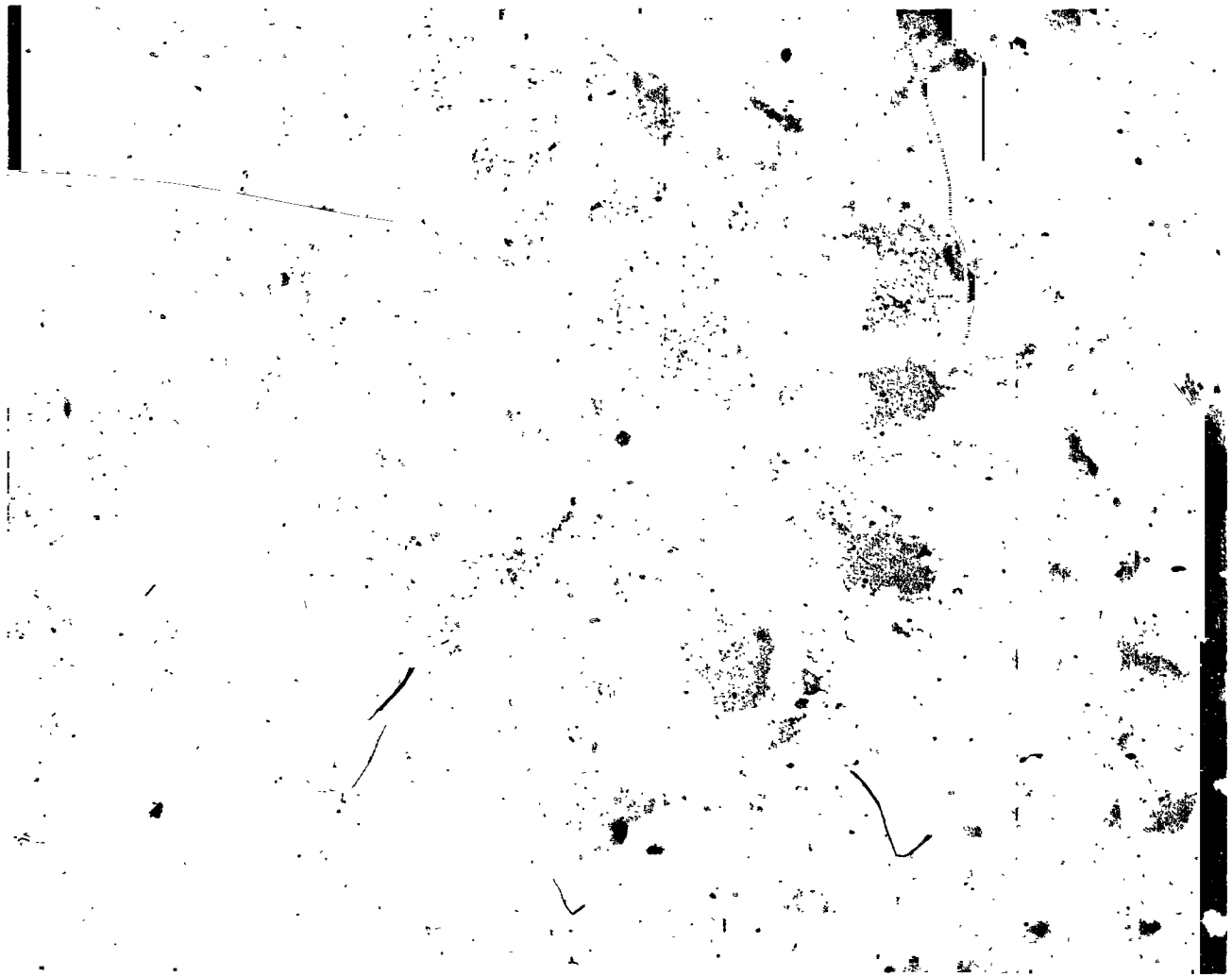

FIGURE 5.23-3 Transmission electron photomicrograph of that area of the film shown in Figure 5.23-2 from which electron diffraction pattern indicating crystallinity was obtained. Note the similarity between the fine granular structure shown in this figure and the much coarser structure of the air-deposited material of Figure 5.21-4.

that our light colored air-deposited material also exhibits a strong backscattering peak. The materials evaporated under less oxidizing conditions, in a graphite crucible in argon or in a vacuum, showed considerable darkening as would be expected.

The formation of particulate matter by the condensation of vaporized components of hot lava is undoubtedly important in the origin of terrestrial volcanic clouds and atmospheric aerosols. The volcanic evaporation-condensation mechanism may also be one of the mechanisms which has contributed to the "fairy-castle" structure of the visible portion of the moon's surface.

5.3 AEROSOL STUDIES OF THE SURTSEY VOLCANOS

In early June of 1965 a new phreatic eruption began a few hundred meters from the Island of Surtsey off the south coast of Iceland. We took advantage of this unusual opportunity by carrying out a sampling program to collect the particulate matter in the volcano cloud. As the program took place from June 24, 1965 to June 29, 1965, there was insufficient time remaining within the contract period to do more than a preliminary analysis on the material collected. However, we believe that the samples will provide valuable information about the mechanics of volcanic eruptions when combined with later theoretical and experimental studies. Below we describe the sampling methods used in the program and discuss the results of the preliminary analysis.

5.31 The Sampling Program

Particles were collected primarily by filtration using the Millipore filter field monitors or by impaction on glass slides. The Millipore field monitors are especially designed for air sampling work; the units are assembled in ultraclean environments so background is low; they are efficient collectors of particulate matter in the submicron range; the collected matter can be preserved indefinitely in the plastic container without fear of contamination; and they are amenable to a variety of well-worked-out analytical techniques including electron microscopy and NMR. Glass slides have an advantage over Millipore filters in that they are more suitable for microscopic observation of submicron particles. The Millipore filter is not wholly satisfactory for microscopic observation

of small particles because of its surface structure.

On three separate occasions an airplane was rented and used to collect samples of the particulates in the cloud emanating from the new Surtsey volcano. On two of these occasions samples were collected by the simple process of holding the filter or glass slide outside the airplane. When the Millipore filter units were used in this fashion, the top section of the monitor was replaced with a retaining ring to allow full utilization of the filter surface. The unit was usually mounted on a modified pipe "T", the center of which was adapted to a rod used to hold the unit outside the cockpit. At the usual airplane speed of 100 mph, the estimated flow through the Millipore filter was about 3 liters per minute. On the other occasion when the airplane was used for sampling, the Millipore filter unit was affixed to a sampling probe, placed outside the airplane, and a flow of 12.5 lpm through the filter was obtained by use of a portable 6 volt Gast pump. Under these conditions the flow was much closer to isokinetic conditions than when impact pressure was used to provide the flow. However, even with the pump the flow was less than isokinetic and while we would expect very little error for particles up to a few microns in diameter, the collection of larger particles would be favored by these conditions.

The fishing boat "Ran", owned and operated by August Olafsson, was rented twice for trips to the old Surtsey Island. The Gast pump was used to provide flow through the Millipore filter on these occasions when the boat was near the plume. On one occasion, we passed directly under the plume and samples of rain were also obtained on glass slides and a Millipore filter.

On the surface of Surtsey, a number of samples were collected using the Millipore units and the Gast pump. Since the wind was blowing the smoke plume away from the island, it is unlikely that these samples are significant. However, on one occasion the unit was set up in the lava field close to the new Surtsey volcano and the emanations from this lava field were sampled. We were unable to transport the battery to the top of the old Surtsey crater but the particulate matter which was being emitted was collected on glass slides and Millipore filters placed

downwind of the crater.

5.32 Analysis of Collected Particulates

We have just begun to analyze the material collected in our sampling program. Table 5.32-1 lists the results of a particle size analysis of material collected on glass slides. This is the analysis of the total material collected and we would hope to repeat this study later for the magnetic fraction.

An attempt was also made to classify the particles as spherical and non-spherical and these data are also listed in Table I. It should be noted that our values for the fraction of spherical particles are greater than those determined by Hodge and Wright (1964) for volcanic material. This may be due to the fact that our data are for the total dust rather than the magnetic fraction or may be simply due to the adoption of less stringent criteria for classification as spherical.

Table 5.32-1 shows that by far the largest percentage of particulate matter is in the micron range. (The microscope and electron microscope also show that many of the larger particles are composed of aggregates of smaller particles.) The smoke from the crater of the old volcano is smaller than that in the plume of the new volcano as might be anticipated from the differences in the primary methods of cloud formation. The smoke from the old volcano is very light and probably the result of evaporation and condensation processes whereas the new volcano generates a large amount of coarser material by mechanical means. A large percentage of the > 10-micron particle collected at the crater undoubtedly results from the contamination of the slide by blowing surface dust.

Photomicrographs, both with the optical and electron microscopes, have been taken of some of the glass slides and Millipore filter samples. These pictures and subsequent planned analytical processes, such as electron diffraction and electron microprobe studies, may in the future add appreciably to our understanding of the mechanics of volcanic eruptions.

5.4 CONCLUSIONS ABOUT THE BEHAVIOR OF VOLATILES ESCAPING FROM LUNAR MAGMAS

In addition to their influence on the rheological properties of magma and their ability to provide pressure for expulsion of magmas from

TABLE 5.32-I

GLASS SLIDE PARTICLE ANALYSIS

% Smaller than Stated Size

Size Range	Airplane Samples									Rain Samples		Crater Samples				
	#1	#2	#3	#4	#5	#6	#7	#14	Ave.	#8	#9	#10	#11	#12	#13	Ave.
< 1 μ	55	47	64	47	49	67	7.9	46	57	49	-	60	65	70	65	65
1 μ - 3 μ	76	89	90	75	90	85	94	76	85	85	-	93	97.5	97.3	97.7	96.4
3 μ - 10 μ	90	95	94	87	94	99.2	98.2	84	92.7	97	-	96	99.2	98.7	99.2	98.3
10 μ - 25 μ	99	98.8	97.3	96.3	98.7	99.7	99.6	95	98.2	98.8	-	97.6	99.7	99.8	99.9	99.1
25 μ - 50 μ	99.7	-	99.1	99.1	99.6	99.9	99.9	98.6	99.5	99.6	-	99.7	-	-	-	99.7
50 μ - 100 μ	99.95	-	-	-	-	-	-	-	99.9	99.8	-	99.8	-	-	-	99.8
>100 μ	-	-	-	-	-	-	-	-	-	-	-	-	-	-	-	-
% Spherical in 10 μ - 100 μ range	0.6	1.1	0.7	1.5	0.2	0.4	-	-	0.8	0.6	0.1	0.02	-	1.2	-	-

the secondary chamber, volatiles may condense to form deposits of their own. We have investigated several aspects of the behavior, after escaping from the melt, of those substances which exist as gases at relatively low temperatures and of those which vaporize at lava temperatures. Our more significant conclusions are summarized below.

The vapor pressures of several of the clathrate gas hydrates have been extrapolated to the region of 120°K using the best available data, which in most cases leaves much to be desired. All the hydrates have higher vapor pressures than ice but much lower vapor pressures than the pure substance values used in previous studies of the stability of volatiles on the moon. Even these lower pressures appear to be too high to permit accumulation of clathrate gas hydrates in cold traps on the moon under equilibrium conditions. Once formed, however, the clathrates may be stable under cold trap conditions. Thus the clathrates, if found, will provide a valuable record of the conditions existing at an earlier stage of the moon's history.

From existing data the vapor pressures and evaporation rates of pure metal oxides found in basalt has been assembled. Vapor pressures of such oxides as K_2O, Na_2O and P_4O_{10} appear to be high enough to result in considerable evaporation from basalt lava. Deposits formed above basalt heated in air in an argon atmosphere and in a vacuum of 10^{-4} torr confirm that appreciable evaporation from molten lava will take place. Evaporation from any molten lava extruded onto the moon would be expected to contribute to the formation of "fairy-castle" structure by vapor depositing material over hundreds of thousands of square kilometers.

We also believe that an appreciable fraction of the aerosol particles produced in a phreatic eruption on earth may be the result of condensation of material from the vapor phase. On the moon this type of condensation may be less significant.

6. SUMMARY AND CONCLUSIONS

After examining the available evidence, we have found no compelling reasons to assume that the moon's composition differs significantly from that postulated by Ringwood and others for the earth's mantle. We have approximated the composition by a mixture of basalt and dunite and have used published data on silicate minerals to predict the thermal properties and melting relationships as functions of pressure and temperature. The more important aspects of these predicted functions have been selected and used to extend the normal thermal history calculations of the moon to include the effects of differentiation through igneous activity. The calculations indicate that a brief period of intense volcanic activity is likely to have occurred; the time at which this activity took place will be primarily a function of the moon's temperature at the time of its formation and the concentration of radioactive heat sources. Properly selected samples of the moon's surface rocks should thus make it possible to determine the temperature at the time of formation. The total thickness of extrusive and intrusive igneous rocks is strongly dependent on the efficiency of radiative heat transfer in removing heat from the interior. Further experimental work on heat conduction in silicates seems to be required.

We have made use of the predicted melting relationships and heats of fusion to propose a mechanism for sudden generation of magma which appears to be consistent with terrestrial geological evidence. There seems to be no reason that a similar mechanism could not have operated on the moon.

Calculations, using published data on the viscosity of basalts in conjunction with a simple model for dike propagation, have yielded dike dimensions which agree with field observations. When lunar pressure gradients are substituted into the model, the minimum width of a dike which can transport appreciable amounts of material from the region of generation is predicted to be roughly 2.5 times wider than a similar dike in the earth. The flow of material through this lunar dike should also be about 2.5 times larger than through its terrestrial counterpart.

There is substantial evidence that magma migration through a dike should terminate as a result of a rapid increase in viscosity whenever pressures become low enough for nucleation of bubbles of water and other volatile constituents. This would be consistent with the observation that most magmas erupted into the earth's surface appear to have been differentiated from a primary basaltic magma in a near-surface chamber. If the volatile hypothesis is correct, the depth at which migration stops and differentiation begins should be primarily controlled by pressure; secondary magma chambers should therefore be found about six times as deep on the moon as they are on the earth. As the evidence for the effects of exsolution of volatiles on viscosity is incomplete and partially contradictory, we believe experimental and theoretical investigations in this are necessary.

Based on our present knowledge, it does not appear unlikely that a variety of rocks, representing different stages of differentiation of basaltic magmas, will be found at or near the surface of the moon. However, the interaction between the volatile constituents and the melt is of such importance that there seems to be no logical basis at this time on which to predict crystal size, rock texture, or mineral assemblage. Such predictions will have to wait until direct experimental evidence of the properties of a volatile-magma mixture is available on which to found a quantitative theory.

The evidence which we have at this time indicates that electrification observed in terrestrial phreatic eruptions does not take place in the atmosphere and thus the generation of charge must be considered in conjunction with the mechanism of eruption.

It appears that although the clathrate gas hydrates have much lower vapor pressures than the pure substance values, the pressures are not low enough for these materials to be stable under "cold trap" conditions. However, if they were formed under conditions different from those existing at the present time, they could persist in the cold traps.

There is strong evidence that evaporation of some of the metallic oxide components of the melt takes place during volcanic eruptions. These oxides would be expected to distribute themselves over several

hundreds of thousands of square kilometers possibly contributing to the formation of a "fairy-castle" type structure.

In summary, then, we believe that although there are many interesting unsolved problems of volcanism, the most pressing needs for the purposes of lunar exploration are: determination of the radiative component of thermal conductivity for model rock types; experimental and theoretical studies to determine the interaction of volatiles with a melt, with particular emphasis on the rheological properties; and theoretical study of the dynamics of eruption using the experimental data on the effects of volatiles.

REFERENCES

Anderson, D.L., 1964, Universal dispersion tables 1. Love waves across oceans and continents on a spherical earth: Bull Seism. Soc. Am, v. 54, pp. 681-726.

Anderson, R., Bjornsson, S., Blanchard, D., Gathman, S., Hughes, J., Jonasson, S., Moore, C., Survilas, H., Vonnegut, B., 1965, Electricity in volcanic clouds: Science, May, v. 148, pp.1179-1189

Balchan, A.S., and Drickamer, H.C., 1959, Effect of pressure on the spectra of olivine and garnet: J. Appl. Phys., v.30, p. 1446.

Barrer, R.M., and Stuart, W.I., 1957, Non - Stoicheiometric compounds of water: Proc. Roy. Soc., A243, 172-189.

Birch, Francis, 1964, Density and composition of mantle and core: J. Geophy. Res., v. 69, p. 4377-4388.

Birch, F., and Clark, H., 1940, The thermal conductivity of rocks and its dependence upon temperature and composition: PartII: Am. Jour. Sc., v. 238, p. 613-635.

Birch, F., and P. Le Comte, 1960, Temperature-pressure plane for albite compositions: Am J. Sci., v. 258, p. 209.

Birch, F., Schairer, J.F., Spicer, H.C., editors, 1942, Handbook of physical constants: GSA Special Paper, No. 36.

Blackman, M., and Lisgarten, N.D., 1958, Electron diffraction investigations into the cubic and other structural forms of ice: Adv. in Phys., 7, 189-198.

Blanchard, D.C., 1965, Charge separation from saline drops on hot surfaces: Nature, v. 201, pp. 1164-1166.

Bockris, J. O'M., Mackenzie, J.D., and Kitchener, J.A., 1955, Viscous flow in silica and binary liquid silicates: Trans. Fara. Soc., v. 51, p. 1734.

Bodvarsson, G., and Walker, G.P.L., 1964, Crustal drift in Iceland: Geophys. Jour. Roy. Astron. Soc., v. 8, p. 285-300.

Boyd, F.R., 1964, Geological aspects of high-pressure research: Science, v. 45, p. 13.

Boyd, F.R., and England, J.L., 1960, Yearbook 59: Carnegie Institution of Washington, p. 48.

Boyd, F.R., and England, J.L., 1963, Effect of pressure on the melting of diopside, $CaMgSi_2O_6$, and albite, $NaAlSi_3O_8$, in the range up to 50 kilobars: J. Geophys. Res., v. 68, p. 311-323.

Boyd, F.R., and England, J.L., 1964, The system enstatite-pyrope: Yearbook 63, Carnegie Institution of Washington, p. 157-161.

Boyd, F.R., England, J.L., and Davis, B.T.C., 1964, Effects of pressure on the melting and polymorphism of enstatite, $MgSiO_3$: J. Geophys. Res., v. 69, p. 2101-2109.

Bradley, R.S., 1962, Thermodynamic calculations on phase equilibria involving fused salts. Part II Solid solutions and applications of the olivines: Am. J. of Science, v. 260, p. 550-554.

Bridgeman, P.W., 1949, Physics of high pressure, G. Bell, London.

Bundy and Strong, 1962, High temperature and pressures: Solid State Physics, v. 13, p. 118, Academic Press, N.Y.

Burdecki, F., 1964, Meteorological phenomena after volcanic eruptions: Weather, 19, p. 113.

Chao, E.C.T., 1963, The petrographic and chemical characteristics of tektites: in Tektites, ed. J.A. O'Keefe, University of Chicago Press, p. 51-94.

Clark, Jr., S.P., 1956, Effect of radiative transfer on temperature in the earth: Geol. Soc. America Bull, v. 67, p. 1123-1124.

Clark, Jr., S.P., 1957a, Absorption spectra of some silicates in the visible and near infrared: Am. Mineralogist, v. 42, p. 732-742.

Clark, Jr., S.P., 1957b, Radiative transfer in the earth's mantle: Trans. Amer. Geophys. Union, v. 38, p. 931-938.

Clark, Jr., S.P., de Neufville, J., 1962, Crystalline phases in the system diopside-$CaAl_2SiO_6$-silica at high pressures: J. Geophys. Res., v. 67, p. 3550.

Davis, B.T.C., England, J.L., 1964, The melting of forsterite up to 50 kilobars: J. Geophys. Res., v. 69, p. 1113-1116.

deBary, E. and Bullrich, K., 1959, "Zur Theorie des Bishop Ringes" Met. Rdsch, Berlin 12, 89.

Dekker, A.J., 1957, Solid State Physics, p. 366: Englewood Cliffs, N.J., Prentice-Hall, Inc.

Eaton, J.P., Murata, K.J., 1960, How volcanos grow: Science, v. 132, p. 925-938.

Einarrson, T., 1949, The flowing lava. Studies of its main physical and chemical properties: from "The eruption of Hekla 1947-1948": edited by T. Inarsson, G. Kjarteasson and S. Thorarinsson, published jointly with The Museum of Natural History, Reykjavik.

Eitel, W., 1965, Silicate Science, Academic Press, v. IIA par. 89.

Engel, A.E.J., and Engel, C.G., 1964, Reports: Composition of basalts from the mid-atlantic ridge: Science, v. 144, p. 1330-1333.

Engelke, J., 1965, Personal communication.

Euler, R., and Winkler, H.G.F., 1957, Glastech. Ber. 30, 325.

Fourier, J., 1822, Theorie analytique de la chaleur, F. Didot Père et fils, Paris.

Fricker, P.E., and Reynolds, R.T., 1965, Thermal history of the moon: paper presented at Forty-sixth Annual Meeting of the Amer. Geoph. Union, Washington, D.C.

Friedman, I., Long, W., and Smith, R.L., 1963, Viscosity and water content of rhyolite glass: J. Geophys. Res., v. 68, p. 6523.

Giauque, W.F., and Stout, J.W., 1936, The heat capacity of ice,: Jour. Am. Chem. Soc., 58, 1144-1150.

Gilvarry, J.J., 1956, The Lindemann and Gruneisen laws: Phys. Rev., v. 102, p. 308-316.

Gilvarry, J.J., 1956, Gruneisen's law and the fusion curve at high pressure: Phys. Rev., v. 102, p. 317-325.

Gilvarry, J.J., 1956, Equation of the fusion curve: Phys. Rev., v. 102, p. 325-331.

Gilvarry, J.J., 1956, Variation of the amplitude of thermal vibration on the fusion curve: Phys. Rev., v. 104, p. 908-913.

Gilvarry, J.J., 1956, Amplitudes of thermal vibration at fusion: Phys. Rev., v. 103, p. 1700-1704.

Glasstone, S., Laidler, K.J., and Eyring, H., 1941, The theory of rate processes: McGraw-Hill, New York.

Green, D.H., Ringwood, A.E., 1963, Mineral assemblages in a model mantle composition: J. Geophys. Res., v. 68, p. 937-945.

Gryvnak, D.A., and Burch, D.E., 1965, Optical and infrared properties of Al_2O_3 at elevated temperatures: J. Opt. Soc. Am., v. 55, p. 625-629.

Hapke, B., 1964, Packing properties of fine powders and the depth of the lunar dust layer: J. Geophys. Res., v. 69, p. 1146-1151.

Hapke, B., and Goldberg, L.S., 1965, Molecular flow through soils and the possibility of lunar permafrost layers. Paper presented at 46th annual meeting of American Geophysical Union, Washington, D.C.

Hapke, B., and Van Horn, H., 1963, Photometric studies of complex surfaces with applications to the moon. Jour. Geoph. Res., v. 68, p. 4545.

Hodge, P.W., and Wright, F.W., 1964, Studies of particles for extra-terrestrial origin, v. 69, No. 12, Jour. of Geophy. Res.

Jacobs, J.A., 1956, The interior of the earth: Advances in Geophysics, ed. H.E. Landsberg, Academic Press Inc., New York, P. 183-239.

Jacobs, J.A., Russell, R. D., Wilson, J.T., 1959, Physics and geology: New York, McGraw-Hill.

Johannsen, A., 1939, A descriptive petrography of the igneous rocks: v. I, introduction textures, classifications and glossary, University of Chicago Press, Chicago, Ill.

Kaula, W.M., 1963, Tidal dissipation in the moon: Jour. Geophys. Res. v. 68, p. 4959-4965.

Kennedy, G.C., 1948, Equilibrium between volatiles and iron oxides in igneous rocks: Amer. J. Sci., v. 246, p. 529-49.

Kingery, W.D., Francl, J., Coble, R.L., Vasilos, T., 1954, Thermal conductivity. X, Data for several pure oxide materials corrected to zero porosity: Jour. Am. Ceramic Soc., v. 37, p. 107-110.

Kittel, Charles, 1956, Introduction to Solid State Physics: New York, John Wiley and Sons, Inc.

Kopal, T., 1963, Gravitational heating of the moon: Icarus, v.1, p. 412-421.

Kozakevitch, P., 1961, Viscosity of lime-alumina-silica melts between

1600 and 2100C: AIME Metallurgical Society Conf, v. 3, p. 97, Interscience Publishers, New York.

Kubachewski, O., and E. Evans, 1957, Metallurgical thermochemistry: Academic Press, New York.

Langmuir, I., 1948, The growth of particles in smokes and clouds and the production of snow from supercooled clouds: Proc. Amer. Phil. Soc. 92, 167.

Lawson, A. W., 1957, On the high temperature heat conductivity of insulators: J. Phys. Chem. Solids, v.3, p. 155.

Lawson, A.W., Jamieson, J.C., 1958, Energy transfer in the earth's mantle: J. Geology, v.66, p. 540-551.

Lee, D.W., Kingery, W.D., 1960, Radiation energy transfer and thermal conductivity of ceramic oxides: Jour. Am. Ceram. Soc., v.43, p. 594-607.

Lee, W.H.K., 1963, Heat flow data analysis: Reviews of Geophysics, v.1, p. 449-479.

Levin, E.M., Robbins, C.R., McMurdie, H.F., 1964, Phase diagrams for ceramists: Amer. Ceramic Soc.

Lippincott, E.R., Weir, C.E., Van Valkenburg, A., and Bunting, E.N., 1960, Studies of infrared adsorption spectra of solids at high pressures: Spectrochim. Acta, v. 60, p. 58.

Lovering, J.F., 1958, The nature of the mohorovicic discontinuity: Trans. Amer. Geophys. Union, v. 39, p. 947-955.

Lowman, P.D., 1963, The relation of tektites to lunar igneous activity: Icarus, v. 2 p. 35-48.

Lubimova, H.A., 1958, Thermal history of the earth with consideration of the variable thermal conductivity of its mantle: Geophy. J. of Roy. Astr. Soc., v. 1, p. 115-134.

McConnell, R.K., 1963, The visco-elastic response of a layered earth to the removal of the Fennoscandian ice sheet: Unpublished Ph.D. Thesis, University of Toronto.

McConnell, R., 1965, Isostatic Adjustment in a Layered Earth: Jour. of Geophys. Res. v. 70, p. 5171-5188.

McConnell, R.K., Jr., and McTaggart-Cowan, G.M., 1963, Crustal seismic refraction profiles - a compilation, Univ. of Toronto, Toronto.

MacDonald, G.J.F., 1954, A critical review of geologically important thermochemical data: Ph.D. Thesis, Harvard Univ.

MacDonald, G.J.F., 1959, Calculations on the thermal history of the earth: J. Geophysical Res., v. 64, p. 1967-2000.

MacDonald, G.J.F., 1962, On the internal constitution of the inner planets: J. Geophys. Res., v. 67, p. 2945-2974.

MacDonald, G.J.F., 1964, Dependence of the surface heat flow on the radioactivity of the earth: J. Geophy. Res., v. 69, p. 2933-2946.

Macedo, P.B., and Litovitz, T.A., 1965, On the relative roles of free volume and activation energy in the viscosity of liquids: J. Chem. Phys., v. 42, p. 245.

Machin, J.S., and Hanna, D.L., 1945, Viscosity studies of system $CaO-MgO-Al_2O_3-SiO_2$: I, 40% SiO_2: J. Am. Cer. Soc., v. 28, p. 310-316.

Machin, J.S., and Yee, T.B., 1948, Viscosity studies of system $CaO-MgO-Al_2O_3-SiO_2$: II, $CaO-Al_2O_3-SiO_2$: J. Am. Cer. Soc., v.31, p. 200-204.

Machin, J.S., Yee, T.B., and Hanna, D.L., 1952, Viscosity studies of system $CaO-MgO-Al_2O_3-SiO_2$: III, 35, 45, and 50% SiO_2: J. Am. Cer. Soc., v. 35, p. 322-325.

Mackenzie, J.D., 1957, The discrete ion theory and viscous flow in liquid silicates: Trans Fara. Soc., v. 53, p. 1488.

Mellor, J.W., 1930, Comprehensive Treatise on Inorganic and Theoretical Chemistry, v. X, p. 132, Longmans, Green Co., N.Y.

Miller, S.L., 1961, The Occurrence of Gas Hydrates in the Solar System. Proc. Nat. Acad. Sci. (U.S.A.), 47, 1798-1808.

Neufville, J. de, Clark, Jr., S.P., and Schairer, J.F., 1962, Effect of pressure on the liquidus in the plane diopside-anorthite-silica: J. Geophys. Res., v. 67, p. 3583.

Newton, R.C., Jayaraman, A., and G.C. Kennedy, 1962, The fusion curves of the alkali metals up to 50 kilobars: J. Geophys. Res., v. 67, p. 2559-2566.

O'Keefe, J.A., 1963, The origin of tektites: in Tektites, University of Chicago Press, p. 167-188.

Partington, J.R., 1951, Adv. Treatise on phys. chem: v. 2, p. 217, Longmans, Green and Co. New York.

Ringwood, A.E., 1959, On the chemical evolution and densities of the planets: Geochim. Cosmochim. Acts, v. 15, p. 257-283.

Ringwood, A.E., 1962, Mineralogical constituition of the deep mantle: J. Geophys. Res., v. 67, p. 4005-4010.

Ringwood, A.E., 1962, A model for the upper mantle: J. Geophys. Res. v. 67, p. 857-867.

Rogers, A.F., and Kerr, P.F., 1942, Optical Mineralogy, N.Y., McGraw-Hill Co.

Roscoe, R., 1953, Suspensions: ChapterI, in flow properties of disperse systems: Edited by J.J. Hermans, Interscience, N.Y.

Shaw, Herbert R., 1963, Obsidian - H_2O viscosities at 1000 and 2000 bars in the temperature range 700° to 900°C: J. Geophys. Res., v. 68, p. 6337-6343.

Shaw, H.R., 1964, Theoretical solubility of H_2O in silicate melts - quasi-crystalline models: J. Geology, v. 72, p. 601.

Sokolnikoff, I.S., 1956, Mathematical theory of elasticity: N.Y., McGraw-Hill.

Steele, W.A., and Webb, W., 1963, High pressure physics and chemistry; Chap. 411, v.1: Edited by R.S. Bradley, Academic Press, N.Y.

Sterrett, K.F., Klement, W., Kennedy, G.C., 1965, Effect of pressure on the melting of iron: J. Geoph. Res., v. 70, p. 1979-1984.

Stull, D.R., 1947, Vapor pressure of pure substances, Ing, Eng. Chem., 39, 517-550.

Thorarinsson, 1965, Personal communication.

Tilton, G.R., and Reed, G.W., 1963, Radioactive heat production in eclogite and some ultramafic rocks: Earth Science and Meteorites, J. Geiss and E.D. Goldberg editors. North Holland, Amsterdam.

Turkdogan, E.T., and Bills, P.M., 1960, Critical review of viscosity of $CaO-MgO-Al_2O_3-SiO_2$ melts: J. Am. Cer. Soc., v. 39, p. 682.

Turner, F.J., Verhoogen, J., 1960, Igneous and metamorphic petrology: second ed. New York, McGraw-Hill.

Urey, H.C., Craig, H., 1953, The composition of the stone meteorites and the origin of the meteorites: Geochim. Cosmochim. Act. v. 4, p. 36-82.

van der Waals, J.H., and Plateeuw, J.C., 1959, Clathrate Solutions, Adv. in Chem. Phys., 2, 1-58.

Washburn, E.W., 1933, International Critical Tables, McGraw-Hill, N.Y.

Wasserburg, G.J., MacDonald, G.J.F., Hoyle, F., Fowler, W.A., 1964, Relative contributions of Uranium, thorium, and potassium to heat production in the earth: Science, v. 143, p. 465-467.

Watson, K., Murray, B.C., and Brown, H., 1961, On the Possible Presence of Ice on the Moon: Jour. Geophys. Res., 66, 1558-1600.

Watson, K., Murray, B.C., and Brown, H., 1961, The Behavior of Volatiles on the Lunar Surface: Jour. Geophys. Res., 66, 3033-3045.

Yoder, Jr., H.S., Tilley, C.E., 1962, Origin of basalt magmas: an experimental study of natural and synthetic rock systems: J. of Petrology, v. 3, p. 342-532.